博士学位論文

アオリイカ生態研究への安定同位体比技術の応用

Ecological applications of stable isotopic technique on bigfin reef squid *Sepioteuthis lessoniana*

2021 年 2 月

長崎大学大学院水産・環境科学総合研究科

江　俊億

Acknowledgements

First, I truly appreciate all teaching and support from my supervisor, Dr. Chia-Hui Wang, during such a difficult way of academic research for me. I could not imagine how I finish my dissertation without you. I would like to take this opportunity to express my sincere appreciation to my supervisor Dr. Atsuko Yamaguchi. You always took patiently care of me and arranged a wonderful practical farm of aquaculture for conducting my experiment. I also thank Dr. Tin-Yam Chan very much for your instruction and suggestion when I encountered difficulties in studying and submitting manuscripts. I truly appreciate Dr. Ming-Tsung Chung for his assistance and expertise, making the ideas and analysis in this research be realized and significantly improving this dissertation.

I would like to thank my committee, Dr. Yoshiki Matsushita and Dr. Naoki Yagishita, who not only provided a lot of useful comments but also helped me to adapt the different culture and language during my stay in Japan.

Thanks also go to all my friends and colleagues at Nagasaki University, Dr. Keisuke Furumitsu, Dr. Kojiro Hara, Yoshimi Ogino of Marine Zoology Lab, and Jungmo Jung of Fishing Technology Lab for taking me a great time with their accompanying. I particularly thank Sen Hao for taking care of me when I was seriously injured. You took me commuting between campus and hospital many times and assisted things within my daily japan life, but never complained. I also would like to thank a lot all members of Biogeochemistry Lab at National Taiwan Ocean University. I will remain my gratitude to you in another dissertation of NTOU.

I also want to extend particular thanks to all people, CC Cheng, KF Huang, PH Hung, BN Jenq, RY Li, TH Lin, LW Liu, Dr. JC Shiao, Dr. TW Shih, Dr. NJ Su, SY Teng, YH Tsai, MH Wang, Dr. PL Wang, Dr. YC Wang, and MR Yang, for their sample collection, experimental support, chemical analysis, statistical suggestion and manuscript editing.

In final, I am grateful to my family for their long-term financial and daily supports, allowing me to complete my research without any worries, and to my soulmate, Chiu-Chen Tsai, you gave me the courage to face all the difficulties in my life.

Abstract

Stable isotopic analytical technique has been applied on ecology of varied marine organisms but with few cases on cephalopods. *Sepioteuthis lessoniana* is a neritic squid species distributed in the Indo-Pacific Ocean. Fisheries management of the species is difficult due to inadequate ecological information, e.g. habitat use, movement pattern, metabolism and dietary shift of each life history stage. Therefore, the aim of this study is to apply stable isotopic technique for ecological studies on *S. lessoniana* in Taiwan waters as a pioneer example.

This study first evaluated the efficacy of enriched stable isotopic mass-marking technique on hatchlings for further larval dispersal tracking purpose and the potential mass-marking effects on hatchling size and statolith chemistry of *S. lessoniana*. *S. lessoniana* egg capsules were collected from northern Taiwan and assigned randomly to ^{137}Ba-spiking experimental groups at 0.2, 0.5 and 1 ppm and three immersion durations (1, 3 and 7 days). Immersion duration >3 days produced significantly lower ^{138}Ba : ^{137}Ba ratios, with 100% marking success, indicating that it is a reliable marking technique. The ^{137}Ba mass marking had a positive effect on size at hatch and was likely to affect statolith trace element incorporation, including Cu, Zn and Pb. These findings highlight that it is necessary to consider the species-specific effects on hatchling size and physiological responses when using stable isotopes mass-marking techniques.

Subsequently, the daily growth and δ^{18}O and δ^{13}C values from the core to the edge of statoliths on *S. lessoniana* collected in northern Taiwan and the Penghu Islands were analyzed to predict the ontogenetic temperature and metabolic rate changes. The probability of occurrence in a given area at each life stage in three seasonal groups was determined using salinity values, deduced and measured temperatures, and the known ecology of *S. lessoniana*. The results showed that ontogenetic variation in the statolith δ^{18}O values in *S. lessoniana* reflected the seasonal temperature fluctuation observed in Taiwanese waters, which indicated the reliability of the prediction method. Highly diverted dispersal and movement patterns

were observed. The results indicated the importance of the waters near the coast of northeastern Taiwan and the Penghu Islands as spawning grounds. Based on a model prediction, the distribution of *S. lessoniana* is likely associated with water temperature and upwelling, which supports high primary production and sustains the prey of the squid in the waters. The geographical overlap and a potential migration route between northeastern Taiwan and the Penghu Islands suggests the possibility of population connectivity in *S. lessoniana* between the two sites.

Finally, the $\delta^{13}C$ and $\delta^{15}N$ in muscles of *S. lessoniana* in northern Taiwan were analyzed to investigate the diet composition shifting resulting from habitat change as growth. The $\delta^{13}C$ values in muscles and statoliths are further used to assess the proportion of metabolically derived carbon (M value), evaluating the metabolic change along the ontogeny. The results showed an increasing pattern of $\delta^{15}N$ and relatively consistent $\delta^{13}C$ in squid muscles with the ontogenetic change, suggesting that they consume consistent species composition of prey in the same latitude region, whereas the prey size increases within ontogenetic change. A high level of metabolic rate, regarding high M value, found in adult individuals suggested obvious mobility for overwintering, and a high feeding rate and energy consummation during the reproductive period.

This study evaluated the potential of stable isotopic mass-marking approach to track hatchling dispersal of *S. lessoniana*, and provided information on the spatial-temporal movement and dietary shift of bigfin reef squid at various ontogenetic stages, which is essential for resource management and conservation of the species. These findings extend the limited knowledge about the life history of *S. lessoniana* in Taiwan. Future developments can reduce the uncertainty associated with this approach and provide more accurate species-specific interpretations of the variations of stable isotopic signatures within individuals and stocks of free-moving cephalopods.

Table of Contents

1. Introduction 1

1.1. ^{137}Ba mass-marking techniques 2

1.2. The analysis of oxygen isotope ratio 4

1.3. The analysis of carbon and nitrogen isotope ratio 5

1.4. Research purpose 7

2. Evaluation of the ^{137}Ba mass-marking technique and potential effects in the early life history stages of *Sepioteuthis lessoniana* 9

2.1. Materials and methods 10

2.2. Results 12

2.2.1. Barium isotope ratios and mark success 12

2.2.2. Hatchling size and growth condition factor 13

2.2.3. Element discrimination and correlation 14

2.3. Discussion 14

3. Seasonal movement patterns of the bigfin reef squid *Sepioteuthis lessoniana* predicted using statolith δ^{18}O values 18

3.1. Materials and methods 19

3.1.1. Squid collection and age estimation 19

3.1.2. Isotopic analysis 19

3.1.3. Prediction of movement patterns 21

3.1.4. Statistical analysis 23

3.2. Results 24

3.2.1. Oxygen isotopic composition of the statolith 25

3.2.2. Predicted occurrence area and movement pattern 26

3.2.3. The geographical overlap during sexual maturity 28

3.3. Discussion 29

3.3.1. Variation in statolith δ^{18}O values in relation to experienced temperature 29

3.3.2. **P**rediction of ontogenetic movement and distribution 30

3.3.3. Method improvement and applications in future 37

4. The ecological inferences using stable carbon and nitrogen isotopes on spatial preferences of *S. lessoniana* in Taiwan 40

4.1. Materials and Methods 41

4.1.1. Squid collection and measurement 41

4.1.2. Isotopic analysis 42

4.1.3. Data analysis 42

4.2. Results 44

4.3. Discussion 46

5. Conclusion 53

6. References 56

List of Tables

Table 1 Summary of the mantle length, body weight, Fulton's condition factor *K* and $^{138}Ba/^{137}Ba$ ratio among the control group and all experimental treatments. 78

Table 2 Nonparametric analysis of variance results for the difference in ^{137}Ba-spiked concentrations (0, 0.2, 0.5 and 1 ppm) and immersion durations (0, 1, 3 and 7 days) for Ba isotopes ratios in the statoliths of hatchlings. 79

Table 3 Structure matrix coefficients for Discriminant Function (DF) 1 and DF2 for each mean element : Ca ratio used in canonical discriminant analysis for hatchling statoliths among the control and experimental groups. 80

Table 4 The cross-validated classification success for the statoliths of hatchlings in the control and experimental groups based on the discriminant function analysis scores. 81

Table 5 Summary of Spearman's ρ test between Ba stable isotopes and trace elements in the statoliths of hatchlings..... 82

Table 6 Sampling date, mantle length, age estimation, and back-calculated hatching date and season for each *S. lessoniana* individual used in statolith oxygen isotopic anlysis. ……....83

Table 7 Results of nonparametric analysis of variance to test the differences in *S. lessoniana* statolith oxygen isotopes ratios among seasonal groups (spring, summer, and autumn) and ontogenetic (embryonic–paralarval, juvenile, juvenile–subadult, and subadult–adult) stages. 85

Table 8 Sample size, morphology and stable isotopic composition of muscles and statoliths of *S. lessoniana* from two sampling sites..... 86

Table 9 The width of growth increment, estimated ML, and estimated BW of *S. lessoniana* in early (embryonic-juvenile) and later (subadult-adult) life history stages from two collection sites. 87

Table 10 Results of multiple linear regressions correlating statolith $\delta^{13}C_{statolith}$ values with predicted variables for all, early (embryonic-juvenline) and later (subadult-adult) life history stages. 88

List of Figures

Figure 1 Mean (±s.d.) Ba isotope ratios in the statoliths of hatchlings immersed in water with ^{137}Ba-spiked concentrations of 0.2 (light gray bars), 0.5 (dark gray bars) and 1 ppm (black bars) for 1, 3 and 7 days. 89

Figure 2 Mantle length, bodyweight and Fulton's condition factor *K* of hatchlings immersed in water with different concentrations of ^{137}Ba spike, namely 0.2 ppm (light grey bars), 0.5 ppm (dark grey bars) and 1 ppm (black bars), for 1, 3 and 7 days and the control group..... 90

Figure 3 Forward stepwise canonical discriminant analysis using Mg, Sr, Zn, Cu and Pb in the statoliths of hatchlings among control and all experimental groups immersed in water containing different concentrations of ^{137}Ba spike (0.2, 0.5 and 1 ppm) for 1, 3 and 7 days..... 91

Figure 4 Linear regressions between mean element : Ca ratios and ^{138}Ba : Ca in the statoliths of hatchlings..... 92

Figure 5 Map showing the collection locations (slanted lines). 93

Figure 6 Polished *S. lessoniana* statolith (K180116012) with the drilling paths for powder collection. 94

Figure 7 Determination of matching between deduced and measured temperature from the two-sample t test. 95

Figure 8 $\delta^{18}O_{statolith}$ values in *S. lessoniana* hatched in 2017 from northern Taiwan in three seasonal groups and at four ontogenetic stages..... 96

Figure 9 $\delta^{18}O_{statolith}$ profiles of *S. lessoniana* from the statolith core to the edge of each individual in the spring group of 2017-Northern Taiwan. 97

Figure 10 $\delta^{18}O_{statolith}$ profiles of *S. lessoniana* from the statolith core to the edge of each individual in the summer group of 2017-Northern Taiwan. 98

Figure 11 $\delta^{18}O_{statolith}$ profiles of *S. lessoniana* from the statolith core to the edge of each individual in the autumn group of 2017-Northern Taiwan. 99

Figure 12 $\delta^{18}O_{statolith}$ values in *S. lessoniana* hatched in 2017 from Penghu Islands in three seasonal groups and at five ontogenetic stages. 100

Figure 13 $\delta^{18}O_{statolith}$ profiles of *S. lessoniana* from the statolith core to the edge of

each individual in the spring group of 2017-Penghu Islands. 101

Figure 14 $\delta^{18}O_{statolith}$ profiles of *S. lessoniana* from the statolith core to the edge of each individual in the summer group of 2017-Penghu Islands. 102

Figure 15 $\delta^{18}O_{statolith}$ profiles of *S. lessoniana* from the statolith core to the edge of each individual in the autumn group of 2017-Penghu Islands. 103

Figure 16 The linear relationship between deduced temperatures from $\delta^{18}O$ values of individual statolith edges and corresponding measured temperatures in the same period. 104

Figure 17 Probability distribution based on experienced temperatures in *S. lessoniana* individuals in the spring group at each life stages of 2017-Northern Taiwan. 105

Figure 18 Probability distribution based on experienced temperatures in *S. lessoniana* individuals in the summer group at each life stage of 2017-Northern Taiwan. 106

Figure 19 Probability distribution based on experienced temperatures in *S. lessoniana* individuals of the autumn group at each life stage of 2017-Northern Taiwan. 107

Figure 20 Probability distribution based on experienced temperatures in *S. lessoniana* individuals of the spring group at each life stage of 2017-Penghu Islands. 108

Figure 21 Probability distribution based on experienced temperatures in *S. lessoniana* individuals of the summer group at each life stage of 2017-Penghu Islands. 109

Figure 22 Probability distribution based on experienced temperatures in *S. lessoniana* individuals of the autumn group at each life stage of 2017-Penghu Islands. 110

Figure 23 Overlapping rates at the subadult-adult stages of *S. lessoniana* individuals among three seasonal groups between northern Taiwan and the Penghu Islands. 111

Figure 24 The relationship between deduced temperature and $\delta^{13}C_{statolith}$ value for all life history stage of Penghu Islands individuals. 112

Figure 25 The relationship between alternative metabolic indexes (deduced temperature and estimated body weight) and $\delta^{13}C_{statolith}$ value for the later life history stage of northern Taiwan individuals. 113

Figure 26 The relationship between alternative metabolic indexes (deduced temperature and estimated body weight) and $\delta^{13}C_{statolith}$ value for the (a, b) early and (c) later life history stage of Penghu Islands individuals..... 114

Figure 27 The variations of residual values of seasonal hatching groups (green: spring; blue: summer; orange: autumn) among different life history stages. 115

Figure 28 The residuals of the Penghu Islands minus these of northern Taiwan at each life history stage. 116

Figure 29 $\delta^{13}C$ values in muscles and statolith edge of northern Taiwan individuals (n = 19). 117

Figure 30 The relationship between $\log_{10}$(body weight) and $\delta^{13}C_{muscle}$ values of northern Taiwan individuals (n = 77). 118

Figure 31 The variations of $\delta^{13}C_{muscle}$ and $\delta^{15}N_{muscle}$ values of northern Taiwan individuals (n = 77) over the sampling duration. 119

Figure 32 $\delta^{13}C$ and $\delta^{15}N$ values in muscles of northern Taiwan individuals. Ellipses represent the standard ellipse area (SEA) estimated for each sexual maturity stage. 120

1. Introduction

Cephalopods exist in almost all marine environments (Okutani, 2015) and are important species for commercial fisheries and are considered as important model species for neurobiological and behavioral researches (Jereb and Roper, 2005; Kobayashi et al., 2013; Sugimoto and Ikeda, 2013). They share common biological characteristics including short life cycles, high metabolic rates, complex behaviors and high plasticity life history characteristics. Their growth and population dynamics respond sensitively to environmental conditions, such as food abundance, temperature and water (Jackson and Moltschaniwskyj, 2002; Forsythe, 2004). Cephalopod movement happens during all stages of the life history, from the passive drifting of egg and paralarvae with coastal and oceanic currents (O'Dor and Balch, 1985) to active vertical and spatial schooling migration at the adult stage for feeding or spawning (O'Dor, 1998a). Similar to most marine organisms, the movement pattern and distributional range of cephalopods is critical in determining population connectivity and dispersal, recruitment success and population gene exchange (O'dor, 1998b; Moreno et al., 2008), which are key factors for fishery management (Swearer et al., 1999; Cowen and Sponaugle, 2009). However, most squid distributions and movement patterns are difficult to observe and so are poorly understood.

The bigfin reef squid, *Sepioteuthis lessoniana*, is widely distributed in the neritic waters of the Indo-Pacific Ocean, which includes the waters surrounding Taiwan (Roper et al., 1984; Okutani, 2015). Field observations have revealed that adults migrate from offshore areas to shallow inshore areas for spawning (Segawa, 1987). In the waters off the northern coast of Taiwan, *S. lessoniana* hatching occurs almost throughout the entire year with two hatching peaks in May and August-September, respectively (Chen et al., 2015). The population can therefore be divided into at least two seasonal groups (spring and autumn) on the basis of back-calculated hatching date and life history traits (Ching et al., 2017). This species of squid is important to fisheries and is caught by a variety of fishing methods, including jigging, lured-hooks, purse seines, set nets and trawls. Although it has the highest economic value among squids in Taiwan, empirical evidence concerning the movement and distribution

during the ontogenetic stages is similarly scarce.

Several methods for investigating dispersal and movements of squids have been developed, but are not always applicable. Movement patterns of squids have been collected directly through external tagging (e.g. Ueta and Jo, 1990; Jackson et al., 2005; Gilly et al., 2006; Kanamaru et al., 2007a; Bazzino et al., 2010). Ueta and Jo (1990) studied the migration of subadult–adult individuals of *S. lessoniana* around Tokushima Prefecture in Japan by using the tag–recapture method along with fishery data and suggested that this species stayed in inshore waters and migrated to offshore waters for overwintering. Kanamaru et al. (2007a) evaluated past tagging studies for *S. lessoniana* migration in Japan and reported that individuals released in autumn moved farther than those released in spring. However, external tags may harm organisms and increase mortality rates (Sauer et al. 2000; Kanamaru et al., 2007b; Barry et al. 2011). In addition, low recapture rates and the size of the electronic device usually limit the success of squid tagging experiments (Semmens et al., 2007). Although alternative biomarkers, such as parasite communities and molecular markers, are not limited by squid body size and can be applied on larval stage individuals, these methods cannot provide detailed information on larval dispersal and movement patterns (Bower and Margolis 1991; Buresch et al. 2006). On the other hand, the movements of squids are attributed to suitable temperature and food abundance because squids are highly vulnerable to drastic changes in temperature and food availability. Elemental signatures (e.g. Sr:Ca ratio) of the hard structures of squid provide a potential method to trace the ambient water temperatures experienced (Ikeda et al., 2003; Yamaguchi et al., 2015, Liu et al., 2016; Yamaguchi et al., 2018), although the relationships between the Sr:Ca ratio and temperature are inconsistent in different species (Elsdon and Gillanders, 2002, 2003; Gillanders et al., 2013). Other than elemental signatures, stable isotopic tracers that are more commonly applied to teleost otolith should be considered to apply on cephalopod statolith for improving the accuracy and reliability of predictions.

1.1. ^{137}Ba mass-marking techniques

In recent years, enriched stable isotope marking techniques have been used on fishes, such as injecting enriched stable isotopes into mature females (Thorrold et al. 2006; Almany et al. 2007) or immersing offspring in water with enriched stable isotopes (Munro et al. 2008; Smith and Whitledge 2011; Woodcock et al. 2011a). These techniques can be used to produce unique isotopic signatures in the biogenic carbonates of experimental offspring, which are distinguishable from natural populations (Munro *et al.* 2008; Smith and Whitledge 2011). Stable isotopes of barium and strontium have similarities in their ionic radius to Ca^{2+} and will likely be a substitute for Ca^{2+} in biogenic carbonates (Speer 1983), thus both elements are commonly used in the marking experiments. Because barium concentrations are relatively low in natural seawater (varying in the range 0.007–15 ppm in seawater and fresh water; Bernat et al. 1972; Kresse et al. 2007), performing this technique with barium for marine organisms is easier. In addition, marking by feeding Ba-enriched dietary items has been suggested as a more effective method in marine systems (Woodcock and Walther 2014). The ^{137}Ba isotope is stable in lower abundance (11.23%) and is not the major barium isotope (71.1% for ^{138}Ba; Rosman and Taylor 1998). When enrichment with ^{137}Ba in calcified structures is greater than environmental levels, the mark is easily detected and shows a difference from natural seawater signatures (Thorrold et al. 2006). Therefore, ^{137}Ba mass-marking techniques are likely suitable for tracking larval dispersal and movement patterns of squids in the natural environment.

To date, only two studies have evaluated the ^{137}Ba mass-marking technique in the early life stages of cephalopods (Pecl *et al.* 2010; Payne *et al.* 2011). Due to the difficulty in determining the oocyte maturity stage in cephalopod ovaries (Pecl et al., 2010), maternal injection of stable isotopes may not be available for all cephalopod species. In contrast, Payne et al. (2011) combined two ^{137}Ba spiked concentrations (0.3 and 1 ppb) with three immersion durations (2, 5 and 8 days) for marking *Sepia apama* eggs hatchlings, and demonstrated the potential of using stable isotopes to assess the population dynamics of cephalopods in the field. Given the efficacy of enriched isotope marking technique varies among species, the method producing

high-quality marking with lower cost in the species of interest has to be evaluated (Warren-Myers *et al.* 2018).

On the other hand, compared with other fluorescent dyes (e.g. alizarin complexone), mass-marking methods with enriched isotopes are usually considered non-toxic to experimental offspring (Williamson et al. 2009; Woodcock et al. 2011a; Warren-Myers et al. 2018). However, increasing evidence suggests that this technique may affect hatchling size (Williamson et al. 2009; Starrs *et al.* 2014a, 2014b). The size at hatch is crucially related to swimming and foraging ability, which consequently affects survival rate and reproduction (Sogard, 1997). It is unclear if the enriched isotope marking method affects the hatchling size of cephalopod species. Moreover, the physiological regulation may be altered during the process of enriched isotope marking, causing erroneous interpretations for cephalopod behaviours (de Vries et al. 2005). Such effects must be validated and considered carefully in stable isotope mass-marking experiments.

1.2. The analysis of oxygen isotope ratio

Besides enriched isotopes marking, natural isotopic signatures in biogenic carbonate can be modified by environmental and biological activity, and thus are considered powerful tools for assessing organism dispersal and ecological connectivity (Rodgers and Wing, 2008; Kato et al., 2020; Kawazu et al., 2020). In fishes, the isotopic composition in otolith formed $CaCO_3$ can provide important information on environmental and biological processes (Campana, 1999). Oxygen has three forms of stable isotopes: ^{16}O, ^{17}O and ^{18}O, and their relative abundances are 99.76, 0.04 and 0.20 %, respectively. Due to greater abundances and mass differences between ^{16}O and ^{18}O, the oxygen isotope ratio generally focuses on $^{18}O/^{16}O$ ratio (Rohling, 2013). Oxygen isotope ratios in seawater have been considerably linked with thermal mechanisms within the hydrological cycle, such as evaporation, vapor transport, precipitation and freshwater runoff (Rohling, 2013). The oxygen isotope ratio ($\delta^{18}O$) in fish otoliths is in equilibrium with that in the ambient water, and $\delta^{18}O$ value uniformly increases with a decrease in seawater temperature in various species

of fish (Elsdon and Gillanders, 2002; Høie et al., 2004a). Squid statoliths are composed of calcium carbonate, and the fundamental mechanism between statolith and ontogeny/environment is similar to that of fish otoliths (Arkhipkin et al., 2004; Arkhipkin 2005; Gillanders et al., 2013). Therefore, statolith $\delta^{18}O$ value can be analogously used as proxies for reconstructing the ontogenetic preferences of squids (Radtke, 1983; Landman et al., 2004; Trasviña-Carrillo et al., 2018, Chung et al. 2020). There are a few literatures that predicted the environmental preferences with $\delta^{18}O$ value in cephalopod statoliths. Landman et al. (2004) assessed the experienced temperature of the giant squid *Architeuthis sanctipauli* to be in the range of 10.5 ºC–12.9 ºC and average living depths to be 125–250 m by analyzing the $\delta^{18}O$ values in one entire statolith, which are considered to provide lifelong average temperature data. Trasviña-Carrillo et al. (2018) analyzed the $\delta^{18}O$ values in the entire statolith of the jumbo squid *Dosidicus gigas* and found that spatial and trophic preference did not differ between sexes, but did among ontogenetic stages because of vertical migration for larger individuals. The temporal resolution of their ontogenetic movement and distribution history can be increased by micromill sampling, which was used on fish otoliths (Høie et al., 2004b), for higher temporal resolution of isotopic information. Recently, Chung et al. (2020) conducted a temperature-controlled experiment to define the statolith $\delta^{18}O$ values of *sepia pharaonis* exposed to the different ambient water temperature. To date, this is the first temperature-dependent equation for $\delta^{18}O$ values in cephalopod statoliths. Combining the temporal resolution of isotopic composition and temperature-dependent equation offers a valuable opportunity to study cephalopod movement and their thermal responses to climate change.

1.3. The analysis of carbon and nitrogen isotope ratio

Like the expression of oxygen isotopes, carbon isotopes typically was expressed as $^{13}C/^{12}C$ ratio (99.89 % and 0.11%, respectively). The carbon isotope composition in seawater is mainly controlled by biological and inorganic processes as well as air-sea exchange (e.g. Schmittner et al., 2013). For example, living plants preferentially incorporate lighter ^{12}C, compared to ^{13}C, into their biomass and have less value of stable carbon isotope ratio ($\delta^{13}C$) (about -28‰) for C_3 photosynthetic pathway than

the value (about -14‰) for C_4 pathway (O'Leary, 1988). Factors affecting $\delta^{13}C$ value in biogenic carbonate are more complex than those affecting oxygen isotope (McConnaughey 1989; McConnaughey et al., 1997). The $\delta^{13}C$ value in fish otoliths is derived from dissolved inorganic carbon in water ($\delta^{13}C_{DIC}$) and dietary carbon ($\delta^{13}C_{diet}$). In general, $\delta^{13}C_{DIC}$ values are relatively uniform in marine systems, varying from 0 to 3‰ on the horizontal distribution and 1‰ in vertical gradient (Lin et al., 1999; Schmittner et al., 2013; Becker et al., 2016). With a given value of apparent oxygen utilization (AOU), $\delta^{13}C_{DIC}$ values can be calculated from a simple linear relationship between $\delta^{13}C_{DIC}$ values and AOU in the global ocean (Kroopnick, 1985). On the other hand, $\delta^{13}C_{diet}$ values in benthic/neritic prey are commonly higher than those of pelagic prey (France, 1995). The stable isotopic composition of a consumer shows an integrated value of isotopic composition of their prey, suggesting that habitat and food utilization affect the carbon isotope composition in the predator body (Hobson, 1999). Moreover, carbon sources for biogenic carbonates are derived from blood and endolymph of organisms (Campana, 1999). The proportion of respiratory and dietary carbon in body fluid increases with faster metabolic rates, reducing the $\delta^{13}C$ value (Schwarcz et al., 1998; Soloman et al., 2006; Tohse and Mugiya, 2008). The $\delta^{13}C$ value in biogenic carbonate in such instances records information on physiological processes regulating the metabolic rate (Chung et al., 2019a, 2019b), such as the swimming activity and growth of organism (Sherwood and Rose, 2003). We therefore used the $\delta^{13}C$ values in statoliths as a supplement for inferring the movement between coastal and offshore seawater corresponding to metabolism and dietary shifts.

Similarly, the analysis of $\delta^{13}C$ and $\delta^{15}N$ of soft tissues is a considerable method to infer the trophic relationship in response to foraging ecology and habitat use (Rodgers and Wing, 2008; Green et al., 2012). This two stable isotope analysis shows the dietary information over a time period from weeks to months depending on size at catch and turnover rate (Hobson, 1999). The trophic shifting throughout lifetime has not been evaluated for *S. lessoniana* in the field. Based on empirical observations in rearing experiments (Lee et al., 1994; Ikeda et al., 2003), *S. lessoniana* mainly feeds

on crustaceans and fishes, and is sometimes cannibalistic, resulting in similar trophic patterns. Due to the presence of different life history stages, which may show a distinct habitat use, some degree of spatial, seasonal and bathymetric variability in diet may be found using carbon and nitrogen stable isotope analysis of soft tissues.

1.4. Research purpose

The demographic dynamic has not been fully evaluated for *S. lessoniana* in Taiwan. Given the presence of different life history stages of *S. lessoniana*, which may exhibit distinct habitat use and movement patterns, there is an evident need to integrate overall temporal-spatial shifts on dispersal and movement of this species in Taiwan waters. This is a fundamental step to having a better understanding about the environmental role in the distribution and the population connectivity of this species. This study therefore evaluated potential techniques and investigated the movement patterns and distribution of *S. lessoniana* in terms of the individual, seasonal, geographical, and population scales by combining stable oxygen and carbon isotopes in statoliths, which deduced the experienced temperature and metabolic information among life history stages, with stable carbon and nitrogen isotope of muscle tissues, available for assessing dietary shifting in each habitat. The objectives of this study are:

(I) Evaluate the efficiency of marking statoliths of *S. lessoniana* embryos with enriched ^{137}Ba and the potential effects on the size-at-hatch and statolith chemistry of individuals after marking for future application in the field.

(II) First analysis of spatial-temporal stable oxygen and carbon isotope in cephalopod statoliths. Then investigate the ontogenetic movement patterns of different seasonal and geographical groups of *S. lessoniana* around Taiwan through statolith $\delta^{18}O$ and $\delta^{13}C$ analyses.

(III) Examine whether $\delta^{13}C$ values in statoliths could be a proxy of metabolic rate, then $\delta^{13}C$ values in muscles and statoliths are used to assess the proportion of

metabolically derived carbon (M value). In addition, stable carbon and nitrogen isotopes in *S. lessoniana* muscles were used to provide evidence of diet between habitat shifting as growth.

2.

Evaluation of the ^{137}Ba mass-marking technique and potential effects in the early life history stages of *Sepioteuthis lessoniana*

2.1. Materials and methods

S. lessoniana egg capsules were collected by SCUBA diving from artificial bamboo reefs (depth ~20–25 m) at Wanghaixiang Bay in northern Taiwan in August 2015. The egg capsules were put in an opaque plastic bucket with natural seawater and immediately transported (<2 h) to the aquaculture station of the National Museum of Marine Science and Technology (Keelung, Taiwan). Before the experiments, all the egg capsules were suspended on nylon threads in a 200-L tank for initial acclimation. Natural seawater was collected from Wanghaixiang Bay and pumped through a filter bed to supply the rearing system. During the experiment, the seawater temperature was maintained at a mean (±s.d.) temperature of 25 ± 1°C, salinity was maintained at 34.1–34.7 PSU and experiments were conducted under a 12-h light–dark cycle.

In all, 150 eggs with visible embryos at 23–25 developmental stages, which were classified according to Segawa (1987), were randomly selected for each group stage and reared in a 10-L tank. There were nine experimental groups in total: three ^{137}Ba spike concentrations (0.2, 0.5 and 1 ppm) and three immersion durations (1, 3 and 7 days). These groups were compared against a control group with no spiking. Different ^{137}Ba concentrations were prepared by dissolving ^{137}Ba-enriched $BaCO_3$ (≥91% ^{137}Ba and 8% ^{138}Ba; Trace Sciences International, Richmond Hill, ON, Canada) in ultrapure water. For groups immersed for >1 day, half the rearing seawater was replaced daily and extra ^{137}Ba spike was added to maintain the concentration of the ^{137}Ba spike. After immersion, eggs were returned to the natural seawater until they hatched. The Mantle length (ML, mm) and body weight (BW, mg) of the hatchlings were measured. Individuals were then sacrificed by exposure to a high concentration of ethyl alcohol and their statoliths extracted. The experimental procedures followed the Guidelines for the Care and Welfare of Cephalopods in Research – A Consensus Based on an Initiative by CephRes, FELASA and the Boyd Group (Fiorito et al., 2015). The growth condition factor of hatchlings was estimated based on Fulton's condition factor *K*, calculated as follows (Ricker 1975):

$$K = (\mathrm{BW} \div \mathrm{ML}^3) \times 100$$

Statoliths were extracted under a stereomicroscope (SteREO Discovery, V12; Carl Zeiss Microscopy GmbH, Jena, Germany), cleaned ultrasonically with 70% hydrogen peroxide to remove adhering tissue, rinsed three times in ultrapure water, placed into acid-washed Eppendorf microcentrifuge tubes and oven dried overnight. The statoliths were then transferred to 1.5-mL acid-washed high-density polyethylene vials and weighed on a microbalance to the nearest 10 μg. Individual pairs of statoliths were dissolved in 0.5 mL of 0.3 M ultrapure nitric acid. Solutions were analysed using inductively coupled plasma–mass spectrometry (ICP-MS; ELEMENT XR ICP-MS; Thermo Scientific, Bremen, Germany) at the Institute of Earth Science, Academia Sinica, Taipei, Taiwan. Nine isotopes (^{25}Mg, ^{43}Ca, ^{55}Mn, ^{88}Sr, ^{137}Ba, ^{138}Ba and ^{208}Pb) were analysed in a low-resolution mode and two isotopes (^{63}Cu and ^{64}Zn) were evaluated in a medium-resolution mode. Element concentration is shown as a ratio relative to the concentration of calcium (mean element (Me) : Ca ratio). The carbonate (otolith)-certified reference material FEBS-1 (National Research Council, Ottawa, ON, Canada) was used to determine the Me : Ca ratio of samples and analysed every fifth sample to instrument drift. In regard to the matrix effect, statolith solutions in various calcium concentrations (0.5, 1, 5, 25 and 50 ppm) were tested and the Me : Ca ratios of every sample were normalised at the same level of matrix concentration. The relative standard deviations of the Me : Ca ratio measurements of FEBS-1 were lower than 4% for most elements expect Mn : Ca (Mg : Ca 3.37%; Mn : Ca 5.16%; Sr : Ca 1.79%; Ba : Ca 3.44%; Pb : Ca 2.46%; Cu : Ca 1.85%; Zn : Ca 3.06%), and the percentage accuracy of the Me : Ca ratios was better for Mg : Ca, Sr : Ca, Ba : Ca and Pb : Ca (1.04, 0.36; 0.60 and 1.21% respectively) than for Mn : Ca, Cu : Ca and Zn : Ca (7.20, 7.91 and 6.76% respectively). However, Mn concentrations detected were close to the background level and were excluded from further analyses.

Statistical analyses in present study were performed using SPSS (ver. 20, IBM Corp., Armonk, NY, USA), as described below. A Shapiro–Wilk was used to assess the normality of the data, and Ba stable isotope ratios were found to be non-normally distributed. Therefore, a non-parametric Scheirer Ray Hare extension of the Kruskal–

Wallis test was used to examine the effects of spiked concentration and immersion duration on $^{138}Ba : {}^{137}Ba$ ratios. In addition, the effect of ^{137}Ba spikes on the size and condition of marked hatchlings were analysed by two-way analysis of variance (ANOVA). If significant differences were detected, Tukey's post hoc test was used to evaluate the difference between groups. For statolith chemistry, a forward stepwise canonical discriminant analysis was used to evaluate variations in element composition (Mg : Ca, Sr : Ca, Zn : Ca, Cu : Ca and Pb : Ca) among the control and all treatment groups, and cross-validation was further conducted to assess the percentage of successful classifications. In addition, Spearman's ρ test was used to assess correlations between barium stable isotopes ($^{137}Ba : Ca$ and $^{138}Ba : Ca$) and other trace elements.

2.2. Results

2.2.1. Barium isotope ratios and mark success

The ^{137}Ba spike was successfully marked in statoliths because $^{138}Ba : {}^{137}Ba$ values decreased with increasing spike concentration or immersion duration. The mean (±s.d.) $^{138}Ba : {}^{137}Ba$ ratio in statoliths in the control group was 6.28 ± 0.17, which decreased to 3.50 ± 0.22 after 7 days of immersion in 1-ppm ^{137}Ba-spiked solution (Table 1, Fig. 1). Significant interactions were found between immersion duration and the concentration of the ^{137}Ba spike on $^{138}Ba : {}^{137}Ba$ ratios in hatchling statoliths (Scheirer–Ray–Hare extension of the Kruskal–Wallis test, d.f. = 9, SS = 166601.9, $H = 34.577$, $P < 0.001$), so separate Dunn's tests were used to compare the mean $^{138}Ba : {}^{137}Ba$ ratios within groups. Overall, 7 days of immersion produced significantly lower mean $^{138}Ba : {}^{137}Ba$ ratios than 1 day immersion for the same spiked concentration ($Z > 4.057$, $P < 0.001$), and the mean $^{138}Ba : {}^{137}Ba$ ratios of the 1-ppm treatment were significantly lower than those of the 0.2-ppm treatment for the same immersion duration ($Z > 3.510$, $P < 0.01$). Longer immersion durations (3 and 7 days) with higher spiked concentrations (0.5 and 1 ppm) produced significantly lower $^{138}Ba : {}^{137}Ba$ ratios than seen in the control group ($Z > 4.564$, $P < 0.001$). An additional significant difference was detected between 3- and 1-day immersions in the 0.2-ppm ^{137}Ba-spiked group ($Z > 3.510$, $P = 0.015$).

Following the criteria of Payne et al. (2011), the critical value of successfully marked squid was set at 5.78, which was the mean ratio of the control group minus 3 s.d. for ^{138}Ba : ^{137}Ba. A successfully marked statolith was defined as a ^{138}Ba : ^{137}Ba ratio in the hatchling statolith that was lower than this value. Higher spiked concentrations and longer immersion duration both increased the success rate of statolith marking (Fig. 1). For example, no mark was found after 1 day of immersion with 0.2 ppm ^{137}Ba spike, but the success rate increased to 40% after 3 days of immersion with the same concentration. In total, 100% of squid were successfully marked after 3 days of immersion with the 0.5- and 1-ppm concentrations and after 7 days of immersion with all concentrations.

2.2.2. Hatchling size and growth condition factor

All eggs hatched 1–5 days after marking. The mean ML of the hatchlings in each group ranged from 5.54 to 5.99 mm, the mean BW ranged from 24.4 to 31.3 mg and mean Fulton's condition factor *K* ranged from 12.98 to 16.43 (Table 1, Fig. 2). No interaction between spike concentration and immersion duration was found for ML ($F = 0.795$, $P = 0.622$), BW ($F = 1.162$, $P = 0.321$) or Fulton's condition factor *K* ($F = 0.821$, $P = 0.597$) of hatchlings (Table 2). The spiked concentration of ^{137}Ba significantly affected ML ($F = 5.789$, $P = 0.001$) and BW ($F = 6.687$, $P < 0.001$) of hatchlings, but not Fulton's condition factor *K* ($F = 2.530$, $P = 0.058$). Hatchlings exposed to spike concentrations of 0.2 and 1 ppm were significantly longer than those in the control group (Tukey's honest significant difference (HSD), $P = 0.001$ and 0.008 respectively; Fig. 2a). The BW of hatchlings in the control group was significantly lower than that of hatchlings in all spiked groups ($P < 0.01$, Fig. 2b). Conversely, the ML ($F = 5.190$, $P = 0.002$), bodyweight ($F = 8.222$, $P < 0.001$) and Fulton's condition factor *K* ($F = 3.214$, $P = 0.024$) of hatchlings differed significantly among immersion duration treatments. Individuals in most immersion duration groups had a larger size in terms of ML and BW than those in the control group, except for BW observed after 1 day immersion ($P = 0.063$). In addition, there was a significant difference in Fulton's condition factor *K* between 1 and 3 days of immersion ($P =$

0.013; Fig. 2c).

2.2.3. Element discrimination and correlation

According to canonical discriminant analysis, hatchling statolith element composition did not show a clear pattern of discrimination between the control and all experimental groups (Fig. 3). The variations explained by Functions 1 and 2 were 53.9 and 24.0% respectively. Cu primarily contributed to Function 1 and Zn contributed to Function 2 (Table 3). The cross-validated classification success for all hatchlings was 24.7%, and ranged from 0% (7 days of immersion with 0.2 ppm ^{137}Ba) to 53.3% (7 days of immersion with 1 ppm ^{137}Ba) (Table 4).

Although statoliths were enriched with ^{137}Ba, their elemental:Ca ratios (Cu : Ca, Zn : Ca and Pb : Ca) positively correlated not to ^{137}Ba but to ^{138}Ba (Table 2; Fig. 4). The regressions of ^{138}Ba : Ca with Cu : Ca, Zn : Ca and Pb : Ca were significant ($P <$ 0.01), with determination coefficients (R^2) of 0.865, 0.741 and 0.248 respectively.

2.3. Discussion

Because of its crucial role in marine ecosystems and being a highly attractive fishery target, effective ecological monitoring and resource management of *S. lessoniana* are needed. In particular, larval dispersal patterns and demographic population connectivity have significant effects on marine organism resources (Cowen et al., 2000; Thorrold et al., 2001; Jones et al., 2005; Cowen and Sponaugle, 2009). There are many factors influencing the success rate of mass marking (e.g. spike concentration or developmental stage; Payne et al., 2011; Woodcock and Walther, 2014). Consistent achievement of 100% mark success is a vital goal for any mass-marking technique (Warren-Myers et al., 2018). For fish larvae or eggs, concentrations of ≥0.1 ppm ^{137}Ba have been used to achieve 100% mark success by immersion (Woodcock et al., 2011a, 2011b; de Braux et al., 2014, Warren-Myers et al., 2015). However, the eggs of many cephalopod species (e.g. myopsid squid and sepioidea cuttlefish) are coated with encapsulation substances (i.e. a capsule) that are effective barriers against metal uptake into the embryo (Rosa et al., 2015). Therefore,

the present study examined higher ^{137}Ba spike concentrations to mark large numbers of *S. lessoniana* hatchlings and found that 100% mark success was achieved steadily after 3 days of immersion with concentrations >0.5 ppm of the enriched barium stable isotope.

This study revealed that 7 days of immersion with lower spike concentrations could also achieve 100% mark success, indicating that immersion duration is a critical factor for marking *S. lessoniana* statolith through egg immersion. This may be because the perivitelline fluid, which is in the capsule and encasing the embryo, is conducive to ambient seawater influx and swells gradually during the late development stage (Cronin and Seymour, 2000). Extension of immersion during egg swelling results in the uptake of the spiked water, decreasing the ^{138}Ba : ^{137}Ba ratio within eggs. A similar effect of immersion duration on Ba stable isotope ratios in otoliths of fish species has been reported (Munro et al., 2008; de Braux et al., 2014). Yet, this is inconsistent with the results reported for *S. apama* by Payne et al. (2011), who found a significant interaction between the concentration of enriched ^{137}Ba and immersion duration, but no significant differences among immersion durations for the lower concentration tested (0.3 ppb). Species and physiological differences may explain these different results. For example, egg swelling time varies according to embryo development period, thus the longer embryo development of *S. apama* (3–5 months; Hall and Fowler, 2003) would dilute the contribution of immersion time to the ^{138}Ba : ^{137}Ba ratios in *S. apama* statoliths. Moreover, the relatively low enriched ^{137}Ba concentration may need a longer time of immersion, and the effect of immersion duration would become significant. In the study of Payne et al. (2011), extension of immersion duration from 2 to 8 days did decrease ^{138}Ba : ^{137}Ba ratios for the higher-concentration (1 ppb) treatment group. Therefore, determining the appropriate concentration and corresponding time of immersion before using this technique on a species of interest is important, because life history characteristics (e.g. developmental stage) and habitats (e.g. seawater or fresh water) may affect the effectiveness and the costs for mass marking.

The ML of hatchlings in this study was consistent with that reported by Lee et al. (1994), who continuously cultured *S. lessoniana* through three successive generations and whose hatchlings averaged 5.3 mm ML, ranging from 3.5 to 6.4 mm ML. The BW of hatchlings in past studies varies, from a range of 4.3–12.0 mg (mean 8.2 mg; Lee et al., 1994) to 50 mg (Segawa, 1987); the BW of hatchlings in the present study fell between values published in the literature. In the present study, ^{137}Ba mass marking slightly increased the ML and BW of marked hatchlings in some of the experimental groups. Larger hatchling size may benefit from an increased attack speed (Sugimoto and Ikeda, 2013) and a reduction in the distance required to capture prey accurately (Chen et al., 1996). In addition, hatchling size is linked to vulnerability to predators (Blaxter, 1986; Sogard, 1997), so that larger size hatchlings would have a greater survival rate in the early life history stages. Moreover, the growth condition (*K*) is related to embryo development and environmental variables, and individuals in a better condition (K) have higher survivorship and greater growth rate (Bolger and Connolly, 1989). However, the *K* values of hatchlings in the present study only differed significantly between two immersion duration groups, indicating that ^{137}Ba mass marking did not affect hatchling growth condition. Previous experimental results of the effects of transgenerational marking (i.e. injection method) on the condition of larval fish were species specific. Positive (Starrs et al., 2014a, 2014b), negative (Williamson et al., 2009) and no significant effects (Zitek et al., 2013; Warren-Myers et al., 2015) on size at hatch, yolk sac area, oil globule area and eyeball diameter were found among species. The findings of the present study provide additional information on cephalopod species marked using the immersion method. As noted by Starrs et al. (2014b), the effects of such mass marking with stable isotopes on hatchling morphology require additional research, as does the roles of the barium during the development of *S. lessoniana* embryos.

We found different element compositions of statoliths in hatchlings that were related to size at hatch, and significant correlations were found between Me : Ca ratios (Cu : Ca, Zn : Ca and Pb : Ca) and ^{138}Ba : Ca. The effects on element composition of statoliths are not often mentioned in the literature when marking cephalopod offspring

with enriched stable isotopes. Element uptake in cephalopod statoliths is presumably similar to the observations in fish otoliths (Gillanders et al., 2013) and is primarily associated with environmental changes, such as water chemistry composition (Arkhipkin et al., 2004) and ambient temperature (Ikeda et al., 2002; Zumholz et al., 2007). However, in this study the rearing seawater was maintained at consistent conditions and egg capsules in the same cluster were used to eliminate any possible effects from the maternal yolk (e.g. Lloyd et al., 2008). The difference in growth rate between control and experimental groups was a potential explanation for variations in element incorporation. Growth rate has been confirmed to be negatively correlated with the elemental partition coefficient in otoliths of teleost species (Walther et al., 2010). A faster growth rate could result in more calcium-binding proteins, altering relative ion concentrations in the calcifying fluid (Kalish, 1989). Therefore, trace elements such as Cu and Zn have a greater likelihood of being associated with organic matrix protein (Miller et al., 2006). In addition, a fast growth rate usually occurs with higher calcium carbonate accretion rate (Ikeda et al., 1999), which raises the pH of the calcifying fluid and reduces trace element concentrations in the endolymph, resulting in a negative relationship between the Me : Ca ratio and accretion rate (Sinclair, 2005; Sinclair and Risk, 2006; Hamer and Jenkins, 2007). The lower hatchling size in the control group could simultaneously lead to elevated patterns of Me : Ca in statoliths. Although the effects of growth rate on the element composition of cephalopod statoliths have not been adequately clarified, the physiological processes do significantly affect the microchemistry of biogenic carbonates. We emphasis that the mechanisms of trace element incorporation into statoliths should be carefully considered to avoid confounding environmental signatures with artificial marking.

3.

Seasonal movement patterns of the bigfin reef squid *Sepioteuthis lessoniana* predicted using statolith $\delta^{18}O$ values

3.1. Materials and methods

3.1.1. Squid collection and age estimation

Twenty-two and twenty-one adult *S. lessoniana* individuals were collected by jigging from the inshore waters of northern Taiwan and the Penghu Islands (Fig. 5), respectively, between November 2017 and March 2018. The mantle length (ML; in mm) of each individual was measured. Statoliths were extracted, cleaned ultrasonically using 70% hydrogen peroxide, rinsed, oven-dried, and embedded in Epofix resin (Struers, Denmark). The left statolith of each squid was ground and polished along the posterior side to approximately 50–100 μm above the core by using a metallographic grinding and polishing machine (P20FR-HA; Top Tech Machines co. Ltd., Taiwan). This thickness ensured that a sufficient volume of milling powder was available for isotopic analysis (>40 μg per sample). Alternative formation of translucent and opaque growth zones has been previously validated as occurring on a daily basis (Jackson, 1990); thus, the growth increment at the lateral dome region of statolith was examined from the photographs recorded under a compound microscope (400×, DM-2500, Leica Microsystems GmbH, Germany) by using a digital camera (DFC-450, Leica Microsystems [Switzerland] Lt., Switzerland) to estimate age. The growth increments were counted twice, and an average value was used as daily age. If the difference between two counts was >5%, a third count was recorded to minimize measurement error (Arkhipkin and Shcherbich, 2012). The hatching date of each individual was back-calculated from the deduced age (in days) and the date of collection. Each individual was further categorized into the nearest seasonal group according to its hatching month, namely spring (March–May), summer (June–August) and autumn (September–November).

3.1.2. Isotopic analysis

After age counting, statolith slides were drilled using an ESI New Wave Research Micromill and carbonate powders were collected sequentially from the edge to the core at the lateral dome region at intervals of 134–192 μm (Fig. 6). The tip of the drill was approximately 200 μm in diameter (H23RS, Comet, Germany), and milling depth was set at approximately 150 μm. In squid samples from northern

Taiwan, most statoliths involved four drilling paths (except a smaller statolith, K180313003, which had three paths only), and each path was recorded to estimate covered daily growth. Based on the morphological and ecological changes in accordance with growth and age (Segawa, 1987), we defined four stages in *S. lessoniana* from northern Taiwan corresponding to age, namely the embryonic-paralarval (age: 0–20 days), juvenile (age: 20–60 days), juvenile–subadult (age: 60–110 days) and subadult–adult (age: >110 days) stages. Conversely, there are three larger adults of the summer group from Penghu Islands involving five drilling paths, we therefore additionally defined an adult (age: >150 days) stage for the fifth path.

The powder samples of each drilling path were transferred to glass vials and reacted with 100% orthophosphoric acid at 70°C in an automated online system (Kiel Carbonate IV, Thermo Electron Corporation, Germany) to produce CO_2. The values of $\delta^{18}O$ were determined by analyzing the released CO_2 gas by using a mass spectrometer (Finnigan MAT 253, Thermo Electron Corporation, Germany) at National Taiwan University. The long-term reproducibility of the Finnigan MAT 253 is higher than ± 0.08‰ (one standard deviation [s.d.]) for $\delta^{18}O$, based on repeat samples of international reference standards (NBS-19, approximately 40–50 μg). The values of $\delta^{18}O$ (‰) were reported in standard notation relative to standards Vienna Pee Dee Belemnite (VPDB) after calibration against the NBS-19 standard:

$$\delta^{18}O \text{ values} = \left(\frac{^{18}O{:}^{16}O_{sample} - {}^{18}O{:}^{16}O_{standard}}{^{18}O{:}^{16}O_{standard}} \right) \times 1000(‰)$$

The temperature-dependent relationship of $\delta^{18}O$ values in biogenic aragonites is taxonomic and species specific (Shirai et al., 2018). However, no equation has been established for statoliths in *S. lessoniana*; hence, we applied the equation established for statoliths in another cephalopod species, *Sepia pharaonis* (Chung et al., 2020), to deduce experienced temperature in *S. lessoniana*.

$$\delta^{18}O_{statolith,\ VPDB} - \delta^{18}O_{water,\ VSMOW} = 2.88\ (\pm 0.14) - 0.20\ (\pm 5.40 \times 10^{-3}) \times T(^{o}C)$$

where $\delta^{18}O_{statolith,VPDB}$ represents the statolith $\delta^{18}O$ values on a VPDB scale, and $\delta^{18}O_{water,\ VSMOW}$ represents the water $\delta^{18}O$ values on a VSMOW (Vienna Standard Mean Ocean Water) scale. The $\delta^{18}O_{water,\ VSMOW}$ values were derived using the relationship with salinity (S) in Taiwan Strait (Chang, 2000):

$$\delta^{18}O_{water,\ VSMOW} = 0.28 \times S - 9.38$$

To evaluate the feasibility of the equation, the relationship of measured and deduced temperature derived from the edge of statoliths in 67 crossed-season captured individuals were analysed to understand if it followed the 1:1 correspondence. The duration (days) which statolith $\delta^{18}O$ values represented was considered, and the measured temperature was averaged based on the duration at the depth of 50m.

3.1.3. Prediction of movement patterns

To accurately predict the experienced temperature and corresponding living areas of *S. lessoniana*, individual differences in living period and temporal and spatial variations in seawater temperature were considered in the evaluation. The individual living period and season corresponding to each data point of statolith $\delta^{18}O$ values were established through the examination of microstructure. During the defined period, water temperature and salinity were obtained from the HYbrid Coordinate Ocean Model website (HYCOM, http://ncss.hycom.org/thredds/catalog.html) and are presented in a spatial resolution of 0.08° × 0.08° at the depths of 0, 30, 50, and 100 m, according to the living depth of this species (Roper et al., 1984; Tomano et al., 2016; Ammar and Maaroof, 2019). Next, we set the unit of the spatial grid at 0.4° × 0.4° to establish the movement pattern because this spatial grid covers the minimum range of squids captured off northern Taiwan in the present study (Fig. 5). For setting units, the average values of temperature and salinity in each grid at each depth (0, 30, 50, and 100 m) was used to produce $\delta^{18}O_{water,\ VSMOW}$ values based on the equation established by Chang (2000).

The deduced temperature depended on the measured statolith $\delta^{18}O$ value and the variation in water $\delta^{18}O$ values among grids at different depths. Therefore, each data point of statolith $\delta^{18}O$ values was used to deduce the experienced temperature in every grid at various depths, each of which had their specific water $\delta^{18}O$ values. When the deduced temperature matched with the measured temperature (from the HYCOM), the grid thus obtained was considered the possible living area of the squid during a specific period; this period was estimated using the growth rings in the milling area for the statolith $\delta^{18}O$ measurement. The extent of match between the deduced and measured temperature was based on the comparison of probability distributions between these two values determined using Student's t test (Fig. 7). The probability distribution of deduced temperature was modeled using a known living period (days) as well as an average and the uncertainty (SD) associated with the deduced temperature. The uncertainties were estimated by running Monte Carlo simulations 1,000 times and included variations in salinity, instrumental measurements, and parameters of the temperature-dependent equation. Similarly, the probability distribution of measured temperature was modeled using known living periods (days) and average values of measured temperature and associated standard deviations. Once the t test resulted in a *P*-value larger than 0.05, we accepted that the two temperatures did not differ significantly and inferred a possibility of the occurrence of a living area in the grid (Fig. 7). We repeated modeling to determine the matched area and depth of each statolith $\delta^{18}O$ value from individuals at each life stage.

Furthermore, we considered the collection location, spawning site, and movement ability of *S. lessoniana* to determine the possible living areas. The $\delta^{18}O$ value in the outermost portion of statoliths reflected the occurrence of *S. lessoniana* near the collection location. If this value represented the 10-day average of the signal, the maximum movement of *S. lessoniana* was calculated to be approximately 50 km away from the collection location because the mean swimming speed of adult *S. lessoniana* individuals is 5 km per day, according to a study by Kanamaru et al. (2007a). Consequently, grids located farther than 50 km from the collection site were

eliminated. In addition to this “backward” evaluation, based on the collection location, a “forward” method was also used to evaluate the living area at the embryonic-paralarval stage. We excluded the matched areas that were not adjacent to the coast because the egg capsules of *S. lessoniana* are always found in inshore waters (Segawa, 1987). Combining the results of forward and backward calculations and mobility, the possible occurrence of life stages of individuals were further selected from the matched areas found based on the statolith $\delta^{18}O$ value.

After examining the living area at an individual level, we calculated the probability of occurrence in each setting area for each seasonal group. The probability was calculated using the following equation:

$$P_j = \frac{C_{1j} + C_{2j} + \ldots + C_{kj}}{k_j}$$

where C_{kj} represents the occurrence of kth squid in area j, and k_j is the total number of individuals in grid j. If squid sample number 1 exists in grid 1 at a specific life stage, the C_{kj} value is 1; otherwise, the C_{kj} value is 0. Furthermore, the P_j value indicates the probability of occurrence in grid j. If the P_j value is 1, all squid samples at the same ontogenetic stage occur in grid j. If an area with a probability (*p* value) of >0.5 is identified, it would be considered a major residential area for *S. lessoniana* seasonal groups around Taiwan.

3.1.4. Statistical analysis

In order to understand the geographical differences in the movement pattern and distribution, we compared the squid samples in northern Taiwan and the Penghu Islands waters from November 2017 to March 2018. To identify the effects of ontogenetic stage and hatching season on $\delta^{18}O_{statolith}$ value, differences in $\delta^{18}O_{statolith}$ values among all ontogenetic stages over the seasonal groups (spring, summer, and autumn) were examined using a nonparametric Scheirer–Ray–Hare extension of the Kruskal–Wallis test followed by post hoc multiple comparisons tests (Dunn’s tests). A

linear regression and an Analysis of Covariance (ANCOVA) were used to test if the experienced temperature deduced by the equation (Chung et al., 2020) was reasonable and close to 1:1 correspondence between measured and deduced temperature. All statistical tests were conducted using SPSS (ver. 20, IBM Corp., Armonk, USA). The t-test used to evaluate the extent of matching between deduced and measured temperatures and the Monte Carlo simulations were used for uncertainty determination were performed using R (R Core Team 2018).

3.2. Results

Hatching date and season of all *S. lessoniana* samples were back-calculated from statolith daily increment reading. In squid samples collected from northern Taiwan, seven individuals were identified belonging to the spring group with a mean (±s.d.) ML of 264 ± 49 mm and an age ranging from 150 to 167 days. Six individuals were identified as the summer group with a mean ML of 260 ± 24 mm and an age ranging from 146 to 192 days. Nine individuals belonged to the autumn group with a mean ML of 298 ± 45 mm and an age ranging from 140 to 177 days (Table 6). In the samples collected from Penghu Islands, four individuals were found to belong to the spring group with a mean ML of 301 ± 58 mm and an age ranging from 175 to 228 days. More than a half of individuals (n = 12) of Penghu Islands were identified as the summer group with a mean ML of 311 ± 51 mm and an age ranging from 149 to 240 days. Five individuals of the autumn group had a mean ML of 243 ± 37 mm and an age ranging from 143 to 184 days (Table 6).

No significant interaction or differences in ML of squid samples of northern Taiwan were observed between seasonal groups (two-way analysis of variance [ANOVA], $F < 2.470$, $P > 0.097$). Again, there were no significant geographical or seasonal differences in ML of squid samples from northern Taiwan and Penghu Islands ($F < 0.588$, $P > 0.448$). For statolith carbonate sampling, the drilling paths represented an average (±s.d.) of 17.2 ± 8.3, 42.9 ± 7.8, 51.4 ± 8.2, and 58.5 ± 12.5 days growth from the core to the edge that corresponding to the embryonic–paralarval, juvenile, juvenile–subadult, and subadult–adult stages, respectively. In

addition, for the adult stage of three individuals of Penghu Islands, the outermost drilling paths represented an average of 59.8 ± 12.7 days living record.

3.2.1. Oxygen isotopic composition of the statolith

In the squid samples of northern Taiwan, $\delta^{18}O_{statolith}$ values ranged from −2.93 to −0.12‰ with a mean of −1.86 ± 0.79‰. Variations in the $\delta^{18}O_{statolith}$ values were not consistent among seasonal groups (Fig. 8a). Larger variations were observed in the summer and autumn groups than in the spring group; however, the $\delta^{18}O_{statolith}$ values were not significantly different among the seasonal groups (Kruskal–Wallis test, H = 1.506, P = 0.471, Table 7). Ontogenetic stage differences were observed in $\delta^{18}O_{statolith}$ values (Kruskal–Wallis test, H = 39.941, $p < 0.001$, Table 7). The values decreased slightly from embryonic–paralarval stage to the juvenile stage and then increased until the subadult–adult stage (Fig. 8b). The values of $\delta^{18}O_{statolith}$ in the embryonic–paralarval stage were significantly lower than those in the subadult–adult stage (Dunn's tests, Z = –4.078, $p < 0.001$). In addition, the values in the juvenile stage were significantly different from those in the juvenile–subadult and subadult–adult stages. No interaction was observed between the seasonal group and ontogenetic stages in $\delta^{18}O_{statolith}$ values (Table 7). Individual ontogenetic trends showed that the $\delta^{18}O_{statolith}$ values in the spring group ranged between –2.87‰ and –1.61‰ and were relatively stable until the statolith edge (Fig. 9). In the summer group, the $\delta^{18}O_{statolith}$ values in the statolith core varied from –2.54‰ to –1.87‰; they decreased to the lowest levels, between –2.32‰ and –2.83‰, at the juvenile stage and then increased to the highest levels, between –1.06‰ and –0.65‰, in the statolith edge (Fig. 10). The $\delta^{18}O_{statolith}$ values in the autumn group showed a pattern similar to that of the summer group (Fig. 11), but the $\delta^{18}O_{statolith}$ values were higher at the juvenile–subadult stage (–2.23‰ to –0.97‰) and subadult–adult stage (–0.50‰ to –0.12‰) than those in the summer group.

The $\delta^{18}O_{statolith}$ values ranged from −3.26 to −0.20‰ with a mean of −1.88 ± 0.67‰ for the squid samples of Penghu Islands. Significant interactions were found between the seasonal group and ontogenetic stage of the $\delta^{18}O_{statolith}$ values, thus

pairwise Dunn's tests were used to compare the mean $\delta^{18}O_{statolith}$ values within groups (Table 7). Similar to the results of northern Taiwan, the $\delta^{18}O_{statolith}$ values were not significantly different among the seasonal groups (Kruskal–Wallis test, $H = 3.304$, $P = 0.192$, Fig. 12a), but ontogenetic differences were observed (Kruskal–Wallis test, $H = 30.059$, $P < 0.001$, Table 7, Fig. 12b). The value of $\delta^{18}O_{statolith}$ gradually increased from the juvenile stage, and the subadult-adult stage and adult stage showed significantly higher values of $\delta^{18}O_{statolith}$ than other stages (Dunn's tests, $Z = –2.981$, $P < 0.05$). A significant difference between the juvenile stage and the juvenile-subadult stage was observed (Dunn's tests, $Z = –3.318$, $P < 0.01$). Overall, the individual ontogenetic trends of squid samples of the Penghu Islands were slightly different from these of northern Taiwan. The $\delta^{18}O_{statolith}$ values in the spring group ranged between –2.69‰ and –1.40‰ and decreased between the embryonic-paralarval stage and the subadult-adult stage (Fig. 13). Besides three individuals (P171229002, P180117001 and P180304004) which showed $\delta^{18}O_{statolith}$ value patterns similar to that of the summer group of northern Taiwan, the $\delta^{18}O_{statolith}$ values in most individuals in the summer group showed a constantly increasing trend until the statolith edge, varying between –1.86‰ and –0.40‰ at the subadult-adult stage and adult stage (Fig. 14). Again, the $\delta^{18}O_{statolith}$ values in the autumn group increased from the juvenile stage to the highest levels, between –1.65‰ and –0.38‰, in the statolith edge, but the $\delta^{18}O_{statolith}$ value in the statolith core of only one individual (P180313002) was detected (Fig. 15).

3.2.2. Predicted occurrence area and movement pattern

Deduced and measured temperature of individuals in northern Taiwan samples were close and the linear regression showed a well correspondent (Fig. 16, $p < 0.001$). The slope was not significantly different from the line of 1:1 ($F_{1, 34} = 0.83$, $p = 0.37$) indicating that the deduced temperature could reasonably reflect the experienced temperature of *S. lessoniana*.

Figures 17–22 present the distribution of occurrence probability of seasonal groups at different depths of northern Taiwan and the Penghu Islands by comparing

deduced and measured temperatures while considering collection location, spawning site, and movement ability. The probability of occurrence results indicated that the three seasonal groups of *S. lessoniana* around Taiwan have diverse distributions and movement patterns.

For the squid samples of northern Taiwan, the individuals in the spring group had the highest possibility of hatching in neritic waters (approximate depth: 0–50 m) near the coast, extending from northeastern to eastern Taiwan and the Ryukyu Islands (Fig. 17). After hatching and reaching the paralarval stage, individuals were widely distributed in the inshore waters of northeastern Taiwan, possibly from the sea surface to an approximate depth of 50 m; these individuals may have subsequently migrated to relatively deeper waters near the coast of northeastern Taiwan or to the offshore waters of eastern Taiwan. In addition, the waters at a depth of 30-50 m along southern Taiwan were also potential hatchling grounds, and the hatched individuals moved northward as the growth proceeded. Finally, they mainly remained in the northeastern waters during the subadult–adult stages (Fig. 17). The summer group of northern Taiwan was most likely to hatch in the areas near northeastern Taiwan, extending southward to the Penghu Islands (Fig. 18). However, the predicted distribution at the juvenile stage covered a wide area, owing to constant seawater temperatures in summer. Similarly, a wide and deep living area (approximate depth: 100 m), including the inshore waters of northern Taiwan and the waters near the Ryukyu Islands (approximate depth: 100 m), was observed in the last two stages, and it differed from the pattern of the spring group. In the autumn group of northern Taiwan, the predicted hatching sites were similar to those in the summer group (Fig. 19). However, juvenile individuals might have been distributed in the southern waters (Fig. 19), but they were not detected in the waters, with the probability > 0.5, because the deduced temperature at this stage did not completely match the water temperature in the study area. The autumn group then spent their subadult and adult stage (approximately 3–4 months) in the inshore waters of northern Taiwan at depths between 0 and 100 m before capture.

For the squid samples of the Penghu Islands, the highest possibility for hatching in the spring group occurred in neritic waters (approximate depth: 0–50 m) around the both Penghu Islands waters and the waters off northeastern to eastern Taiwan (Fig. 20). At the juvenile stage, they then distributed mainly at depths of 30-50 m waters around the Penghu Islands, or in the inshore waters of northeastern extending to eastern Taiwan; these individuals may have subsequently stayed in relatively deeper waters in eastern Taiwan or between the Penghu Islands and southwestern Taiwan. Finally, they migrated and aggregated to Taiwan Straits during the subadult-adult stage, likely at a depth of 0 – 50 m in northern Penghu Islands and approximately 100 m depth in southern Penghu Islands (Fig. 20). In contrast, the individuals in the summer group of the Penghu Islands were most likely to hatch in the waters from the Penghu Islands to southern Taiwan (Fig. 21). They also exhibited a wide possibility of distribution at the juvenile stage because of the constant seawater temperature in summer. When reaching the subadult stage, the individuals of the summer group highly aggregated around the Penghu Islands, in comparison to the spring group. The depth distribution during subadult and adult stages was random between the sea surface to an approximate depth of 100 m. For the adult stage, the occurrence probability remained in the same regions as the subadult stage for spawning. The individuals in the autumn group of the Penghu Islands seemed to hatch in the waters of southern Taiwan; however, the prediction was based on $\delta^{18}O_{statolith}$ value in the statolith core area from a single squid sample. Similarly, a wide possible living area in the neritic waters (approximate depth: 0 – 50 m), including the inshore waters of northeastern Taiwan and southern Taiwan, was observed in the juvenile stage. The individuals at the juvenile-subadult stage consequently migrated to the Taiwan Strait, and spent their subadult-adult stage in the northern waters at depths between 0 and 50 m and about 50 km from the Penghu Islands, before capture.

3.2.3. The geographical overlap during sexual maturity

The occurrence probabilities in the subadult-adult stages of each seasonal group were multiplied to understand their geographical overlap between northern Taiwan and the Penghu Islands (Fig. 23). The geographical overlap for all seasonal groups mainly

presented in northern Taiwan Strait. The overlapping regions of the spring group were located in 118.8 – 120.4°E, 24.2 – 25.4°N. These of the summer and autumn groups were closer to Taiwan and in 120.0 – 121.2°E, 23.8 – 25.8°N. The overlapping rates among three seasonal groups were lower than 0.5. The highest rate (0.30) was in 0 – 30 m depth of coastal waters near China for the spring group, following (about 0.28) was in 0 – 30 m depth waters by western Taiwan for the summer group.

3.3. Discussion

Stable oxygen isotope ratios recorded in statoliths provide information regarding diverse movement patterns of *S. lessoniana*; differences in ontogenetic distributions were observed among seasonal groups, as well as between geographical stocks. Although the approach for investigating the movement of animals by using $\delta^{18}O$ values in biogenic carbonates has been widely applied in studies on fish (Trueman et al., 2012; Currey et al., 2014; Shiao et al., 2017; Darnaude and Hunter, 2018), thus far, studies have not adopted this method to determine the movement history of cephalopods. We demonstrated the potential of using this approach in studies on cephalopod ecology. Because of the significant effects of larval dispersal and demographic population connectivity on cephalopod resources (O'Dor, 1992; Boyle and Boletzky, 1996; Semmens et al., 2007), the results of the present study may improve the fishery management and conservation for the bigfin reef squid.

3.3.1. Variation in statolith $\delta^{18}O$ values in relation to experienced temperature

The variation in statolith $\delta^{18}O$ values among individuals has been observed in several squid species and is associated with differences in experienced temperature (Radtke, 1983; Landman et al., 2004; Trasviña-Carrillo et al., 2018). The general trend of statolith $\delta^{18}O$ values is to decrease with an increase in temperature; this trend follows the theoretical predictions and observations from other biogenic carbonates (Rexfort and Mutterlose, 2006; Trueman et al., 2012; Kitagawa et al., 2013; Linzmeier et al., 2016). However, assessing the reliability of using statolith $\delta^{18}O$ values to reconstruct experienced temperature in cephalopods is challenging because previous studies have analyzed $\delta^{18}O$ value from an entire statolith, which indicates the mean

experienced temperature throughout its lifespan. Thus, in our study, we evaluated the deduced temperature compared with the seawater temperature and temperature preference of *S. lessoniana* at different life stages.

The deduced temperature of the embryonic stage and an approximate 20-day paralarval stage from the statolith core ranged from 20.0°C to 28.5°C, regardless of seasonal or geographical groups. This finding was consistent with those of other studies that found that *S. lessoniana* hatches in a warm environment of approximately 20°C to 30°C (Segawa, 1987; Walsh et al., 2002; Ikeda et al., 2009). Each squid species has its optimum living temperature, which supports its growth and survival, particularly in its embryonic development and early life stages (Jackson and Choat, 1992; Forsythe et al., 2001). This suggests that the population of *S. lessoniana* around Taiwan shows a constant preference for this temperature at hatch.

Whether the squid samples were collected from which locations, the statolith $\delta^{18}O$ values among seasonal groups exhibited similar patterns of variation after the paralarval stage because of seawater temperature varying with the seasons. For example, the spring group experienced warmer (summer) temperatures at the juvenile and adult stages than at the hatching stage in spring. By contrast, the summer and autumn groups reached their juvenile and adult stages in autumn and winter, respectively, hence, they experienced lower temperatures in their juvenile and adult stages than in their hatching stage. The summer and autumn groups exhibited more positive $\delta^{18}O$ values than the spring group at the juvenile and adult stages because of lower temperatures. Thus, the ontogenetic variation in statolith $\delta^{18}O$ values in the spring group was less obvious than in the summer and autumn groups (Fig. 9-11 and Fig. 13-15). The statolith $\delta^{18}O$ values of *S. lessoniana* ontogenetic variation mirrored the seasonal temperature fluctuation off Taiwan waters, thus indicating the reliability of the prediction method used in the present study.

3.3.2. Prediction of ontogenetic movement and distribution

The seasonal and vertical migration of squid species has been described in the literatures (Bazzino et al., 2010; Argüelles et al., 2012; Yamaguchi et al., 2019); this behavior was also observed in our study. Interpreting time-series data in squids is generally more difficult than interpreting data obtained from bivalves (e.g., Nakashima et al., 2004; Owen et al., 2008; Nishida et al., 2015) because the squid species move freely, unlike bivalves. We converted the measured statolith $\delta^{18}O$ values to the deduced temperature and cross-matched them with the seasonal and depth changes in the seawater temperatures to estimate the probability of the geographical distribution of *S. lessoniana* between two collection sites (northern Taiwan and the Penghu Islands), through using a procedure derived from a widely used method to study fish migration (involving the use of otolith $\delta^{18}O$ values; Thorrold et al., 1997; Weidel et al., 2007; Shiao et al., 2014). In our case, the movement patterns of *S. lessoniana* in ontogenetic stages exhibited diversity among the seasonal and geographical groups (Figs. 17–22). These findings are comparable to the known ecology of *S. lessoniana*, including spawning (Segawa, 1987), migration (Ueta and Jo, 1990; Kanamaru et al., 2007a) and depth distribution (Roper et al., 1984; Tomano et al., 2016). Therefore, we first explored the movement patterns and distribution of *S. lessoniana* in Taiwan, as well as the roles of environmental factors in the processes, and discussed the distribution ranges between northern Taiwan and the Penghu Islands to clarify their population connectivity and dynamics.

3.3.2.1. The squid samples of northern Taiwan

According to statolith $\delta^{18}O$ values, most probably the individuals of the spring and summer groups hatched near the coasts of northeastern Taiwan, with an occurrence probability of 1; these findings support empirical evidence that the waters near the coast of northeastern Taiwan are one of main spawning grounds for *S. lessoniana* (Chen et al., 2015; Ching et al., 2017). The dominant topography in northern Taiwan is that of an eroded coastline with complicated topographical features and structures (Song et al., 1997), forming macroalgae-rich and coral-rich environments for spawning. In addition, the quantity of nutrients supplied by the year-round upwelling of the Kuroshio Current off northeastern Taiwan supports high

primary production and sustains sequential consumers in the waters (Liu et al., 1992; Chen, 1997; Gong et al., 2003). Therefore, this biomass could be a crucial factor sustaining the abundance of *S. lessoniana* near Taiwan (e.g., Otero et al., 2008; Rodhouse et al., 2014). However, the individuals of the autumn group had a high probability (> 0.8) of hatching in the waters of southern and southwestern Taiwan (i.e., the Penghu Islands). The paralarvae were transported northward by the Kuroshio Current or the South China Warm Current into the Taiwan Strait during September and October (Tang et al., 2000; Jan et al., 2002, 2006). Although the results suggest that waters at a depth of 100 m near the coast of southern Taiwan are also potential hatching grounds, adult females are unlikely to have laid eggs at a depth of down to 100 m because the environment is unsuitable for planktonic paralarvae and no egg capsules have been observed on the seabed at the aforementioned depth.

Distribution of juvenile individuals appeared to be widespread around Taiwan, both horizontally and vertically. This distribution pattern has two possible explanations. First, the juvenile squids were passively shifted by ocean currents, thus reflecting the seawater temperatures of a larger region. Second, the consistent seawater temperatures around Taiwan in summer and autumn reduced the precision of distribution prediction. In particular, the estimated probabilities of juvenile distribution in the autumn group were all less than 50%. Compared with the juvenile stage, the subadult–adult stages showed a narrower area of predicted distribution. In the spring group, the subadult individuals remained at a depth of approximately 50 m near the coast of northeastern Taiwan or at a depth of approximately 100 m in the inshore waters of eastern Taiwan. Subsequently, adult individuals migrated to the northeast coasts for mating and spawning. To our knowledge, larger individuals are rarely captured in the eastern waters, which suggests that the eastern waters are not a principal habitat for *S. lessoniana* individuals in the spring group. Nevertheless, the occurrence of *S. lessoniana* in the eastern water needs to be understood through additional surveys using systematic fishery records. By contrast, individuals in the juvenile–subadult stage in the summer group were mostly found in the areas between the coastal waters of China to northeastern Taiwan; furthermore, individuals in this

stage in the autumn group might remain in the waters in northeastern Taiwan or around the Penghu Islands. Both the summer and autumn groups used the northern waters of Taiwan as their main habitat during the adult stage in winter. In addition, adult individuals in the autumn group appeared to move to further offshore waters (about 100 km). During winter months, drastic reductions in temperature occur in northern Taiwan primarily during strong northeasterly monsoon and cold surge events (Chen and Huang, 1999; Chen et al., 2002). In such a turbulent state, the individuals move offshore for overwintering and return to inshore areas for feeding and spawning when the environment becomes relatively stable. This explanation is consistent with the findings of Ueta and Jo (1990), who studied the migration of *S. lessoniana* subadult–adult individuals around Tokushima Prefecture.

3.3.2.2. The squid samples of the Penghu Islands

The waters at depth of 0 – 50 m around the Penghu Islands were the probably hatching ground for the individuals of both spring and summer groups, but the spring group exhibited another potential hatching ground near the coast of northeastern Taiwan (Fig. 20-22). It is commonly believed that *S. lessoniana* aggregated near the coastal waters for spawning (Segawa, 1987; Jereb and Roper, 2005), but the empirical evidence for spawning activity around the Penghu Islands is rather limited than in northeastern Taiwan. These findings therefore further supported that another population of *S. lessoniana* exists in the waters around the Penghu Islands, which have been explored by using life-history traits and statolith elemental signatures (Ching et al., 2017). The Penghu Islands is located on the continental shelf between Taiwan and southeast Mainland China, and has complex and diverse topography (Hong et al., 2011). Hundreds of shallow sandbanks of the Taiwan Bank, with an average depth of 20 m, lie in the southwest of the Penghu Islands. The Penghu Channel, located in the east of the Penghu Islands, is 100 – 200 m depth in south-north direction and the shallower Zhangyun Ridge is to the north of the Penghu Channel. Seasonal variations of wind directions have endured complex coastal current and circulation systems, topographically inducing upwelling to bring nutrient-enriched water resulting in higher primary production, particularly in summer (Hont

et al., 2011; Tseng et al., 2020). These oceanographic features constitute a suitable hatchery for this species, making the waters around the Penghu Islands one of the main habitats in Taiwan. On the other hand, the hatchery of the spring group near the coasts of northeastern Taiwan is related to the connection between the two geographical stocks (explained in the following sections). Although the individual of the autumn group exhibited potential hatching sources from southern Taiwan near the Penghu Channel, this spawning depth (approximate 100 m) is not considered a favorite by the pelagic squid species, especially represented from only one individual.

The squid samples of the Penghu Islands among three seasonal groups were widely distributed in the waters at depths of 0 – 50 m around Taiwan. However, compared with the individuals of northeast Taiwan, the distribution range of the individuals of the Penghu Islands waters may reflect the seasonal variations of the wind directions over the Taiwan Strait (Jen et al., 2006; Hong et al., 2011). For example, weaker southwesterly winds have predominated in summer, and two topographically induced upwelling areas occur around the Penghu Islands and near the Taiwan Bank, respectively (Hu et al., 2003). The juveniles of spring and summer groups aggregated to the two upwelling areas where abundant nutrients are (Fig. 20-21). On the other hand, the winds have switched to stronger and northeast direction and resulted in the China Coastal Water, with low temperature and low salinity, southwards into northern waters of the Penghu Islands. The juveniles of the autumn group thus shifted through the winter monsoon and distributed in southern waters of the Penghu Islands (Fig. 22). At the juvenile-subadult stage, the individuals of the spring group stayed at deeper waters (approximate: 50 – 100 m) in the Penghu Channel or near the coasts of eastern Taiwan (Fig. 20). In contrast, the subadult individuals of the other two groups were distributed in the Taiwan Strait; the summer group was at a depth of 100 m near the Penghu Channel (Fig. 21) and the autumn group was in neritic waters (Fig. 22). Finally, isothermal line spacing around the Penghu Islands might affect the predicted distribution differences of adult individuals among seasonal groups. The spring group took northern regions of the Penghu Islands or deeper waters in the Penghu Channel as the main habitat during their adult stage

and the two areas were topographically inferred as high-nutrient upwelling areas (Hong et al., 2011; Huang et al., 2018). However, the statolith edges of these individuals have reflected main water temperatures from summer to mid-autumn, when the main water mass is warm China Coastal Water (Jan et al., 2010; Huang et al., 2018), affecting the precision of distribution prediction. At the subadult-adult stage, the autumn group showed a shallower distribution range, corresponding to the 20°C isotherm with vertical mixing of water masses, which has been demonstrated to enhance phytoplankton growth and affect the fishing ground of other fish species (i.e. *Mugil cephalus*, Lan et al., 2014).

Due to the technical limitation of the micromill method, it is difficult to analyze more than four drilling paths from one individual except for the larger squid samples of the summer group. The additional fifth path provided an opportunity for estimating the movement patterns of *S. lessoniana* after maturity. Interestingly, these individuals of the summer group exhibited a limited moving distance from the subadult stage to the adult stage, with at most 2 grids in the present study (about 70 – 80 km) (Fig. 21). These individuals stayed and spent their 40 – 50 % (about 80 – 110 days) of their lifetime near the waters of the Penghu Islands. The short life cycle of loliginid squids commonly exhibit a wide variety of reproductive patterns with multiple times of mating and spawning during a spawning season (Iwata et al., 2005; Wade et al., 2005). In addition, male cephalopods usually mature earlier than females, so males may have a longer reproductive period (Rodhouse and Hatfield, 1990; Chen et al, 2015). However, the length of spawning activities of *S. lessoniana* remains unknown. Our results with statolith $\delta^{18}O$ values suggested that *S. lessoniana* hatched in summer may migrate aggregately near the Penghu Islands during autumn and winter (Oct. – Feb.) for spawning. A similar species, *Sepioteuthis australis*, distributed in southwestern coast of Australia and New Zealand, was demonstrated to spawn over months and move over one hundred kilometers but do not leave a spawning ground (Pecl et al., 2006). It is critical to know how long it takes for a species to use a habitat to reside and reproduce so that we can assess the effectiveness of fishery management (e.g. protected area and closed season), and estimate the amount of resources in the

region. Long-term monitoring and more detailed temporal resolution of movement pattern will be helpful to understand the roles of the waters near the Penghu Islands for *S. lessoniana*.

3.3.2.3. The geographic overlap between northern Taiwan and the Penghu Islands

The immaturity individuals of three seasonal groups in the present study exhibited considerable habitat overlap and a possible migration route from the Penghu Islands to northeastern Taiwan. In addition, the results showed that the northern waters of the Taiwan Strait may overlap its habitat for mature individuals from northern Taiwan and the Penghu Islands, suggesting a possibe gene exchange with the individuals in the northern waters of the Taiwan Strait. The female could store the sperm in their sperm storage receptacles for weeks (Wada and Kobayashi, 1995; Wada et al., 2005) until they move to deposit their eggs in inshore shallower waters, consequently improving the genetic exchange between the geographical stocks. In general, loliginid squids spawn throughout the year and consequently exhibit multicohort formations along with highly diverse dispersion patterns; hence, high levels of genetic diversity are achieved in the populations of these cephalopods (O'Dor, 1998). A study reported that the elemental signatures in the entire statolith exhibited less variation between *S. lessoniana* samples from northern Taiwan and the Penghu Islands for the same season (Ching et al., 2017). This finding suggests a high level of population connectivity in *S. lessoniana* in Taiwan. In recent years, the coexistence of three cryptic lineages of *S. lessoniana* has been reported in the Indo-Pacific Ocean (Cheng et al., 2014; Tomano et al., 2016). These cryptic lineages of *S. lessoniana* exhibit similar morphology but are genetically distinct (Akasaki et al., 2006; Hsiao et al., 2016; Shen et al., 2016). Although the extent of cryptic diversity within the *S. lessoniana* species complex in Taiwan remains unclear, a single cryptic lineage may be predominant in northern Taiwan and the Penghu Islands, based on the migration pattern prediction. Additional studies with larger areas of geographic sampling and using a combination of molecular methods are needed to provide more

knowledge regarding the population structure of the bigfin reef squid over its distribution range.

3.3.3. Method improvement and applications in future

As the first study to determine the ontogenetic movement of squid by using statolith $\delta^{18}O$ values, this study provided information on the life history of *S. lessoniana*, although the analytical technique can be improved considerably in the future. First, the $\delta^{18}O$ values in the juvenile statoliths of the autumn group of northern Taiwan suggested high experienced temperatures (approximately 25°C –29°C), and this does not satisfactorily accord with the observed water temperature range from the sea surface to a depth of 100 m depth in autumn. The mechanisms of isotopic fractionation in statoliths (such as the results of fish otolith by Thorrold et al., 1997; Høie et al., 2004a) and other potential sources of variability (e.g., Høie et al., 2004b; Darnaude and Hunter, 2018; Linzmeier, 2019) should be carefully considered in further research. Second, the seawater $\delta^{18}O$ values vary by <1‰ across the surface in the present study area and by approximately 1‰ with depth (LeGrande and Schmidt, 2006), slightly biasing the prediction of experienced temperature. Salinity was used to predict seawater $\delta^{18}O$ values, based on the equation established from the waters in Taiwan Strait (Chang, 2000). The development of location-specific relationships between salinity and seawater $\delta^{18}O$ values can minimize the bias of reconstructed temperature. Third, reducing the minimum analytical powder amount from statolith can increase the temporal sampling resolution and enhance the precision of reconstructed temperature (Leder et al., 1996; Høie et al., 2004b). As reported by Sakamoto et al. (2019) in their otolith study, the weight of drilling powder can be as low as 0.3–11.4 μg, representing a temporal resolution of 10–30 days, which is considerably higher than that of this study (>40 μg and approximately 30–60 days). A statolith analysis with higher temporal resolution can significantly benefit the studies on stock discrimination and individual migration. Fourth, defining minimum and maximum probabilities that can indicate the existence of *S. lessoniana* populations requires additional statistical support. In addition, the size of the spatial grid can be

reduced to match the movement behavior of *S. lessoniana* for a higher precision of habitat determination.

Seawater temperature directly and strongly affects cephalopod ecology and fisheries (Jackson and Moltschaniwskyj, 2002; Forsythe, 2004). Statolith $\delta^{18}O$ is a crucial parameter that provides evidence of general patterns of distributional extent and movement. Statoliths, which are involved in orientation and balance, are found in all cephalopod species; hence, they can be widely used for ecological research on cephalopods (Clarke, 1978; Arkhipkin 2005). For example, the predicted geographical distributions based on statolith $\delta^{18}O$ signatures are comparable to the estimated stock boundaries determined using fishery data or tagging methods. Precise geographic boundary and habitat use (e.g., spawning ground) allow managers to implement suitable management measures to conserve targeted species (Gislason et al., 2000; Hobday et al., 2010). In recent years, in response to variations in the behavior of oceans and difficulties in managing resources, scientists have highlighted the importance of technological improvements through use of finer spatial and temporal scales for near real-time animal tracking (Maxwell et al., 2015; Dunn et al., 2016). Combining the deduced temperatures of the individuals over ontogenetic stages, we have described continuous movement patterns of *S. lessoniana* lifespan. This study thus provided the geographical variations of distribution ranges to supply more information regarding the population connectivity, and to estimate the genetic flow, which may be particularly difficult if complex cryptic lineages of *S. lessoniana* exist in the same region. The intra- and interannual movement patterns also support the decisions pertaining to the establishment of fishing grounds, forecasting of catches, and dynamic fishery management for cephalopods (e.g., Yamaguchi et al., 2019). However, the extent of geographic distribution resolution using statolith $\delta^{18}O$ may be species specific. Our results showed that accurately predicting residence waters during the periods when variations in water temperature of the region are not obvious (from summer to early autumn in Taiwan) is relatively difficult. Thus, statolith $\delta^{18}O$ is unlikely to serve as the main indicator of distribution for tropical cephalopod species. Species with a large diel vertical migration (e.g., Young, 1978; Hunt and Seibel, 2000)

also probably biases the prediction of experienced temperature, thus increasing the risk of misinterpretation when this method is applied to a species. Establishing a temperature-dependent relationship of $\delta^{18}O$ for specific cephalopod species is also necessary for improving the approach in the future.

4.

The ecological inferences using stable carbon and nitrogen isotopes on spatial preferences of *S. lessoniana* in Taiwan

4.1. Materials and Methods

4.1.1. Squid collection and measurement

Seventy-seven *S. lessoniana* individuals were collected by jigging from the coastal and inshore waters of northern Taiwan between November 2017 and December 2018. As this jigging is a directed and squid-specific fishing method, the catch reflected a main size range of the squid, including the recruitment size in northern Taiwan. To obtain statoliths for the carbon isotopic analysis over complete ontogenetic stages, twenty-two adult *S. lessoniana* of northern Taiwan and twenty-one adult individuals from the Penghu islands waters between November 2017 and March 2018 were collected for statolith isotopic analysis. All squid samples were frozen immediately then were transported to the laboratory for the examination.

The mantle length (ML; in mm) and body weight (BW; in g) of each individual was measured. Sexual maturity was determined following given scales for loliginid squid by Boyle and Rodhouse (2005): Stage I and II (immature); III (maturing); IV (mature). Approximate 1 cm × 0.5 cm of muscle tissues were obtained from the mantle of squid individuals. Muscle tissues were rinsed with distilled water, removed the skins, dried at 40 °C for 48 hours, and ground into a fine powder by using a mortar and pestle. Dried muscle powder at about 0.70 – 0.75 mg of each sample was packed into a tin capsule for subsequent analysis. As long turnover rate tissue, the stable isotopes of muscle commonly reflect the ecological records in the recent weeks to months duration (Hobson, 1999). Based on their sampling month, the individuals therefore were categorized into four groups, namely spring (March–May), summer (June–August), autumn (September–November), and winter (December–February) sampling groups.

For twenty-two individuals from northern Taiwan and twenty-one from the Penghu Islands, statoliths of each squid were extracted, cleaned ultrasonically using 70% hydrogen peroxide, rinsed, oven-dried, and embedded in Epofix resin (Struers, Denmark). The left statolith then was ground and polished along the posterior side by using a metallographic grinding and polishing machine (P20FR-HA; Top Tech

Machines co. Ltd., Taiwan) to a distance about 50–100 μm above the core, ensuring more than 40 μg milling powder was available for carbon isotopic analysis. The growth increment (formed daily, Jackson, 1990) at the lateral dome region of statolith was examined from the photographs recorded under a compound microscope (400×, DM-2500, Leica Microsystems GmbH, Germany) by using a digital camera (DFC-450, Leica Microsystems [Switzerland] Lt., Switzerland) to estimate age. The daily age of the individual for statolith carbon isotopic analysis was an average value of two growth increment counts. Another count had to be made when the difference between two counts was >5% to reduce measurement error (Arkhipkin and Shcherbich, 2012). The hatching date of each individual was back-calculated from the deduced age (in days) and the date of collection. Each individual was categorized into the nearest seasonal group according to its hatching month, namely spring (March–May), summer (June–August) and autumn (September–November) hatching groups.

4.1.2. Isotopic analysis

The definition of life history stage and detailed measurement procedure for $\delta^{13}C$ value of statolith ($\delta^{13}C_{statolith}$) is described in above **Section 3.1.2.**. Each drilling path was recorded to determine the life history stage corresponding to covered daily growth.

The bulk $\delta^{13}C$ and $\delta^{15}N$ values of muscle tissues ($\delta^{13}C_{muscle}$ and $\delta^{15}N_{muscle}$) were measured by an automatic Elemental Analyzer (Flash 2000 EA, Thermo Fisher Scientific, Germany) connected to an isotope ratio mass spectrometer (Finnigan MAT 253, Thermo Fisher Scientific, Germany). The standards, namely urea, protein and carbon and nitrogen isotopes in L-glutamic acid (USGS40), were analyzed in groups of seven samples during the measurement process. The reproducibility of the Finnigan MAT 253 is higher than ± 0.06‰ (one standard deviation [s.d.]) and ± 0.15‰ for $\delta^{13}C_{muscle}$ and $\delta^{15}N_{muscle}$ values, respectively.

4.1.3. Data analysis

Metabolic rate can be indexed by the width of daily growth increment of statolith, water temperature, and body mass. Therefore, we explored the effect of these indexes on $\delta^{13}C_{statolith}$ values at geographical (northern Taiwan; the Penghu Islands) and ontogenetic (early stages: embryonic, paralarval, early juvenile; later stages: stage later juvenile, subadult, adult) levels by sample and multiple regressions. The width of daily growth increments was averaged at each life history stage. The deduced temperatures were described in above **Section 3.1.2.**. The mantle length at each life history stage was back-calculated using the logistic growth function in Taiwan (Chen et al., 2015):

$$ML = \frac{a}{(1 + Exp(-b(t - c)}$$

where *a* is 426.55, *b* is 0.02, and *c* is 141.05 for male individuals; *a* is 341.05, *b* is 0.03, and *c* is 125.46 for females. Then the estimated BW were derived using the relationships between ML and BW (Chen et al., 2015):

$$BW = aML^b$$

where *a* is 0.0003; *b* is 2.65 and 2.70 for male and female, respectively. The intermediate dates of each life history stage were used to represent the median ML at each life history stage, so that the estimated BW could correspond to the $\delta^{13}C_{statolith}$ values at these stages. To identify the seasonal and geographical effects on $\delta^{13}C_{statolith}$ value, we eliminated the potential effects of temperature on the $\delta^{13}C_{statolith}$ value through the linear regression of the $\delta^{13}C_{statolith}$ values on deduced temperature. A nonparametric Kruskal–Wallis test was then used to examine the differences in the residual values among seasonal sampling groups and collection sites.

The proportion of metabolically derived carbon (M values) was calculated following a two-component mixing model (Schwarcz et al., 1998; Solomon et al., 2006; Chung et al., 2019a):

$$\delta^{13}C = M * \delta^{13}C_{diet} + (1 - M) * \delta^{13}C_{DIC} + \varepsilon$$

where $\delta^{13}C_{diet}$ and $\delta^{13}C_{DIC}$ values are the $\delta^{13}C$ values of the dietary carbon and dissolved inorganic carbon of seawater, respectively, and the term ε is the total net isotopic fractionation from the sources to biogenic carbonate. In present study, $\delta^{13}C_{diet}$

value was $\delta^{13}C_{muscle}$ value minus 1.6 of trophic enrichment based on *Dosidicus gigas* (Ruiz-Cooley et al., 2006); ε was set as 2.7 for aragonite carbonates following the result from inorganic precipitation of carbonate (Romanek et al., 1992). The $\delta^{13}C_{DIC}$ value was acquired from a modelling prediction (Kroopnick, 1985):

$$\delta^{13}C_{DIC} = 0.0074 \times \mathrm{AOU} + 1.54$$

where AOU is apparent oxygen utilisation, and we set AOU values as annual mean values with a spatial resolution of 1° × 1° from the sea surface to 200 m depth around Taiwan (117.5 – 124.5°E, 20.5 – 24.5°N), which were obtained from National Oceanographic Data Center of NCEI website (https://www.nodc.noaa.gov/cgi-bin/OC5/woa18/woa18oxnu.pl?parameter=A, Garcia et al., 2009). This M value represents the proportion of carbon metabolically derived from the diet.

Finally, to assess the distributions of $\delta^{13}C_{muscle}$ and $\delta^{15}N_{muscle}$ values between ontogenetic stages and sampling seasons, we determined the isotopic niche overlap using the the standard ellipses method of the SIBER (Stable Isotope Bayesian Ellipses in R) package, version 2.1.5 in R version 3.4.2 (R Development Core Team, Vienna, Austria) (Jackson et al., 2011).

4.2. Results

The summarized sample information is shown in Table 8. The mean ML and BW were 217.2 ± 75.0 mm and 637.7 ± 471.8 g for the individuals with muscle isotopic analysis, respectively. The mean $\delta^{13}C_{muscle}$ and $\delta^{15}N_{muscle}$ values were -16.88 ± 0.49‰ and 12.73 ± 0.72‰, and the mean C:N ratio in muscle was 3.49 ± 0.21. In the statolith carbon isotopic analysis, the mean ML and BW were 276.6 ± 43.7 mm and 998.5 ± 382.9 g for individuals from northern Taiwan and 293.1 ± 54.9 mm and 1298.3 ± 626.6 g for individual from the Penghu Islands. The $\delta^{13}C_{statolith}$ values were -9.37 ± 0.71‰ and -8.86 ± 1.30‰ for northern Taiwan and the Penghu Islands individuals, respectively.

Table 9 shows the width of growth increment, estimated ML, and estimated BW of *S. lessoniana* individuals for statolith isotopic analysis in early and later life history

stages from two collection sites. Consequently, the explanatory of growth increment width, deduced temperature, estimated body weight, as alternative metabolic indexes, on $\delta^{13}C_{statolith}$ values at geographical and ontogenetic levels were examined (Table 10). These metabolic indexes have little effect (< 25%) on all life history stages of individuals from both collection sites, and no significant effect ($P = 0.416$) was found on the early life history stage from northern Taiwan. The highest R^2 of 57% was found in the later life history stage of individuals from northern Taiwan. In addition, the explanatory levels of alternative metabolic indexes were generally better in later life history stage than in the early life history stage. The simple linear regression showed that deduced temperature significantly affected the $\delta^{13}C_{statolith}$ value in all life history stages of individuals from the Penghu Islands ($F = 8.51$, $P < 0.01$) (Fig. 24), but not on individuals from northern Taiwan ($F = 3.49$, $P = 0.66$). For individuals from northern Taiwan, deduced temperature ($F = 46.29$, $P < 0.001$) had a significant effect on $\delta^{13}C_{statolith}$ value in the later life history stages (Fig. 25). For individuals from the Penghu Islands, deduced temperature showed significant effect on $\delta^{13}C_{statolith}$ value in both early life history stage ($F = 5.12$, $P < 0.05$) and later life history stage ($F = 12.45$, $P < 0.01$) (Fig. 26). However, estimated body weight showed a positive effect on $\delta^{13}C_{statolith}$ value in the later life history stage of individuals from northern Taiwan ($F = 12.92$, $P < 0.01$) but a negative effect in the early life history stage from the Penghu Islands ($F = 4.22$, $P < 0.05$) (Fig. 25, 26).

The residuals of $\delta^{13}C_{statolith}$ values in the linear regression on deduced temperatures showed significant seasonal variations between two collection sites (Fig. 27). In northern Taiwan, the residuals among three seasonal hatchling groups decreased in the first three life history stages but those of the autumn hatchling group significantly increased at subadult-adult stage ($H = 15.12$, $P < 0.01$). The residuals of the autumn hatching group were significantly higher than that of the spring hatching group (Dunn's tests, $Z = -14.88$, $P < 0.05$). On the other hand, the residuals among three seasonal hatchling groups of the Penghu Islands generally decreased over life history stages. The residuals of each seasonal hatching group had no significant difference between life history stages. The residuals of the autumn hatchling group

were also significantly higher than those of the others (Dunn's tests, $Z < -19.28$, $P < 0.01$). At the geographical level, the residual patterns between two autumn hatching groups had significant differences ($H = 3.95$, $P < 0.05$). Fig. 28 shows the differences in residuals at each life history stage between northern Taiwan and the Penghu Islands. There were little differences in residuals for the spring and summer hatching group between two collection sites except for the subadult-adult stage of the summer hatching group. Conversely, the residuals for the autumn group in the Penghu Islands were larger than these in northern Taiwan over all life history stages.

There was no relationship between $\delta^{13}C_{muscle}$ and $\delta^{13}C_{statolith}$ values (Fig. 29). Based on the AOU acquired in the present study area, the $\delta^{13}C_{DIC}$ values were ranged from -0.22 to 1.67. Therefore, the calculated proportion of metabolically derived carbon (M values) were averaged as 0.66 ± 0.04, ranging between 0.56 to 0.75.

Fig. 30 showed the relationship between $\log_{10}$(BW) and $\delta^{13}C_{muscle}$ values of individuals (n = 77) from northern Taiwan. No significant effect of body weight was found on $\delta^{13}C$ values of muscle tissues. Given the different patterns observed when comparing the $\delta^{13}C_{statolith}$ residuals between life history stages, we next analyzed the variations of $\delta^{13}C_{muscle}$ and $\delta^{15}N_{muscle}$ values at the ontogenetic level. Over sampling duration (Nov. 2017－Dec. 2018), the $\delta^{13}C_{muscle}$ values of individuals from northern Taiwan did not exhibit obvious trends, and the $\delta^{15}N_{muscle}$ values generally increased with months and maturity stages (Fig. 31, 32). The $\delta^{15}N_{muscle}$ values of maturing and mature individuals were significantly higher than those of immature individuals ($H = 37.58$, $P < 0.001$).

4.3. Discussion

The application of stable isotope analysis of carbon and nitrogen in ecological inferences is continually increasing and has provided insight into the dietary and trophic status, habitat use, and movements of a variety of species (Hobson, 1999; Trasviña-Carrillo et al., 2018; Simpson et al., 2019; Kato et al., 2020; Kawazu et al., 2020). Present study investigated the potential methods for inferring the spatial

preferences of *S. lessoniana* using the variations of statolith $\delta^{13}C$ value and muscle $\delta^{13}C$ and $\delta^{15}N$ values. The results demonstrated that the alternative metabolic indexes significantly affected the statolith $\delta^{13}C$ value, and there were ontogenetic and seasonal differences in $\delta^{13}C$ and $\delta^{15}N$ values. Combining previous estimation of movement pattern and distribution using statolith $\delta^{18}O$ values, stable carbon and nitrogen isotopic composition provided a supplementary and valuable test to indicate the habitat and movement differences in different life history stages and seasonal hatching groups.

Statolith growth increment width, deduced temperature and estimated body weight exhibited partial impacts on statolith $\delta^{13}C$ value except for the early life history stage of northern Taiwan (Table 10). The stable carbon isotopic composition varies because of two sources: (1) DIC in environmental water incorporated through the gill or intestine; (2) metabolic carbon from diet and respiration (Kalish, 1991; McConnaughey et al., 1997; Chung et al., 2019a, 2019b). To our knowledge, the evaluation of metabolic proxy using $\delta^{13}C$ value in biogenetic carbonate in cephalopods has not been examined yet. The statolith increment width has demonstrated to reflect the somatic growth rate of squid (Jackson and Moltschaniwskyj, 2001); the temperature and body mass exhibit positive relationships with resting oxygen consumption (Clarke and Johnston, 1999; Gillooly et al., 2001). These alternative metabolic indexes therefore can be used to test if the statolith $\delta^{13}C$ value is a metabolic proxy for cephalopods, such as that in teleost fishes. The results in present study supported this expectation, but might vary with environmental and physiological changes in different life history stages. Cephalopods are poikilothermic animals, and temperature is the most influential factor in altering their life cycle, including egg development, feeding rate and lifespan (Forsythe et al., 2001, 2002; Vidal et al., 2002). Temperature showed a negative effect on statolith $\delta^{13}C$ value, which is consistent with the results of the temperature-controlled studies on fish otoliths (Martino et al., 2019; 2020). However, stronger temperature effects were found in the later life history stage (subadult-adult) (Fig. 25, 26). This is likely because of the narrower temperature range for hatching (20 – 30°C, Segawa, 1987; Walsh et al., 2002; Ikeda et al., 2009) reducing the contribution of ambient

temperature on metabolism, which influenced the variation of statolith $\delta^{13}C$ values in early life history stage (embryonic-juvenile). Estimated body weight contributed a portion effect on statolith $\delta^{13}C$ values, although not consistent between two collection sites (i.e. positive and negative). At the species level, smaller body size has a higher mass specific metabolic rate. We observed that statolith $\delta^{13}C$ values of northern Taiwan individuals increased with estimated body weight, suggesting lower metabolic rate of larger individual, while Penghu Islands individuals had an opposite trend in their early life history stage. The hatchlings of loliginid squids are planktonic, and they switch to active prey capture and highly mobile with the onset of the development process (Boyle and Rodhouse, 2005). The locomotion ability at each development stage may lead different relationships between statolith carbon isotopes and metabolism. In contrast, the statolith growth increment width had a relatively slight effect on the $\delta^{13}C$ values. Although statolith $\delta^{13}C$ values can be a potential indicator of metabolic rate to assess the movement patterns such as swimming efficiency and feeding activities (Sherwood and Rose, 2003), we emphasize that the stable carbon isotopes are altered by the collective effect among multiple factors, and cephalopods have the capability to adjust their cellular and mitochondrial energetic consumption during short- or long-term changes of temperature and environmental conditions (Oellermann et al., 2012). These must be taken into account when using statolith carbon isotopes to make ecological inferences to avoid misinterpretations.

The observed differences in residuals of $\delta^{13}C_{statolith}$ value profiles between seasonal hatching groups and collection sites of *S. lessoniana* indicated the different environmental conditions they experienced (Fig. 27). This result supports our discussion in **section 3.3.**. For example, the autumn hatching group of northern Taiwan individuals had significantly lower residual values at the juvenile-subadult stage, likely associated with higher energetic consumption when migrating between coastal and offshore waters in winter. The residuals of the autumn hatching groups of both two collection sites were relatively higher than that in the other hatching groups, suggesting slower growth rates (corresponding to lower total metabolic rate) were maintained during lifetime for autumn hatching groups. In winter, strong and cold

northeasterly monsoons covers the waters off northern Taiwan and the Taiwan Strait. Searching and staying in suitable habitats may be driven by strategies to avoid drastic reductions in temperature and turbulent environment, but habitat depth and diversity is linked to metabolic energetic demands, thus inhibiting their growth.

Interestingly, the trends of differences in residuals between two collection sites were relatively consistent for the spring and summer hatching groups, but distinct for the autumn hatching group (Fig. 28). Consistent residuals of the spring hatching group and different residuals at only the adult stage of summer hatching group suggested that these individuals from two collection sites might be exposed to environments with similar properties before the subadult stage. By using statolith $\delta^{18}O$ values, the predicted distributions of spring hatching groups from two collection sites did exhibit large overlap (Fig. 17 and 20). Large habitat overlap can be also observed in the two summer hatching groups, but after the subadult stage, they separately distributed in coastal waters near northern Taiwan and the Penghu Islands (Fig. 18 and 21). Although technological limitations had reduced the prediction accuracy for the autumn hatching group distribution in the early life history stage, the previous results by statolith $\delta^{18}O$ values indicated the habitat differences after the subadult stage (Fig. 19 and 22). As per descriptions in **section 3.3.2.3.**, a possible migration route between northeastern Taiwan and the Penghu Islands and a high level of genetic flow in *S. lessoniana* were suggested. Combining variations of statolith oxygen and carbon isotopic compositions, we therefore conclude that: In summer, due to the warm and consistent oceanic environment between northern Taiwan and the Penghu Islands, the individuals hatched in spring and summer have a higher level of population connectivity within two locations; when winter begins, the cold and turbulent environmental condition separates the two geographical stocks, and thus the levels of gene flow for the individuals hatched in autumn may decrease. On the other hand, the spatial distribution of $\delta^{13}C_{DIC}$ value could affect the variations of statolith $\delta^{13}C$ value in present study (Schwarcz et al., 1998). However, because $\delta^{13}C_{DIC}$ value varies in a narrow range (about 0.5 – 1.0‰ around Taiwan according to Sheu et al., 1996; Lin et

al., 1999), the variation of statolith $\delta^{13}C$ value affected by $\delta^{13}C_{DIC}$ value should be less than 1.0‰.

Compared with statolith $\delta^{13}C$ value, we cannot observe a relationship between log-transformed body weight and muscle $\delta^{13}C$ value (Fig. 30). This variation in $\delta^{13}C$ value between statolith and muscle may be explained by differences in isotopic incorporation and conversion because of dietary influences and tissue metabolic turnover. Cephalopods are extremely sensitive to starvation over their lifetime and must feed on sufficient food to fuel their metabolism and growth (Vadal et al., 2002, 2006). The muscle $\delta^{13}C$ value therefore is continuously changing due to variable diet and fast metabolic turnover. For example, the carbon profiles in muscle fatty acid of *Lolliguncula brevis* squids tended to reflect that of their prey in 10 days of feeding (Stowasser et al., 2006). In present study, the carbon isotopic compositions in muscles might be driven by the synthesis of new tissues, which significantly reflected recent feeding before capture, rather than a direct outcome of metabolism. With this assumption, the absence of a metabolic-related signal in muscle might represent more feeding history among northern Taiwan individuals. This also explains why there was no correlation in $\delta^{13}C$ value between statolith and muscle in the present study (Fig. 29). In teleost fishes, the otolith $\delta^{13}C$ value was expected to reflect the same total change in muscle $\delta^{13}C$ value (Elsdon et al., 2010). However, to our best knowledge, this phenomenon has not been examined in cephalopods yet. Additional experimental evaluations are needed to provide more information regarding stable isotopic fractionation among diet, soft tissues and statolith of *S. lessoniana*.

Given that the proportion of metabolically derived carbon (M value), which increases with an increase of metabolism, in cephalopod statolith is unclear, we preliminarily estimated the M values of adult squids (n = 19) by using carbon isotopes in the statolith edge and muscle with known parameters. The determination of M value can help us to clarify how the statolith $\delta^{13}C$ value reflects the chronological changes of total metabolic rates within ontogenetic progress. The M values estimated here was ranged between 0.56 and 0.75, distinctly higher than the M values estimated

by fish otolith $\delta^{13}C$ values in the most previous studies (0 – 0.5, Chung et al., 2019a). This result is consistent with biological properties of loliginid squids, including strong-swimming in neritic waters and maintaining an extremely high level of feeding and growth rate throughout the lifetime. Notably, the statolith $\delta^{13}C$ value generally decreased with ontogenetic changes, indicating a likely lower M value in early life history stage. Strong mobility and long-distance movement after the juvenile stage may explain this result. For example, subadult and adult individuals in northern Taiwan migrate between coastal and offshore waters, causing an increase in metabolic rate. The energy or oxygen consumption of reproductive physiology as maturating can also alter the metabolic performance. However, juvenile and subadult loliginid squids more frequently use energy-efficient movement ways of mantle contraction to replace the energy-consuming jet propulsion in the paralarval stage (Boyle and Rodhouse, 2005; Bartol et al., 2008). In fact, previous estimations of M value were specific to particular life history stages, and the metabolic rate of an individual fluctuates in response to the dynamics of temperature, growth and activity over the lifetime. Moreover, using the $\delta^{13}C$ value in soft tissues (i.e. muscle) is an alternative method for estimating the metabolically derived carbon isotopes as dietary $\delta^{13}C$ value. For cephalopods, the typical isotopic shifts between diet and muscle tissue range from 0.8‰ in coastal marine food webs (France and Peter, 1997) to 1.6‰ of an open sea species of *Dosidicus gigas* (Ruiz-Cooley et al., 2006). Reducing the uncertainty in the $\delta^{13}C_{DIC}$ and $\delta^{13}C_{diet}$ values will improve the precision of M value estimation. It is certain that the metabolism contributes predominant variations of statolith $\delta^{13}C$ value for adult individuals of *S. lessoniana*. We emphasize that further estimating the M values during the ontogeny should be able to more comprehensively describe the population dynamics and migration throughout life history stages for cephalopods.

Increasing $\delta^{15}N$ values, but not $\delta^{13}C$ values, were found in muscle tissue with body size (28 – 1746 g) of northern Taiwan individuals collected in different months (Fig. 31, 32), indicating ontogenetic changes in diet for *S. lessoniana*. The stable isotopic signatures of consumers reflects that of their preys, and carbon and nitrogen isotopic composition in tissues have been used extensively to trace the food sources

and trophic levels among organisms (Hobson and Welch, 1992; Kelly, 2000). Compared to stomach contents analysis, which shows a dietary snapshot in daily scale and may be difficult to conduct for cephalopods because of their fast digestion rate, stable isotopic signatures provide an integrated estimation of diet over times (from weeks to months) and can be used to infer feeding history and movement (Hansson et al., 1997; Hobson and Wassenaar, 1999; Toledo et al., 2020). In present study, the muscle $\delta^{15}N$ values increased from 11.97 ± 0.41‰ in sexual maturity stage I (immature) to 13.24 ± 0.55‰ in stage IV (mature), and the difference was no greater than the trophic enrichment of $\delta^{15}N$ mean values (2.5–3.4‰). By contrast, $\delta^{13}C$ values are mainly used to determine primary sources within a food web. In the marine ecosystems, $\delta^{13}C$ commonly exhibit different values between latitudes, inshore and offshore, or pelagic and benthic, reflecting variations of plankton compositions (Hobson et al., 1994; Hobson, 1999; Argüelles et al., 2012). The muscle $\delta^{13}C$ values of the present study did not exhibit distinguishable trends with sexual maturity stage, ranging from -16.51 ± 0.47‰ in stage I to -16.97 ± 0.45‰ in stage IV. These results are consistent with other trophic position studies with cephalopod muscle. For example, $\delta^{13}C$ values of the oceanic squid *Todarodes filippovae* were unrelated to body size and had approximate 1.3‰ range between different maturity stages (Cherel et al., 2009); Hunsicker et al. (2010) found little variation in the muscle $\delta^{13}C$ values of *Berryteuthis magister* commander squid with increasing ML. Therefore, the ontogenetic diet we have found in *S. lessoniana* can be concluded as that this squid is a highly carnivorous species that consumes consistent species composition of prey in the same latitude region, likely between coasts and inshore (variation in $\delta^{13}C$ value < 1‰), whereas the prey size increases within ontogenetic change (increase in $\delta^{15}N$ values less than one trophic enrichment). The stable isotopic analysis of muscle samples from various latitudes (e.g. the Penghu Islands) can clarify the ontogenetic shift in diet and feeding differences between locations, helping us to infer detailed movement, connection and population dynamic of this species.

5. Conclusion

This study has evaluated the potential of the stable isotopic mass-marking approach to track hatchling dispersal of *S. lessoniana*, and investigated the movement patterns and distribution of *S. lessoniana* around Taiwan by using stable isotopic compositions in the statolith and muscle tissue. There are few previous studies on the migration over the cephalopod lifetime. In addition, the movement and distribution range of *S. lessoniana* in Taiwan have not been examined yet. Therefore, for the first time, our results provide successful marking conditions when using the stable isotope marking technique on *S. lessoniana* and its potential effects on cephalopod statolith, and indicate the differences of movement patterns among seasonal groups between northern Taiwan and the Penghu Islands as well as the possible variations of their distribution ranges within the ontogenetic changes. These findings extend the limited knowledge about the life history of *S. lessoniana*.

Stable isotope mass-marking techniques can be successfully used in fishes. We demonstrated unique signatures in *S. lessoniana* statoliths with 100% marking success after 3 days of immersion in ^{137}Ba and provide an approach to unravel the questions regarding dispersal mechanisms and movement patterns in cephalopods. However, we also found potential effects of stable isotope mass marking on offspring size at hatch that are consistent with those reported by an increasing number of studies. The effects on embryo development and growth may induce variations in element composition in statoliths, probably reflecting physiological processes and statolith accretion, which affect statolith chemistry and may subsequently affect the accuracy of interpreting an individual's environmental history. We highlight that the effects of this technique need to be taken into consideration in field applications. Additional research investigating the relationships among multiple elements and physiological responses to enriched stable isotope incorporation will advance our knowledge for the application of these techniques to wild cephalopods.

All wild squids possess natural isotopic signatures that are incorporated into their statoliths and reflect the environmental temperature or isotopes composition.

Migration between waters may produce shifts in isotopic composition. This study applied sequential sampling to stable oxygen and carbon isotopic compositions of statoliths, and the findings suggest the ecological features of seasonal movement strategies and population connectivity in *S. lessoniana* in Taiwan. As a result, the waters off northeastern Taiwan and the Penghu Islands have proven to be an important spawning ground for *S. lessoniana*. Furthermore, the spring and summer hatching groups between northern Taiwan and the Penghu Islands may be able to be considered as a single stock. Flexible life history traits and a large distribution range are critical for cephalopods and support a high level of genetic diversity and ensure population abundance. This study provides information on the spatial and vertical distribution of *S. lessoniana* at various ontogenetic stages, which is essential for resource management and conservation of this commercial species.

The stable isotopic signatures in muscle tissues reveal more information on the variations of trophic levels and distribution ranges of poorly known *S. lessoniana*. Our example of this species illustrated the usefulness of combining the statolith and muscle isotopic analysis at the community and population in habitat use and degree of specialization of some seasonal groups. In addition to trophic relationships, the carbon isotopic analysis also provides an opportunity to estimate the metabolic rate of *S. lessoniana* in the field. A high level of metabolic rate found in adult individuals suggested obvious mobility for overwintering, and high feeding rate and energy consumption during the reproductive period. The property of continuous accumulation of the statolith together with muscle carbon isotopic compositions, used as dietary signatures, indicate the ontogenetic changes of metabolism, improving our understanding of the activity and oxygen consumption over the lifetime in cephalopods. Our results also showed an increasing pattern of nitrogen isotopes and relatively consistent carbon isotopic signature, suggesting no obvious dietary shift of the squid within the same latitude region. Future developments can reduce the uncertainty associated with this approach and provide more accurate species-specific interpretations of the variations of stable isotopic signatures within individuals and stocks of free-moving cephalopods.

Recent environmental and anthropic threats to marine ecosystems have come into public notice, increasing the importance of fishery management and conservation (Pikitch et al. 2004; Poloczanska et al. 2013; Dunn et al. 2016). Understanding the population connectivity and migration of cephalopods is critical in developing approaches for the resource management and conservation of marine ecosystems. For example, implementing fishery management by restrictions or closed fishing zones during spawning seasons will ensure the recruitment of the *S. lessoniana* population in Taiwan is sustainable. Using a variety of methods to obtain more ecological information on *S. lessoniana* is needed. The geographical distribution can be delineated based on statolith isotopic signatures and be compared to the estimated stock boundaries by fishery data or tagging approaches. These results can be useful to determine the detailed migration routes of the squid in further studies in combination with isotopic mass-marking tracking and statolith elemental compositions. Moreover, the examination of intra- and inter-annual distributions will help us to understand how climate change influences their population dynamic. This biological information provides insights into the past interaction between organisms and the environment, and enables us to better manage cephalopod resources in the future.

6. References

Akasaki, T., Nikaido, M., Tsuchiya, K., Segawa, S., Hasegawa, M. and Okada, N. (2006) Extensive mitochondrial gene arrangements in coleoid Cephalopoda and their phylogenetic implications. Molecular Phylogenetics and Evolution 383, 648-658.

Almany, G. R., Berumen, M. L., Thorrold, S. R., Planes, S. and Jones, G. P. (2007) Local replenishment of coral reef fish populations in a marine reserve. Science 3165825, 742-744.

Ammar, I. and Maaroof, R. (2019) First record of the squid *Sepioteuthis lessoniana* Férussac, 1831 in the Syrian coastal water. SSRG International Journal of Agriculture & Environmental Science 61, 52-55.

Ankjærø, T., Christensen, J. T. and Grønkjær, P. (2012) Tissue-specific turnover rates and trophic enrichment of stable N and C isotopes in juvenile Atlantic cod *Gadus morhua* fed three different diets. Marine Ecology Progress Series 461, 197-209.

Argüelles, J., Lorrain, A., Cherel, Y., Graco, M., Tafur, R., Alegre, A., Espinoza, P., Taipe, A., Ayón, P. and Bertrand, A. (2012) Tracking habitat and resource use for the jumbo squid *Dosidicus gigas*: a stable isotope analysis in the Northern Humboldt Current System. Marine Biology 1599, 2105-2116.

Arkhipkin, A. I. (2005) Statoliths as black boxes (life recorders) in squid. Marine and Freshwater Research 565, 573-583.

Arkhipkin, A. I., Campana, S. E., FitzGerald, J. and Thorrold, S. R. (2004) Spatial and temporal variation in elemental signatures of statoliths from the Patagonian longfin squid (*Loligo gahi*). Canadian Journal of Fisheries and Aquatic Sciences 617, 1212-1224.

Arkhipkin, A. I. and Shcherbich, Z. N. (2012) Thirty years' progress in age determination of squid using statoliths. Journal of the Marine Biological Association of the United Kingdom 926, 1389-1398.

Barry, P. D., Tamone, S. L. and Tallmon, D. A. (2011) A comparison of tagging methodology for North Pacific giant octopus *Enteroctopus dofleini*. Fisheries Research 1092-3, 370-372.

Bartol, I. K., Krueger, P. S., Thompson, J. T. and Stewart, W. J. (2008) Swimming dynamics and propulsive efficiency of squids throughout ontogeny. Integrative and Comparative Biology 486, 720-733.

Bazzino, G., Gilly, W. F., Markaida, U., Salinas-Zavala, C. A. and Ramos-Castillejos, J. (2010) Horizontal movements, vertical-habitat utilization and diet of the jumbo squid (*Dosidicus gigas*) in the Pacific Ocean off Baja California Sur, Mexico. Progress in Oceanography 861-2, 59-71.

Becker, M., Andersen, N., Erlenkeuser, H., Humphreys, M. P., Tanhua, T. and Körtzinger, A. (2016) An internally consistent dataset of δ^{13}C-DIC in the North Atlantic Ocean – NAC13v1. Earth System Science Data 82, 559-570.

Bernat, M., Church, T. and Allegre, C. J. (1972) Barium and strontium concentrations in Pacific and Mediterranean sea water profiles by direct isotope dilution mass spectrometry. Earth and Planetary Science Letters 161, 75-80.

Bolger, T. and Connolly, P. (1989) The selection of suitable indices for the measurement and analysis of fish condition. Journal of Fish Biology 342, 171-182.

Bower, S. and Margolis, L. (1991) Potential use of helminth parasites in stock identification of flying squid, *Ommastrephes bartrami*, in North Pacific waters. Canadian Journal of Zoology 694, 1124-1126.

Boyle, P. and Boletzky, S. (1996) Cephalopod populations: definition and dynamics. Philosophical Transactions of the Royal Society of London. Series B: Biological Sciences 3511343, 985-1002.

Boyle, P. and Rodhouse, P. (2005) Cephalopods: ecology and fisheries. John Wiley & Sons.

Buresch, K. C., Gerlach, G. and Hanlon, R. T. (2006) Multiple genetic stocks of longfin squid *Loligo pealeii* in the NW Atlantic: stocks segregate inshore in summer, but aggregate offshore in winter. Marine Ecology Progress Series 310, 263-270.

Chang, C. C. (2000) Spatial and Temporal Variation of ^{18}O in the Sea Water from the Taiwan Strait. Master's thesis, Institute of Marine Geology and Chemistry,

National Sun Yat-sen University. Available at https://hdl.handle.net/11296/6u9bf9 [Accessed 25 Oct. 2020]

Chen, C. S., Chen, J. Y. and Lin, C. W. (2015) Variation in life-history traits for micro-cohorts of *Sepioteuthis lessoniana* in the waters off northern Taiwan. Fisheries Science 811, 53-64.

Chen, C. S. and Huang, J. M. (1999) A numerical study of precipitation characteristics over Taiwan Island during the winter season. Meteorology and Atmospheric Physics 703-4, 167-183.

Chen, C. T. (1997) The Kuroshio intermediate water is the major source of nutrients on the East China Sea continental shelf. Oceanographic Literature Review 544, 531.

Chen, D. S., Dykhuizen, G., Hodge, J. and Gilly, W. F. (1996) Ontogeny of copepod predation in juvenile squid *(Loligo opalescens*). The Biological Bulletin 1901, 69-81.

Chen, T. C., Yen, M. C., Huang, W. R. and Gallus Jr, W. A. (2002) An East Asian cold surge: case study. Monthly Weather Review 1309, 2271-2290.

Cheng, S., Anderson, F. E., Bergman, A., Mahardika, G., Muchlisin, Z., Dang, B., Calumpong, H., Mohamed, K., Sasikumar, G. and Venkatesan, V. (2014) Molecular evidence for co-occurring cryptic lineages within the *Sepioteuthis cf. lessoniana* species complex in the Indian and Indo-West Pacific Oceans. Hydrobiologia 7251, 165-188.

Cherel, Y., Fontaine, C., Jackson, G. D., Jackson, C. H. and Richard, P. (2009) Tissue, ontogenic and sex-related differences in $\delta^{13}C$ and $\delta^{15}N$ values of the oceanic squid *Todarodes filippovae* (Cephalopoda: Ommastrephidae). Marine Biology 1564, 699-708.

Ching, T. Y., Chen, C. S. and Wang, C. H. (2017) Spatiotemporal variations in life-history traits and statolith trace elements of *Sepioteuthis lessoniana* populations around northern Taiwan. Journal of the Marine Biological Association of the United Kingdom, 1-11.

Chung, M. T., Chen, C. Y., Shiao, J. C., Lin, S. and Wang, C. H. (2020) Temperature-dependent fractionation of stable oxygen isotopes differs between cuttlefish statoliths and cuttlebones. Ecological Indicators 115, 106457.

Chung, M. T., Trueman, C. N., Godiksen, J. A. and Grønkjær, P. (2019a) Otolith $\delta^{13}C$ values as a metabolic proxy: approaches and mechanical underpinnings. Marine and Freshwater Research.

Chung, M. T., Trueman, C. N., Godiksen, J. A., Holmstrup, M. E. and Grønkjær, P. (2019b) Field metabolic rates of teleost fishes are recorded in otolith carbonate. Communications Biology 21, 24.

Clarke, A. and Johnston, N. M. (1999) Scaling of metabolic rate with body mass and temperature in teleost fish. Journal of Animal Ecology 685, 893-905.

Clarke, M. R. (1978) The cephalopod statolithan-introduction to its form. Journal of the Marine Biological Association of the United Kingdom 583, 701-712.

Cowen, R. K., Lwiza, K. M., Sponaugle, S., Paris, C. B. and Olson, D. B. (2000) Connectivity of marine populations: open or closed? Science 2875454, 857-859.

Cowen, R. K. and Sponaugle, S. (2009) Larval dispersal and marine population connectivity. Annual Review of Marine Science 1, 443-466.

Cronin, E. and Seymour, R. (2000) Respiration of the eggs of the giant cuttlefish *Sepia apama*. Marine Biology 1365, 863-870.

Currey, L. M., Heupel, M. R., Simpfendorfer, C. A. and Williams, A. J. (2014) Inferring movement patterns of a coral reef fish using oxygen and carbon isotopes in otolith carbonate. Journal of Experimental Marine Biology and Ecology 456, 18-25.

Darnaude, A. M. and Hunter, E. (2018) Validation of otolith $\delta^{18}O$ values as effective natural tags for shelf-scale geolocation of migrating fish. Marine Ecology Progress Series 598, 167-185.

de Braux, E., Warren-Myers, F., Dempster, T., Fjelldal, P. G., Hansen, T. and Swearer, S. E. (2014) Osmotic induction improves batch marking of larval fish otoliths with enriched stable isotopes. ICES Journal of Marine Science 719, 2530-2538.

De Vries, M. C., Gillanders, B. M. and Elsdon, T. S. (2005) Facilitation of barium uptake into fish otoliths: influence of strontium concentration and salinity. Geochimica et Cosmochimica Acta 6916, 4061-4072.

Dunn, D. C., Maxwell, S. M., Boustany, A. M. and Halpin, P. N. (2016) Dynamic ocean management increases the efficiency and efficacy of fisheries management. Proceedings of the National Academy of Sciences 1133, 668-673.

Elsdon, T. S., Ayvazian, S., McMahon, K. W. and Thorrold, S. R. (2010) Experimental evaluation of stable isotope fractionation in fish muscle and otoliths. Marine Ecology Progress Series 408, 195-205.

Elsdon, T. S. and Gillanders, B. M. (2002) Interactive effects of temperature and salinity on otolith chemistry: challenges for determining environmental histories of fish. Canadian Journal of Fisheries and Aquatic Sciences 5911, 1796-1808.

Elsdon, T. S. and Gillanders, B. M. (2003) Reconstructing migratory patterns of fish based on environmental influences on otolith chemistry. Reviews in Fish Biology and Fisheries 133, 217-235.

Fiorito, G., Affuso, A., Basil, J., Cole, A., de Girolamo, P., D'angelo, L., Dickel, L., Gestal, C., Grasso, F. and Kuba, M. (2015) Guidelines for the Care and Welfare of Cephalopods in Research–A consensus based on an initiative by CephRes, FELASA and the Boyd Group. Laboratory Animals 492[S2], 1-90.

Forsythe, J. (2004) Accounting for the effect of temperature on squid growth in nature: from hypothesis to practice. Marine and Freshwater Research 554, 331-339.

Forsythe, J., Lee, P., Walsh, L. and Clark, T. (2002) The effects of crowding on growth of the European cuttlefish, *Sepia officinalis* Linnaeus, 1758 reared at two temperatures. Journal of Experimental Marine Biology and Ecology 2692, 173-185.

Forsythe, J., Walsh, L., Turk, P. and Lee, P. (2001) Impact of temperature on juvenile growth and age at first egg-laying of the Pacific reef squid *Sepioteuthis lessoniana* reared in captivity. Marine Biology 1381, 103-112.

France, R. and Peters, R. (1997) Ecosystem differences in the trophic enrichment of ^{13}C in aquatic food webs. Canadian Journal of Fisheries and Aquatic Sciences 546, 1255-1258.

France, R. L. (1995) Carbon-13 enrichment in benthic compared to planktonic algae: foodweb implications. Marine Ecology Progress Series 124, 307-312.

Gao, Y., Schwarcz, H. P., Brand, U. and Moksness, E. (2001) Seasonal Stable Isotope Records of Otoliths from Ocean-pen Reared and Wild Cod, Gadus morhua. Environmental Biology of Fishes 614, 445-453.

Garcia, H., Locarnini, R., Boyer, T., Antonov, J., Baranova, O., Zweng, M. and Johnson, D. (2013) World Ocean Atlas 2013, Vol 3: Dissolved Oxygen, Apparent Oxygen Utilization, and Oxygen Saturation. S. Levitus, Ed.; A. Mishonov, Technical Ed. NOAA Atlas NESDIS 75, 27pp.

Gillanders, B. M., Wilkinson, L. M., Munro, A. R. and de Vries, M. C. (2013) Statolith chemistry of two life history stages of cuttlefish: Effects of temperature and seawater trace element concentration. Geochimica et Cosmochimica Acta 101, 12-23.

Gillooly, J. F., Brown, J. H., West, G. B., Savage, V. M. and Charnov, E. L. (2001) Effects of size and temperature on metabolic rate. Science 2935538, 2248-2251.

Gilly, W., Markaida, U., Baxter, C., Block, B., Boustany, A., Zeidberg, L., Reisenbichler, K., Robison, B., Bazzino, G. and Salinas, C. (2006) Vertical and horizontal migrations by the jumbo squid *Dosidicus gigas* revealed by electronic tagging. Marine Ecology Progress Series 324, 1-17.

Gislason, H., Sinclair, M., Sainsbury, K. and O'boyle, R. (2000) Symposium overview: incorporating ecosystem objectives within fisheries management. ICES Journal of Marine Science 573, 468-475.

Gong, G. C., Wen, Y. H., Wang, B. W. and Liu, G. J. (2003) Seasonal variation of chlorophyll *a* concentration, primary production and environmental conditions in the subtropical East China Sea. Deep Sea Research Part II: Topical Studies in Oceanography 506, 1219-1236.

Green, B. C., Smith, D. J., Grey, J. and Underwood, G. J. (2012) High site fidelity and low site connectivity in temperate salt marsh fish populations: a stable isotope approach. Oecologia 1681, 245-255.

Hall, K. and Fowler, A. (2003) The fisheries biology of the cuttlefish *Sepia apama* Gray. South Australian waters. Final Report to the FRDC (Project 98/151). South Australian Research and Development Institute, Adelaide.

Hamer, P. A. and Jenkins, G. P. (2007) Comparison of spatial variation in otolith chemistry of two fish species and relationships with water chemistry and otolith growth. Journal of Fish Biology 714, 1035-1055.

Hansson, S., Hobbie, J. E., Elmgren, R., Larsson, U., Fry, B. and Johansson, S. (1997) The stable nitrogen isotope ratio as a marker of food-web interactions and fish migration. Ecology 787, 2249-2257.

Hobday, A. J., Hartog, J. R., Timmiss, T. and Fielding, J. (2010) Dynamic spatial zoning to manage southern bluefin tuna (*Thunnus maccoyii*) capture in a multi-species longline fishery. Fisheries Oceanography 193, 243-253.

Hobson, K. A. (1999) Tracing origins and migration of wildlife using stable isotopes: a review. Oecologia 1203, 314-326.

Hobson, K. A., Piatt, J. F. and Pitocchelli, J. (1994) Using stable isotopes to determine seabird trophic relationships. Journal of Animal Ecology, 786-798.

Hobson, K. A. and Wassenaar, L. I. (1999) Stable isotope ecology: an introduction. Oecologia 1203, 312-313.

Hobson, K. A. and Welch, H. E. (1992) Determination of trophic relationships within a high Arctic marine food web using $\delta^{13}C$ and $\delta^{15}N$ analysis. Marine Ecology Progress Series, 9-18.

Høie, H., Folkvord, A. and Otterlei, E. (2003) Effect of somatic and otolith growth rate on stable isotopic composition of early juvenile cod (*Gadus morhua* L) otoliths. Journal of Experimental Marine Biology and Ecology 2891, 41-58.

Høie, H., Otterlei, E. and Folkvord, A. (2004a) Temperature-dependent fractionation of stable oxygen isotopes in otoliths of juvenile cod (*Gadus morhua* L.). ICES Journal of Marine Science 612, 243-251.

Høie, H., Andersson, C., Folkvord, A. and Karlsen, Ø. (2004b) Precision and accuracy of stable isotope signals in otoliths of pen-reared cod (*Gadus morhua*) when sampled with a high-resolution micromill. Marine Biology 1446, 1039-1049.

Hong, H., Chai, F., Zhang, C., Huang, B., Jiang, Y. and Hu, J. (2011) An overview of physical and biogeochemical processes and ecosystem dynamics in the Taiwan Strait. Continental Shelf Research 316, S3-S12.

Hsiao, C. D., Shen, K. N., Ching, T. Y., Wang, Y. H., Ye, J. J., Tsai, S. Y., Wu, S. C., Chen, C. H. and Wang, C. H. (2016) The complete mitochondrial genome of the cryptic "lineage A" big-fin reef squid, *Sepioteuthis lessoniana* (Cephalopoda: Loliginidae) in Indo-West Pacific. Mitochondrial DNA Part A 274, 2433-2434.

Hu, J., Kawamura, H., Hong, H. and Pan, W. (2003) A review of research on the upwelling in the Taiwan Strait. Bulletin of Marine Science 733, 605-628.

Huang, T. H., Lun, Z., Wu, C. R. and Chen, C. T. A. (2018) Interannual carbon and nutrient fluxes in Southeastern Taiwan Strait. Sustainability 102, 372.

Hubbs, C. and Blaxter, J. (1986) Ninth larval fish conference: Development of sense organs and behaviour of Teleost larvae with special reference to feeding and predator avoidance. Transactions of the American Fisheries Society 1151, 98-114.

Hunsicker, M. E., Essington, T. E., Aydin, K. Y. and Ishida, B. (2010) Predatory role of the commander squid *Berryteuthis magister* in the eastern Bering Sea: insights from stable isotopes and food habits. Marine Ecology Progress Series 415, 91-108.

Hunt, J. and Seibel, B. (2000) Life history of *Gonatus onyx* (Cephalopoda: Teuthoidea): ontogenetic changes in habitat, behavior and physiology. Marine Biology 1363, 543-552.

Ikeda, Y., Arai, N., Kidokoro, H. and Sakamoto, W. (2003) Strontium: calcium ratios in statoliths of Japanese common squid *Todarodes pacificus* (Cephalopoda: Ommastrephidae) as indicators of migratory behavior. Marine Ecology Progress Series 251, 169-179.

Ikeda, Y., Okazaki, J., Sakurai, Y. and Sakamoto, W. (2002) Periodic variation in Sr/Ca ratios in statoliths of the Japanese Common Squid *Todarodes pacificus* Steenstrup, 1880 (Cephalopoda: Ommastrephidae) maintained under constant water temperature. Journal of Experimental Marine Biology and Ecology 2732, 161-170.

Ikeda, Y., SAKURAZAWA, I., SAKURAI, Y. and MATSUMOTO, G. (2003) Initial trials of squid rearing, maintenance and culture at the Brain Science Institute of RIKEN. Aquaculture Science 514, 391-400.

Ikeda, Y., Ueta, Y., Anderson, F. and Matsumoto, G. (2009) Reproduction and life span of the oval squid *Sepioteuthis lessoniana* (Cephalopoda: Loliginidae): comparison between laboratory-cultured and wild-caught squid. Marine Biodiversity Records 2.

Ikeda, Y., Wada, Y., Arai, N. and Sakamoto, W. (1999) Note on size variation of body and statoliths in the oval squid *Sepioteuthis lessoniana* hatchlings. Journal of the Marine Biological Association of the United Kingdom 794, 757-759.

Iwata, Y., Munehara, H. and Sakurai, Y. (2005) Dependence of paternity rates on alternative reproductive behaviors in the squid *Loligo bleekeri*. Marine Ecology Progress Series 298, 219-228.

Jackson, A. L., Inger, R., Parnell, A. C. and Bearhop, S. (2011) Comparing isotopic niche widths among and within communities: SIBER–Stable Isotope Bayesian Ellipses in R. Journal of Animal Ecology 803, 595-602.

Jackson, G. and Moltschaniwskyj, N. (2001) The influence of ration level on growth and statolith increment width of the tropical squid *Sepioteuthis lessoniana* (Cephalopoda: Loliginidae): an experimental approach. Marine Biology 1384, 819-825.

Jackson, G. and Moltschaniwskyj, N. (2002) Spatial and temporal variation in growth rates and maturity in the Indo-Pacific squid *Sepioteuthis lessoniana* (Cephalopoda: Loliginidae). Marine Biology 1404, 747-754.

Jackson, G. D. (1990) Age and growth of the tropical nearshore loliginid squid *Sepioteuthis lessoniana* determined from statolith growth-ring analysis. Fishery Bulletin 88, 113-118.

Jackson, G. D. and Choat, J. H. (1992) Growth in tropical cephalopods: an analysis based on statolith microstructure. Canadian Journal of Fisheries and Aquatic Sciences 492, 218-228.

Jackson, G. D., O'Dor, R. K. and Andrade, Y. (2005) First tests of hybrid acoustic/archival tags on squid and cuttlefish. Marine and Freshwater Research 564, 425-430.

Jan, S., Sheu, D. D. and Kuo, H. M. (2006) Water mass and throughflow transport variability in the Taiwan Strait. Journal of Geophysical Research: Oceans 111C12.

Jan, S., Tseng, Y. H. and Dietrich, D. E. (2010) Sources of water in the Taiwan Strait. Journal of Oceanography 662, 211-221.

Jan, S., Wang, J., Chern, C.-S. and Chao, S.-Y. (2002) Seasonal variation of the circulation in the Taiwan Strait. Journal of Marine Systems 353-4, 249-268.

Jereb, P. and Roper, C. F. (2005). "*Sepioteuthis lessoniana* Férussac in Lesson, 1831", in Cephalopods of the World: An Annotated and Illustrated Catalogue of Cephalopod Species Known to Date, Volume 2, Myopisd and Oegopsid Squids, eds P. Jereb and C. F. E. Roper (FAO: Rome, Italy), 95–97.

Jones, G. P., Planes, S. and Thorrold, S. R. (2005) Coral reef fish larvae settle close to home. Current Biology 1514, 1314-1318.

Kalish, J. M. (1989) Otolith microchemistry: validation of the effects of physiology, age and environment on otolith composition. Journal of Experimental Marine Biology and Ecology 1323, 151-178.

Kalish, J. M. (1991) ^{13}C and ^{18}O isotopic disequilibria in fish otoliths: metabolic and kinetic effects. Marine Ecology Progress Series 752–3, 191-203.

Kanamaru, H., Umeda, T. and Morikawa, A. (2007a) Migration of the oval squid, *Sepioteuthis lessoniana* in northern and western waters of the Kyushu. Bulletin of Saga Prefectural Genkai Fisheries Research and Development Center 4, 51-57.

Kanamaru, H., Umeda, T. and Ootu, Y. (2007b) Investigation of tagging method of the ovai squid, *Sepioteuthis lessoniana*. Bulletin of Saga Prefectural Genkai Fisheries Research and Development Center 4, 45-50.

Kato, Y., Togashi, H., Kurita, Y., Kamauchi, H. and Tayasu, I. (2020) Discrimination of nursery locations of juvenile Japanese flounder *Paralichthys olivaceus* on the Pacific coast of northern Japan based on carbon and nitrogen stable isotope ratios. Fisheries Science, 1-9.

Kawazu, M., Tawa, A., Ishihara, T., Uematsu, Y. and Sakai, S. (2020) Discrimination of eastward trans-Pacific migration of the Pacific bluefin tuna *Thunnus orientalis* through otolith $\delta^{13}C$ and $\delta^{18}O$ analyses. Marine Biology 1678, 1-7.

Kelly, J. F. (2000) Stable isotopes of carbon and nitrogen in the study of avian and mammalian trophic ecology. Canadian Journal of Zoology 781, 1-27.

Kitagawa, T., Ishimura, T., Uozato, R., Shirai, K., Amano, Y., Shinoda, A., Otake, T., Tsunogai, U. and Kimura, S. (2013) Otolith $\delta^{18}O$ of Pacific bluefin tuna *Thunnus orientalis* as an indicator of ambient water temperature. Marine Ecology Progress Series 481, 199-209.

Kobayashi, S., Takayama, C. and Ikeda, Y. (2013) Ontogeny of the brain in oval squid *Sepioteuthis lessoniana* (Cephalopoda: Loliginidae) during the post-hatching phase. Marine Biological Association of the United Kingdom. Journal of the Marine Biological Association of the United Kingdom 936, 1663.

Kresse, R., Baudis, U., Jäger, P., Riechers, H. H., Wagner, H., Winkler, J. and Wolf, H. U. (2007) Barium and barium compounds. In 'Ullmann's encyclopedia of industrial chemistry', ed. Pelc H. (Wiley-VCH Verlag GmbH & Co. KGaA: Weinheim, Germany), 621-640.

Kroopnick, P. (1985) The distribution of ^{13}C of ΣCO_2 in the world oceans. Deep Sea Research Part A. Oceanographic Research Papers 321, 57-84.

Lan, K. W., Lee, M. A., Zhang, C. I., Wang, P. Y., Wu, L. J. and Lee, K. T. (2014) Effects of climate variability and climate change on the fishing conditions for grey mullet (*Mugil cephalus* L.) in the Taiwan Strait. Climatic Change 1261-2, 189-202.

Landman, N., Cochran, J., Cerrato, R., Mak, J., Roper, C. and Lu, C. (2004) Habitat and age of the giant squid (*Architeuthis sanctipauli*) inferred from isotopic analyses. Marine Biology 1444, 685-691.

Leder, J., Swart, P. K., Szmant, A. and Dodge, R. (1996) The origin of variations in the isotopic record of scleractinian corals: I. Oxygen. Geochimica et Cosmochimica Acta 6015, 2857-2870.

Lee, P. G., Turk, P. E., Yang, W. T. and Hanlon, R. T. (1994) Biological characteristics and biomedical applications of the squid *Sepioteuthis lessoniana* cultured through multiple generations. The Biological Bulletin 1863, 328-341.

LeGrande, A. N. and Schmidt, G. A. (2006) Global gridded data set of the oxygen isotopic composition in seawater. Geophysical Research Letters 3312.

Lin, H. L., Wang, L. W., Wang, C. H. and Gong, G. C. (1999) Vertical distribution of $\delta^{13}C$ of dissolved inorganic carbon in the northeastern South China Sea. Deep Sea Research Part I: Oceanographic Research Papers 465, 757-775.

Linzmeier, B. J. (2019) Refining the interpretation of oxygen isotope variability in free-swimming organisms. Swiss Journal of Palaeontology 1381, 109-121.

Linzmeier, B. J., Kozdon, R., Peters, S. E. and Valley, J. W. (2016) Oxygen isotope variability within Nautilus shell growth bands. PLOS ONE 114, e0153890.

Liu, B. L., Cao, J., Truesdell, S. B., Chen, Y., Chen, X. J. and Tian, S. Q. (2016) Reconstructing cephalopod migration with statolith elemental signatures: a case study using *Dosidicus gigas*. Fisheries Science 823, 425-433.

Liu, K. K., Gong, G. C., Lin, S., Yang, C. Y., Wei, C. L., Pai, S. C. and Wu, C. K. (1992) The year-round upwelling at the shelf break near the northern tip of Taiwan as evidenced by chemical hydrography. Terrestrial, Atmospheric and Oceanic Sciences 33, 243-275.

Lloyd, D. C., Zacherl, D. C., Walker, S., Paradis, G., Sheehy, M. and Warner, R. R. (2008) Egg source, temperature and culture seawater affect elemental signatures in *Kelletia kelletii* larval statoliths. Marine Ecology Progress Series 353, 115-130.

Martino, J. C., Doubleday, Z. A., Chung, M. T. and Gillanders, B. M. (2020) Experimental support towards a metabolic proxy in fish using otolith carbon isotopes. Journal of Experimental Biology 2236.

Martino, J. C., Doubleday, Z. A. and Gillanders, B. M. (2019) Metabolic effects on carbon isotope biomarkers in fish. Ecological Indicators 97, 10-16.

Maxwell, S. M., Hazen, E. L., Lewison, R. L., Dunn, D. C., Bailey, H., Bograd, S. J., Briscoe, D. K., Fossette, S., Hobday, A. J. and Bennett, M. (2015) Dynamic ocean management: Defining and conceptualizing real-time management of the ocean. Marine Policy 58, 42-50.

McConnaughey, T. (1989) ^{13}C and ^{18}O isotopic disequilibrium in biological carbonates: I. Patterns. Geochimica et Cosmochimica Acta 531, 151-162.

McConnaughey, T. A., Burdett, J., Whelan, J. F. and Paull, C. K. (1997) Carbon isotopes in biological carbonates: respiration and photosynthesis. Geochimica et Cosmochimica Acta 613, 611-622.

Miller, M. B., Clough, A. M., Batson, J. N. and Vachet, R. W. (2006) Transition metal binding to cod otolith proteins. Journal of Experimental Marine Biology and Ecology 3291, 135-143.

Moreno, A., Dos Santos, A., Piatkowski, U., Santos, A. M. P. and Cabral, H. (2008) Distribution of cephalopod paralarvae in relation to the regional oceanography of the western Iberia. Journal of Plankton Research 311, 73-91.

Munro, A. R., Gillanders, B. M., Elsdon, T. S., Crook, D. A. and Sanger, A. C. (2008) Enriched stable isotope marking of juvenile golden perch (*Macquaria ambigua*) otoliths. Canadian Journal of Fisheries and Aquatic Sciences 652, 276-285.

Nakashima, R., Suzuki, A. and Watanabe, T. (2004) Life history of the Pliocene scallop Fortipecten, based on oxygen and carbon isotope profiles. Palaeogeography, Palaeoclimatology, Palaeoecology 2113-4, 299-307.

Nishida, K., Suzuki, A., Isono, R., Hayashi, M., Watanabe, Y., Yamamoto, Y., Irie, T., Nojiri, Y., Mori, C., Sato, M., Sato, K. and Sasaki, T. (2015) Thermal dependency of shell growth, microstructure, and stable isotopes in laboratory-reared *Scapharca broughtonii* (Mollusca: Bivalvia). Geochemistry, Geophysics, Geosystems 167, 2395-2408.

O'Dor, R. (1992) Big squid in big currents. South African Journal of Marine Science 121, 225-235.

O'Dor, R. (1998) Can understanding squid life-history strategies and recruitment improve management? South African Journal of Marine Science 201, 193-206.

O'Dor, R. (1998) Squid life-history strategies. FAO Fisheries Technical Paper, 233-254.

O'DOR, R. and Balch, N. (1985) Properties of *Illex illecebrosus* egg masses potentially influencing larval oceanographic distribution. N. NAFO scientific. Council Studies 9, 69-76.

Oellermann, M., Pörtner, H. O. and Mark, F. C. (2012) Mitochondrial dynamics underlying thermal plasticity of cuttlefish (*Sepia officinalis*) hearts. Journal of Experimental Biology 21517, 2992-3000.

Okutani, T. (2015). *Sepioteuthis lessoniana* Férussac in Lesson, 1832. In 'Cuttlefishes and Squids of the World.' pp. 97. (Tokai University Press: Tokyo, Japan.) Available at http://www.zen-ika.com/zukan/pdf/cs184.pdf?idx=1 [Accessed 25 Oct. 2019].

O'Leary, M. H. (1988) Carbon isotopes in photosynthesis. Bioscience 385, 328-336.

Otero, J., Álvarez-Salgado, X. A., González, Á. F., Miranda, A., Groom, S. B., Cabanas, J. M., Casas, G., Wheatley, B. and Guerra, Á. (2008) Bottom-up control of common octopus *Octopus vulgaris* in the Galician upwelling system, northeast Atlantic Ocean. Marine Ecology Progress Series 362, 181-192.

Owen, E. F., Wanamaker, A. D., Feindel, S. C., Schöne, B. R. and Rawson, P. D. (2008) Stable carbon and oxygen isotope fractionation in bivalve (*Placopecten magellanicus*) larval aragonite. Geochimica et Cosmochimica Acta 7219, 4687-4698.

Payne, N. L., Semmens, J. M. and Gillanders, B. M. (2011) Elemental uptake via immersion: a mass-marking technique for the early life-history stages of cephalopods. Marine Ecology Progress Series 436, 169-176.

Pecl, G. T., Doubleday, Z. A., Danyushevsky, L., Gilbert, S. and Moltschaniwskyj, N. A. (2010) Transgenerational marking of cephalopods with an enriched barium isotope: a promising tool for empirically estimating post-hatching movement and population connectivity. ICES Journal of Marine Science 677, 1372-1380.

Pecl, G. T., Tracey, S. R., Semmens, J. M. and Jackson, G. D. (2006) Use of acoustic telemetry for spatial management of southern calamary *Sepioteuthis australis*,

a highly mobile inshore squid species. Marine Ecology Progress Series 328, 1-15.

Pikitch, E. K., Santora, C., Babcock, E. A., Bakun, A., Bonfil, R., Conover, D. O., Dayton, P., Doukakis, P., Fluharty, D. and Heneman, B. (2004) Ecosystem-based fishery management, American Association for the Advancement of Science.

Poloczanska, E. S., Brown, C. J., Sydeman, W. J., Kiessling, W., Schoeman, D. S., Moore, P. J., Brander, K., Bruno, J. F., Buckley, L. B. and Burrows, M. T. (2013) Global imprint of climate change on marine life. Nature Climate Change 310, 919.

Post, D. M. (2002) Using stable isotopes to estimate trophic position: models, methods, and assumptions. Ecology 833, 703-718.

R Core Team (2018). R: A language and environment for statistical computing. Available at: http://www.r-project.org/ [Accessed 1 Jan. 2018].

Radtke, R. (1983) Chemical and structural characteristics of statoliths from the short-finned squid *Illex illecebrosus*. Marine Biology 761, 47-54.

Rexfort, A. and Mutterlose, J. (2006) Stable isotope records from *Sepia officinalis*—a key to understanding the ecology of belemnites? Earth and Planetary Science Letters 2473-4, 212-221.

Ricker, W. E. (1975) Computation and interpretation of biological statistics of fish populations. Bulletin – Fisheries Research Board of Canada 191, 209-210

Rodgers, K. L. and Wing, S. R. (2008) Spatial structure and movement of blue cod *Parapercis colias* in Doubtful Sound, New Zealand, inferred from $\delta^{13}C$ and $\delta^{15}N$. Marine Ecology Progress Series 359, 239-248.

Rodhouse, P. G. and Hatfield, E. (1990) Dynamics of growth and maturation in the cephalopod *Illex argentinus* de Castellanos, 1960 (Teuthoidea: Ommastrephidae). Philosophical Transactions of the Royal Society of London. Series B: Biological Sciences 3291254, 229-241.

Rodhouse, P. G., Pierce, G. J., Nichols, O. C., Sauer, W. H., Arkhipkin, A. I., Laptikhovsky, V. V., Lipiński, M. R., Ramos, J. E., Gras, M. and Kidokoro, H. (2014) "Environmental effects on cephalopod population dynamics:

implications for management of fisheries," in the Advances in Marine Biology, Elsevier). 67, 99-233.

Rohling, E. J. (2013) Oxygen isotope composition of seawater. The Encyclopedia of Quaternary Science. Amsterdam: Elsevier 2, 915-922.

Romanek, C. S., Grossman, E. L. and Morse, J. W. (1992) Carbon isotopic fractionation in synthetic aragonite and calcite: effects of temperature and precipitation rate. Geochimica et Cosmochimica Acta 561, 419-430.

Roper, C. F., Sweeney, M. J. and Nauen, C. (1984). "*Sepioteuthis lessoniana* Lesson, 1830," in FAO species catalogue Vol. 3 Cephalopods of the world. An annotated and illustrated catalogue of species of interest to fisheries, FAO.

Rosa, I. C., Raimundo, J., Lopes, V. M., Brandão, C., Couto, A., Santos, C., Cabecinhas, A. S., Cereja, R., Calado, R. and Caetano, M. (2015) Cuttlefish capsule: an effective shield against contaminants in the wild. Chemosphere 135, 7-13.

Rosman, K. and Taylor, P. (1998) Isotopic compositions of the elements 1997 (Technical Report). Pure and Applied Chemistry 701, 217-235.

Ruiz-Cooley, R., Markaida, U., Gendron, D. and Aguíñiga, S. (2006) Stable isotopes in jumbo squid (*Dosidicus gigas*) beaks to estimate its trophic position: comparison between stomach contents and stable isotopes. Journal of the Marine Biological Association of the United Kingdom 862, 437-445.

Sakamoto, T., Komatsu, K., Shirai, K., Higuchi, T., Ishimura, T., Setou, T., Kamimura, Y., Watanabe, C. and Kawabata, A. (2019) Combining microvolume isotope analysis and numerical simulation to reproduce fish migration history. Methods in Ecology and Evolution 101, 59-69.

Sauer, W., Lipinski, M. and Augustyn, C. (2000) Tag recapture studies of the chokka squid *Loligo vulgaris reynaudii* d'Orbigny, 1845 on inshore spawning grounds on the south-east coast of South Africa. Fisheries Research 453, 283-289.

Schmittner, A., Gruber, N., Mix, A., Key, R., Tagliabue, A. and Westberry, T. (2013) Biology and air–sea gas exchange controls on the distribution of carbon isotope ratios ($\delta^{13}C$) in the ocean. Biogeosciences 109, 5793-5816.

Schwarcz, H., Gao, Y., Campana, S., Browne, D., Knyf, M. and Brand, U. (1998) Stable carbon isotope variations in otoliths of Atlantic cod (*Gadus morhua*). Canadian Journal of Fisheries and Aquatic Sciences 558, 1798-1806.

Segawa, S. (1987) Life history of the oval squid, *Sepioteuthis lessoniana*, in Kominato and adjacent waters central Honshu, Japan. Journal of Tokyo University of Fisheries 74, 67-105.

Semmens, J. M., Pecl, G. T., Gillanders, B. M., Waluda, C. M., Shea, E. K., Jouffre, D., Ichii, T., Zumholz, K., Katugin, O. N. and Leporati, S. C. (2007) Approaches to resolving cephalopod movement and migration patterns. Reviews in Fish Biology and Fisheries 172-3, 401.

Shen, K. N., Yen, T. C., Chen, C. H., Ye, J. J. and Hsiao, C. D. (2016) The complete mitochondrial genome of the cryptic "lineage B" big-fin reef squid, *Sepioteuthis lessoniana* (Cephalopoda: Loliginidae) in Indo-West Pacific. Mitochondrial DNA Part A 273, 2100-2101.

Sherwood, G. D. and Rose, G. A. (2003) Influence of swimming form on otolith $\delta^{13}C$ in marine fish. Marine Ecology Progress Series 258, 283-289.

Sheu, D., Lee, W., Wang, C., Wei, C., Chen, C., Cherng, C. and Huang, M. (1996) Depth distribution of δ^{13} of dissolved ΣCO_2 in seawater off eastern Taiwan: Effects of the Kuroshio current and its associated upwelling phenomenon. Continental Shelf Research 1612, 1609-1619.

Shiao, J. C., Itoh, S., Yurimoto, H., Iizuka, Y. and Liao, Y. C. (2014) Oxygen isotopic distribution along the otolith growth axis by secondary ion mass spectrometry: Applications for studying ontogenetic change in the depth inhabited by deep-sea fishes. Deep Sea Research Part I: Oceanographic Research Papers 84, 50-58.

Shiao, J. C., Sui, T. D., Chang, N. N. and Chang, C. W. (2017) Remarkable vertical shift in residence depth links pelagic larval and demersal adult jellynose fish. Deep Sea Research Part I: Oceanographic Research Papers 121, 160-168.

Shirai, K., Otake, T., Amano, Y., Kuroki, M., Ushikubo, T., Kita, N. T., Murayama, M., Tsukamoto, K. and Valley, J. W. (2018) Temperature and depth distribution

of Japanese eel eggs estimated using otolith oxygen stable isotopes. Geochimica et Cosmochimica Acta 236, 373-383.

Simpson, S. J., Sims, D. W. and Trueman, C. N. (2019) Ontogenetic trends in resource partitioning and trophic geography of sympatric skates (Rajidae) inferred from stable isotope composition across eye lenses. Marine Ecology Progress Series 624, 103-116.

Sinclair, D. J. (2005) Correlated trace element "vital effects" in tropical corals: a new geochemical tool for probing biomineralization. Geochimica et Cosmochimica Acta 6913, 3265-3284.

Sinclair, D. J. and Risk, M. J. (2006) A numerical model of trace-element coprecipitation in a physicochemical calcification system: Application to coral biomineralization and trace-element 'vital effects'. Geochimica et Cosmochimica Acta 7015, 3855-3868.

Smith, K. T. and Whitledge, G. (2011) Evaluation of a stable-isotope labelling technique for mass marking fin rays of age-0 lake sturgeon. Fisheries Management and Ecology 182, 168-175.

Sogard, S. M. (1997) Size-selective mortality in the juvenile stage of teleost fishes: a review. Bulletin of Marine Science 603, 1129-1157.

Solomon, C. T., Weber, P. K., Cech, J., Joseph J, Ingram, B. L., Conrad, M. E., Machavaram, M. V., Pogodina, A. R. and Franklin, R. L. (2006) Experimental determination of the sources of otolith carbon and associated isotopic fractionation. Canadian Journal of Fisheries and Aquatic Sciences 631, 79-89.

Song, G. S., Chang, Y. C. and Ma, C. P. (1997) Characteristics of submarine topography off northern Taiwan. Terrestrial, Atmospheric and Oceanic Sciences 8(4), 461-480.

Speer, J. A. (1983). Crystal chemistry and phase relations of orthorhombic carbonates. Reviews in Mineralogy and Geochemistry 11, 145–190.

Starrs, D., Davis, J. T., Schlaefer, J., Ebner, B. C., Eggins, S. M. and Fulton, C. J. (2014a) Maternally transmitted isotopes and their effects on larval fish: a validation of dual isotopic marks within a meta-analysis context. Canadian Journal of Fisheries and Aquatic Sciences 713, 387-397.

Starrs, D., Ebner, B., Eggins, S. and Fulton, C. (2014b) Longevity in maternal transmission of isotopic marks in a tropical freshwater rainbowfish and the implications for offspring morphology. Marine and Freshwater Research 655, 400-408.

Steven, E. C. (1999) Chemistry and composition of fish otoliths: pathways, mechanisms and applications. Marine Ecology Progress Series 188, 263-297.

Stowasser, G., Pierce, G. J., Moffat, C. F., Collins, M. A. and Forsythe, J. W. (2006) Experimental study on the effect of diet on fatty acid and stable isotope profiles of the squid *Lolliguncula brevis*. Journal of Experimental Marine Biology and Ecology 3331, 97-114.

Sugimoto, C. and Ikeda, Y. (2013) Comparison of the Ontogeny of Hunting Behavior in Pharaoh Cuttlefish (*Sepia pharaonis*) and Oval Squid (*Sepioteuthis lessoniana*). The Biological Bulletin 2251, 50-59.

Sugimoto, C., Yanagisawa, R., Nakajima, R. and Ikeda, Y. (2013) Observations of schooling behaviour in the oval squid *Sepioteuthis lessoniana* in coastal waters of Okinawa Island. Marine Biodiversity Records 6.

Swearer, S. E., Caselle, J. E., Lea, D. W. and Warner, R. R. (1999) Larval retention and recruitment in an island population of a coral-reef fish. Nature 4026763, 799-802.

Sweeting, C., Barry, J., Polunin, N. and Jennings, S. (2007) Effects of body size and environment on diet-tissue $\delta^{13}C$ fractionation in fishes. Journal of Experimental Marine Biology and Ecology 3521, 165-176.

Tang, T., Tai, J. and Yang, Y. (2000) The flow pattern north of Taiwan and the migration of the Kuroshio. Continental Shelf Research 204-5, 349-371.

Thorrold, S. R., Campana, S. E., Jones, C. M. and Swart, P. K. (1997) Factors determining $\delta^{13}C$ and $\delta^{18}O$ fractionation in aragonitic otoliths of marine fish. Geochimica et Cosmochimica Acta 6114, 2909-2919.

Thorrold, S. R., Jones, G. P., Planes, S. and Hare, J. A. (2006) Transgenerational marking of embryonic otoliths in marine fishes using barium stable isotopes. Canadian Journal of Fisheries and Aquatic Sciences 636, 1193-1197.

Thorrold, S. R., Latkoczy, C., Swart, P. K. and Jones, C. M. (2001) Natal homing in a marine fish metapopulation. Science 2915502, 297-299.

Tohse, H. and Mugiya, Y. (2008) Sources of otolith carbonate: experimental determination of carbon incorporation rates from water and metabolic CO_2, and their diel variations. Aquatic Biology 13, 259-268.

Toledo, P., Niklitschek, E. J., Darnaude, A. M., Leiva, F. P., Harrod, C., Lillo, S., Ojeda, V., Klarian, S., Molina-Burgos, B. E. and Gálvez, P. (2020) The trophic ecology of partial migration: insights from *Merluccius australis* off NW Patagonia. ICES Journal of Marine Science 775, 1927-1940.

Tomano, S., Sanchez, G., Kawai, K., Kasaoka, N., Ueta, Y. and Umino, T. (2016) Contribution of *Sepioteuthis* sp. 1 and *Sepioteuthis* sp. 2 to oval squid fishery stocks in western Japan. Fisheries Science 824, 585-596.

Trasviña-Carrillo, L. D., Hernández-Herrera, A., Torres-Rojas, Y. E., Galván-Magaña, F., Sánchez-González, A. and Aguíñiga-García, S. (2018) Spatial and trophic preferences of jumbo squid *Dosidicus gigas* (D'Orbigny, 1835) in the central Gulf of California: ecological inferences using stable isotopes. Rapid Communications in Mass Spectrometry 3215, 1225-1236.

Trueman, C. N., MacKenzie, K. and Palmer, M. (2012) Identifying migrations in marine fishes through stable-isotope analysis. Journal of Fish Biology 812, 826-847.

Tseng, H. C., You, W. L., Huang, W., Chung, C. C., Tsai, A. Y., Chen, T. Y., Lan, K. W. and Gong, G. C. (2020) Seasonal Variations of Marine Environment and Primary Production in the Taiwan Strait. Frontiers in Marine Science 738.

Ueta, Y. and Jo, Y. (1990) Migration of the oval squid, *Sepioteuthis lessoniana* around Tokushima prefecture. Suisanzoshoku 38, 221-226.

Vidal, E. A., DiMarco, F. P., Wormuth, J. H. and Lee, P. G. (2002) Influence of temperature and food availability on survival, growth and yolk utilization in hatchling squid. Bulletin of Marine Science 712, 915-931.

Vidal, É. A., DiMarco, P. and Lee, P. (2006) Effects of starvation and recovery on the survival, growth and RNA/DNA ratio in loliginid squid paralarvae. Aquaculture 2601-4, 94-105.

Wade, Y, and Kobayashi, T. (1995) On an iteroparity of the oval squid *Sepioteuthis lessoniana*. Nippon Suisan Gakkaishi 612, 151-158.

Wada, T., Takegaki, T., Mori, T. and Natsukari, Y. (2005) Alternative male mating behaviors dependent on relative body size in captive oval squid *Sepioteuthis lessoniana* (Cephalopoda, Loliginidae). Zoological Science 226, 645-651.

Walsh, L., Turk, P., Forsythe, J. and Lee, P. (2002) Mariculture of the loliginid squid *Sepioteuthis lessoniana* through seven successive generations. Aquaculture 2121-4, 245-262.

Walther, B. D., Kingsford, M. J., O'Callaghan, M. D. and McCulloch, M. T. (2010) Interactive effects of ontogeny, food ration and temperature on elemental incorporation in otoliths of a coral reef fish. Environmental Biology of Fishes 893-4, 441-451.

Warren-Myers, F., Dempster, T., Fjelldal, P. G., Hansen, T. and Swearer, S. E. (2015) Immersion during egg swelling results in rapid uptake of stable isotope markers in salmonid otoliths. Canadian Journal of Fisheries and Aquatic Sciences 725, 722-727.

Warren-Myers, F., Dempster, T. and Swearer, S. E. (2018) Otolith mass marking techniques for aquaculture and restocking: benefits and limitations. Reviews in Fish Biology and Fisheries 283, 485-501.

Weidel, B. C., Ushikubo, T., Carpenter, S. R., Kita, N. T., Cole, J. J., Kitchell, J. F., Pace, M. L. and Valley, J. W. (2007) Diary of a bluegill (*Lepomis macrochirus*): daily $\delta^{13}C$ and $\delta^{18}O$ records in otoliths by ion microprobe. Canadian Journal of Fisheries and Aquatic Sciences 6412, 1641-1645.

Williamson, D. H., Jones, G. P. and Thorrold, S. R. (2009) An experimental evaluation of transgenerational isotope labelling in a coral reef grouper. Marine Biology 15612, 2517-2525.

Woodcock, S., Gillanders, B., Munro, A. R., McGovern, F., Crook, D. and Sanger, A. (2011a) Using enriched stable isotopes of barium and magnesium to batch mark otoliths of larval golden perch (*Macquaria ambigua*, Richardson). Ecology of Freshwater Fish 201, 157-165.

Woodcock, S. H., Gillanders, B. M., Munro, A. R., Crook, D. A. and Sanger, A. C. (2011b) Determining mark success of 15 combinations of enriched stable isotopes for the batch marking of larval otoliths. North American Journal of Fisheries Management 315, 843-851.

Woodcock, S. H. and Walther, B. D. (2014) Concentration-dependent mixing models predict values of diet-derived stable isotope ratios in fish otoliths. Journal of Experimental Marine Biology and Ecology 454, 63-69.

Wurster, C. M. and Patterson, W. P. (2003) Metabolic rate of late Holocene freshwater fish: evidence from $\delta^{13}C$ values of otoliths. Paleobiology 294, 492-505.

Yamaguchi, T., Aketagawa, T., Miyamoto, M., Hirose, N. and Matsuyama, M. (2018) The use of statolith analyses and particle-tracking experiments to reveal the migratory route of the swordtip squid (*Uroteuthis edulis*) caught on the Pacific side of Japan. Fisheries Oceanography 276, 517-524.

Yamaguchi, T., Aketagawa, T., Takayama, K., Hirose, N. and Matsuyama, M. (2019) Migratory routes of different sized swordtip squid (*Uroteuthis edulis*) caught in the Tsushima Strait. Fisheries Research 209, 24-31.

Yamaguchi, T., Kawakami, Y. and Matsuyama, M. (2015) Migratory routes of the swordtip squid *Uroteuthis edulis* inferred from statolith analysis. Aquatic Biology 241, 53-60.

Young, R. E. (1978) Vertical distribution and photosensitive vesicles of pelagic cephalopods from Hawaiian waters. Fishery Bulletin 763, 583-615.

Zitek, A., Irrgeher, J., Kletzl, M., Weismann, T. and Prohaska, T. (2013) Transgenerational marking of brown trout *Salmo trutta f.f.*, using an ^{84}Sr spike. Fisheries Management and Ecology 204, 354-361.

Zumholz, K., Hansteen, T., Hillion, F., Horreard, F. and Piatkowski, U. (2007) Elemental distribution in cephalopod statoliths: NanoSIMS provides new insights into nano-scale structure. Reviews in Fish Biology and Fisheries 172-3, 487-491.

Table 1 Summary of the mantle length, body weight, Fulton's condition factor *K* and $^{138}Ba/^{137}Ba$ ratio among the control group and all experimental treatments.

		Mantle length (mm)		Body weight (mg)		Fulton's condition factor (*K*)		$^{138}Ba/^{137}Ba$ ratio	
Treatment	n	Mean ± s.d.	Range	Mean ± s.d.	Range	Mean ± s.d.	Range	Mean ± s.d.	Range
Control	15	5.54 ± 0.50	4.89 - 6.37	24.40 ± 6.28	10 - 33	14.21 ± 2.79	8.55 - 20.31	6.28 ± 0.17	6.08 - 6.52
0.2 ppm, 1 day	15	5.96 ± 0.44	5.21 - 6.63	27.53 ± 4.03	17 - 32	13.12 ± 2.27	9.61 - 18.07	6.18 ± 0.17	5.98 - 6.51
0.5 ppm, 1 day	15	5.78 ± 0.58	4.52 - 6.66	26.73 ± 4.32	16 - 30	14.15 ± 3.25	10.20 - 21.66	6.01 ± 0.15	5.75 - 6.29
1 ppm, 1 day	15	5.99 ± 0.28	5.41 - 6.60	27.67 ± 1.99	24 - 31	12.98 ± 1.63	10.37 - 16.42	5.85 ± 0.24	5.25 - 6.10
0.2 ppm, 3 day	15	5.93 ± 0.33	5.14 - 6.27	29.40 ± 3.25	22 - 35	14.13 ± 1.58	12.41 - 17.78	5.83 ± 0.13	5.60 - 6.06
0.5 ppm, 3 day	15	5.77 ± 0.31	5.17 - 6.13	31.27 ± 2.66	27 - 37	16.43 ± 2.50	13.79 - 23.16	5.30 ± 0.18	4.97 - 5.64
1 ppm, 3 day	15	5.78 ± 0.17	5.37 - 5.95	28.93 ± 1.83	25 - 32	15.04 ± 1.17	13.77 - 17.44	4.57 ± 0.36	4.12 - 5.44
0.2 ppm, 7 day	15	5.91 ± 0.25	5.34 - 6.17	28.40 ± 3.54	22 - 36	13.76 ± 1.62	11.23 - 16.48	5.34 ± 0.24	4.89 - 5.78
0.5 ppm, 7 day	15	5.77 ± 0.31	4.96 - 6.16	28.87 ± 3.50	21 - 33	15.10 ± 1.94	12.75 - 18.59	4.61 ± 0.28	4.29 - 5.21
1 ppm, 7 day	15	5.84 ± 0.19	5.57 - 6.16	29.00 ± 2.70	25 - 36	14.54 ± 1.12	12.16 - 16.83	3.50 ± 0.22	3.20 - 3.99

Table 2 Nonparametric analysis of variance results for the difference in ^{137}Ba-spiked concentrations (0, 0.2, 0.5 and 1 ppm) and immersion durations (0, 1, 3 and 7 days) for Ba isotopes ratios in the statoliths of hatchlings. Boldface indicates significant *P*-values.

	df	MS	F	*p*
Mantle length				
Immersion duration	3	0.913	5.190	**0.002**
Concentration	3	1.018	5.789	**0.001**
Immersion duration × Concentration	9	0.140	0.795	0.622
Residual	224	0.176		
Body weight				
Immersion duration	3	188.949	8.222	**< 0.001**
Concentration	3	153.682	6.687	**< 0.001**
Immersion duration × Concentration	9	26.697	1.162	0.321
Residual	224	22.982		
Fulton's condition *K*				
Immersion duration	3	18.235	3.214	**0.024**
Concentration	3	14.353	2.530	0.058
Immersion duration × Concentration	9	4.660	0.821	0.597
Residual	224	5.674		

Table 3 Structure matrix coefficients for Discriminant Function (DF) 1 and DF2 for each mean element : Ca ratio used in canonical discriminant analysis for hatchling statoliths among the control and experimental groups. Main contributed elements are represented in bold.

Elements	DF1	DF2
Cu/Ca	**0.689**	0.254
Zn/Ca	0.506	**0.484**
Pb/Ca	0.336	-0.339
Mg/Ca	0.094	0.042
Sr/Ca	0.082	0.350

Table 4 The cross-validated classification success for the statoliths of hatchlings in the control and experimental groups based on the discriminant function analysis scores. Correct classifications are represented in bold.

Treatments	Control	0.2 ppm 1 day	0.5 ppm 1 day	1 ppm 1 day	0.2 ppm 3 days	0.5 ppm 3 days	1 ppm 3 days	0.2 ppm 7 days	0.5 ppm 7 days	1 ppm 7 days
Control	**26.7**	26.7	0.0	0.0	6.7	13.3	13.3	6.7	6.7	0.0
0.2 ppm, 1 day	20.0	**20.0**	0.0	13.3	0.0	20.0	6.7	13.3	6.7	0.0
0.5 ppm, 1 day	0.0	0.0	**13.3**	20.0	6.7	26.7	6.7	6.7	6.7	13.3
1 ppm, 1 day	6.7	20.0	13.3	**26.7**	0.0	0.0	26.7	0.0	0.0	6.7
0.2 ppm, 3 days	13.3	6.7	13.3	0.0	**6.7**	13.3	13.3	13.3	13.3	6.7
0.5 ppm, 3 days	13.3	6.7	6.7	0.0	6.7	**20.0**	0.0	13.3	26.7	6.7
1 ppm, 3 days	0.0	13.3	0.0	6.7	6.7	6.7	**40.0**	6.7	6.7	13.3
0.2 ppm, 7 days	20.0	0.0	6.7	0.0	0.0	13.3	6.7	**0.0**	20.0	33.3
0.5 ppm, 7 days	6.7	0.0	6.7	0.0	0.0	13.3	13.3	0.0	**40.0**	20.0
1 ppm, 7 days	0.0	6.7	0.0	0.0	0.0	6.7	0.0	13.3	20.0	**53.3**

Table 5 Summary of Spearman's ρ test between Ba stable isotopes and trace elements in the statoliths of hatchlings. Significant correlations ($P < 0.05$) are in bold.

	Mg : Ca (mmol mol^{-1})	Sr : Ca (mmol mol^{-1})	Zn : Ca (μmol mol^{-1})	Cu : Ca (μmol mol^{-1})	Pb : Ca (μmol mol^{-1})
^{137}Ba : Ca (μmol mol^{-1})					
r_s	0.503	–0.122	0.055	–0.067	–0.030
P-value	0.138	0.738	0.881	0.855	0.934
^{138}Ba : Ca (μmol mol^{-1})					
r_s	0.588	0.012	**0.794**	**0.794**	**0.794**
P-value	0.074	0.973	**0.006**	**0.006**	**0.006**

Table 6 Sampling date, mantle length, age estimation, and back-calculated hatching date and season for each *S. lessoniana* individual used in statolith oxygen isotopic analysis.

Sample code	Mantle length (mm)	Age (days)	Sampling date	Hatching date	Seasonal group
2017-Northern Taiwan					
K171102001	323	166	2 Nov. 2017	20 May 2017	Spring
K171102003	285	167	2 Nov. 2017	19 May 2017	Spring
K171102004	279	153	2 Nov. 2017	2 Jun. 2017	Spring
K171102006	313	152	2 Nov. 2017	3 Jun. 2017	Spring
K171102010	239	159	2 Nov. 2017	27 May 2017	Spring
K171102011	215	167	2 Nov. 2017	19 May 2017	Spring
K171102012	194	150	2 Nov. 2017	5 Jun. 2017	Spring
K180116002	256	148	16 Jan. 2018	21 Aug. 2017	Summer
K180116003	231	147	16 Jan. 2018	22 Aug. 2017	Summer
K180116005	261	146	16 Jan. 2018	23 Aug. 2017	Summer
K180116007	244	153	16 Jan. 2018	16 Aug. 2017	Summer
K180116012	264	160	16 Jan. 2018	9 Aug. 2017	Summer
K180313003	302	192	13 Mar. 2018	2 Sep. 2017	Summer
K180313001	339	176	13 Mar. 2018	18 Sep. 2017	Autumn
K180313002	302	172	13 Mar. 2018	22 Sep.2017	Autumn
K180313004	271	163	13 Mar. 2018	1 Oct. 2017	Autumn
K180313007	253	140	13 Mar. 2018	24 Oct. 2017	Autumn
K180313008	234	143	13 Mar. 2018	21 Oct. 2017	Autumn
K180329001	354	177	29 Mar. 2018	3 Oct. 2017	Autumn
K180329002	360	164	29 Mar. 2018	16 Oct. 2017	Autumn
K180329003	285	176	29 Mar. 2018	4 Oct. 2017	Autumn
K180329004	281	174	29 Mar. 2018	6 Oct. 2017	Autumn
2017-Penghu Islands					
P171122001	243	175	22 Nov. 2017	31 May 2017	Spring
P171122002	263	181	22 Nov. 2017	25 May 2017	Spring
P171229001	330	207	29 Dec. 2017	5 Jun. 2017	Spring
P180107001	367	228	7 Jan. 2018	24 May 2017	Spring

Table 6 Continued.

Sample code	Mantle length (mm)	Age (days)	Sampling date	Hatching date	Seasonal group
2017-Penghu Islands					
P171127002	200	149	27 Nov. 2017	1 Jul. 2017	Summer
P171228002	311	198	28 Dec. 2017	13 Jun. 2017	Summer
P171229002	301	181	29 Dec. 2017	1 Jul. 2017	Summer
P180116002	312	198	16 Jan. 2018	2 Jul. 2017	Summer
P180117001	300	184	17 Jan. 2018	17 Jul. 2017	Summer
P180118001	274	189	18 Jan. 2018	13 Jul. 2017	Summer
P180118002	287	195	18 Jan. 2018	7 Jul. 2017	Summer
P180302005	382	240	2 Mar. 2018	5 Jul. 2017	Summer
P180304001	378	219	4 Mar. 2018	28 Jul. 2017	Summer
P180304004	327	190	4 Mar. 2018	26 Aug. 2017	Summer
P180304005	291	201	4 Mar. 2018	15 Aug. 2017	Summer
P180313001	372	198	13 Mar. 2018	27 Aug. 2017	Summer
P180302001	246	143	2 Mar. 2018	10 Oct. 2017	Autumn
P180302002	244	169	2 Mar. 2018	14 Sep. 2017	Autumn
P180304002	188	149	4 Mar. 2018	6 Oct. 2017	Autumn
P180304003	247	163	4 Mar. 2018	22 Sep. 2017	Autumn
P180313002	292	184	13 Mar. 2018	10 Sep. 2017	Autumn

Table 7 Results of nonparametric analysis of variance to test the differences in *S. lessoniana* statolith oxygen isotopes ratios among seasonal groups (spring, summer, and autumn) and ontogenetic (embryonic–paralarval, juvenile, juvenile–subadult, and subadult–adult) stages. Boldface indicates significant *P*-values.

	df	SS	MS	H	*P*
Northern Taiwan					
Seasonal group	2	696.40		1.506	0.471
Ontogenetic stage	3	18472.92		39.941	< **0.001**
Seasonal group × Ontogenetic stage	6	4558.88		9.857	0.131
Total	73	33762.50	462.50		
Penghu Islands					
Seasonal group	2	1820.61		3.304	0.1916
Ontogenetic stage	3	16562.20		30.059	< **0.001**
Seasonal group × Ontogenetic stage	6	8787.57		15.949	**0.014**
Total	73	40222.72	551.00		

Table 8 Sample size, morphology and stable isotopic composition of muscles and statoliths of *S. lessoniana* from two sampling sites.

Collection site	N	Mantle length (mm) Range Mean ± s.d.	Body weight (g) Range Mean ± s.d.	$\delta^{13}C_{muscle}$ (‰) Range Mean ± s.d.	$\delta^{15}N_{muscle}$ (‰) Range Mean ± s.d.	C:N ratio of muscle Range Mean ± s.d.	$\delta^{13}C_{statolith}$ (‰) Range Mean ± s.d.
Northern Taiwan	77	72 — 360 217.2 ± 75.0	28 — 1746 623.7 ± 471.8	-18.21 — -15.35 -16.88 ± 0.49	11.11 — 14.40 12.73 ± 0.72	2.97 — 3.96 3.49 ± 0.21	- -
Northern Taiwan	22	194 — 360 276.6 ± 43.7	382 — 1746 998.5 ± 382.9	- -	- -	- -	-11.17 — -7.89 -9.37 ± 0.71
Penghu Islands	21	188 — 382 293.1 ± 54.9	417 — 2510 1298.3 ± 626.6	- -	- -	- -	-11.37 — -4.41 -8.86 ± 1.30

Table 9 The width of growth increment, estimated ML, and estimated BW of *S. lessoniana* in early (embryonic-juvenile) and later (subadult-adult) life history stages from two collection sites. The estimated mantle length (ML) and estimated body weight (BW) at each life history stage was back-calculated using the logistic growth function and the ML-BW relationship, respectively, in Taiwan (Chen et al., 2015).

Collection site	Early life history stage		Later life history stage	
	Mean ± s.d.	Range	Mean ± s.d.	Range
Northern Taiwan				
Growth increment width (μm)	3.7 ± 0.7	2.4 - 4.9	2.6 ± 0.5	1.5 - 3.5
Estimated ML (mm)	34.1 ± 15.3	8.3 - 73.4	148.2 ± 56.4	57.8 - 255.3
Estimated BW (g)	4.6 ± 4.1	0.1 - 16.9	221.0 ± 199.6	17.2 - 717.2
Penghu Islands				
Growth increment width (μm)	4.0 ± 0.6	2.6 - 5.3	2.8 ± 0.5	1.8 - 4.2
Estimated ML (mm)	34.4 ± 15.1	9.0 - 73.4	172.8 ± 76.9	54.3 - 317.5
Estimated BW (g)	5.8 ± 5.7	0.1 - 26.4	360.3 ± 367.1	14.5 - 1278.9

Table 10 Results of multiple linear regressions correlating statolith $\delta^{13}C_{statolith}$ values with predicted variables for all, early (embryonic-juvenile) and later (subadult-adult) life history stages. The equations of form $\delta^{13}C_{statolith} = a + b_1 \times$ (growth increment width) + $b_2 \times$ (deduced temperature) + $b_3 \times$ (body weight). SE_{est} is standard error of estimate. Boldface indicates significant *P*-values.

Data set	N	*a*	b_1	b_2	b_3	R^2	*P*	SE_{est}
Northern Taiwan								
All stages	74	-8.881	0.33	-0.06	0.0004	0.14	**0.013**	0.68
Early stage	36	na	na	na	na	na	0.416	na
Later stage	38	-6.795	0.25	-0.13	0.0004	0.57	< **0.001**	0.45
Penghu Islands								
All stages	80	-4.125	0.55	-0.26	-0.001	0.24	< **0.001**	1.15
Early stage	35	-2.725	0.31	-0.26	-0.052	0.28	**0.016**	1.00
Later stage	45	-2.449	0.21	-0.29	-0.001	0.29	**0.002**	1.24

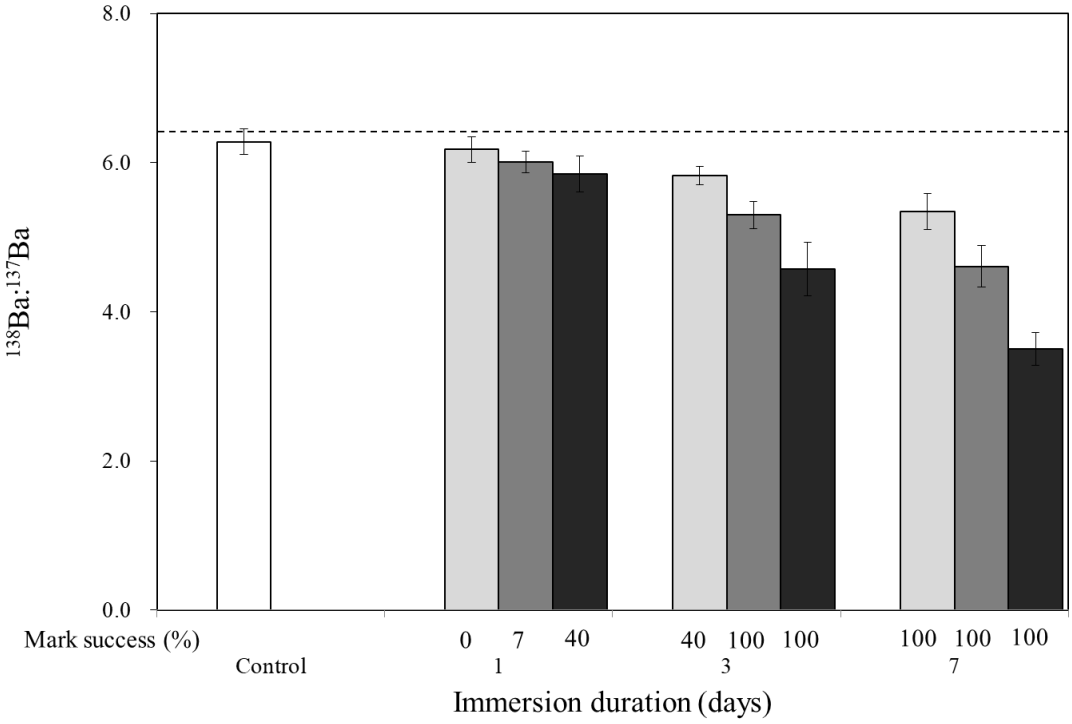

Figure 1 Mean (±s.d.) Ba isotope ratios in the statoliths of hatchlings immersed in water with ^{137}Ba-spiked concentrations of 0.2 (light gray bars), 0.5 (dark gray bars) and 1 ppm (black bars) for 1, 3 and 7 days. Error bars indicate standard deviations, and labels below the columns indicate the percent of mark success for each group. The dashed line indicates the natural ^{138}Ba/^{137}Ba ratio.

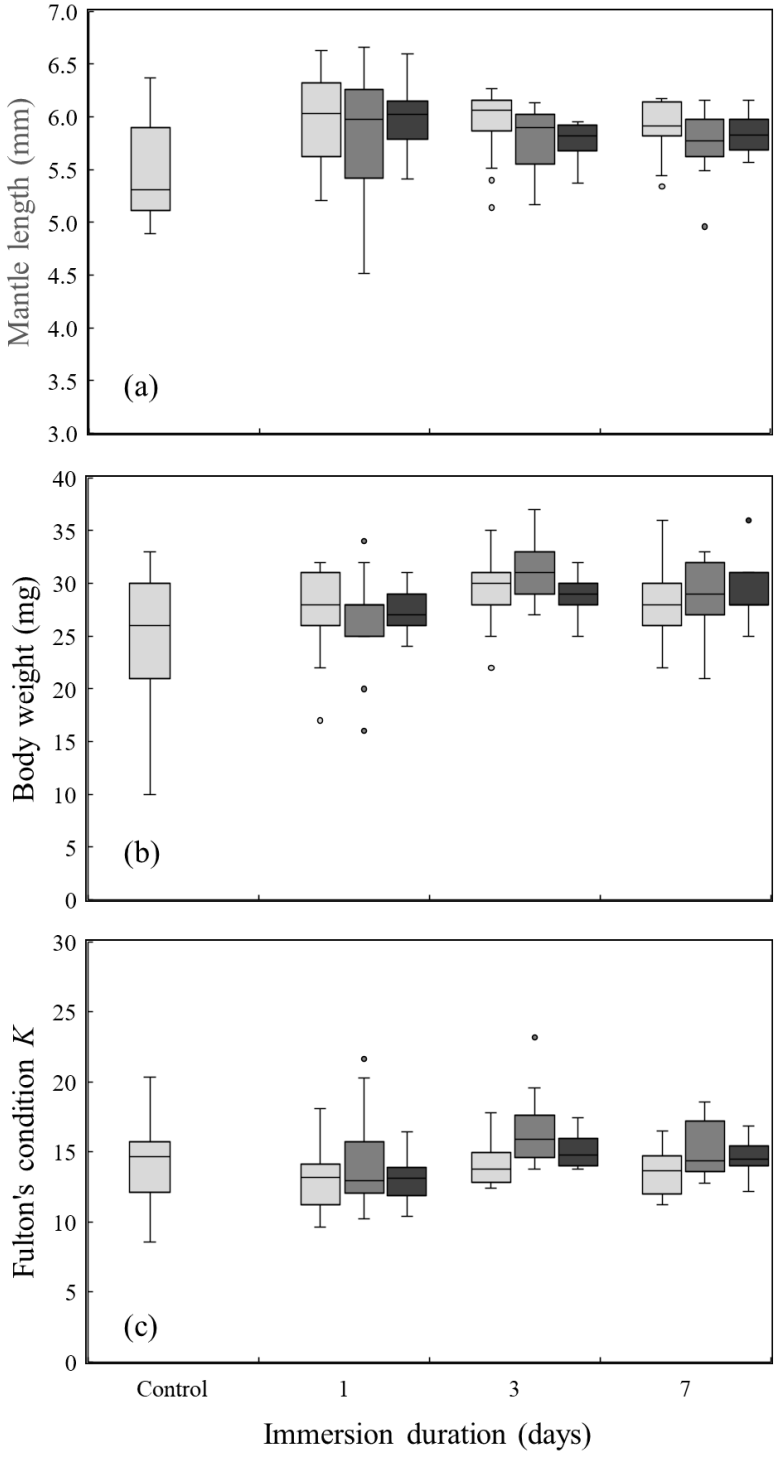

Figure 2 Mantle length, bodyweight and Fulton's condition factor *K* of hatchlings immersed in water with different concentrations of ^{137}Ba spike, namely 0.2 ppm (light grey bars), 0.5 ppm (dark grey bars) and 1 ppm (black bars), for 1, 3 and 7 days and the control group. The boxes show the interquartile range, with the median value indicated by the horizontal line; whiskers show the range. Circles indicate outliers in each experimental group.

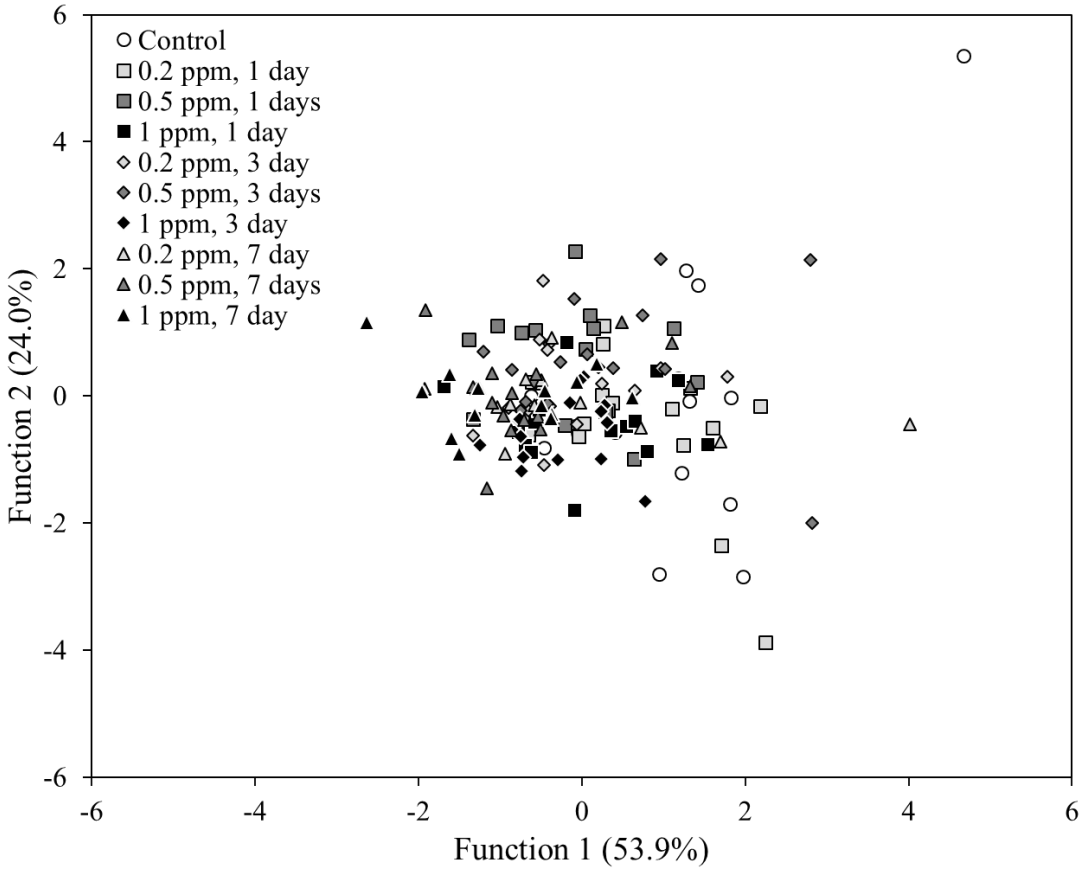

Figure 3 Forward stepwise canonical discriminant analysis using Mg, Sr, Zn, Cu and Pb in the statoliths of hatchlings among control and all experimental groups immersed in water containing different concentrations of ^{137}Ba spike (0.2, 0.5 and 1 ppm) for 1, 3 and 7 days.

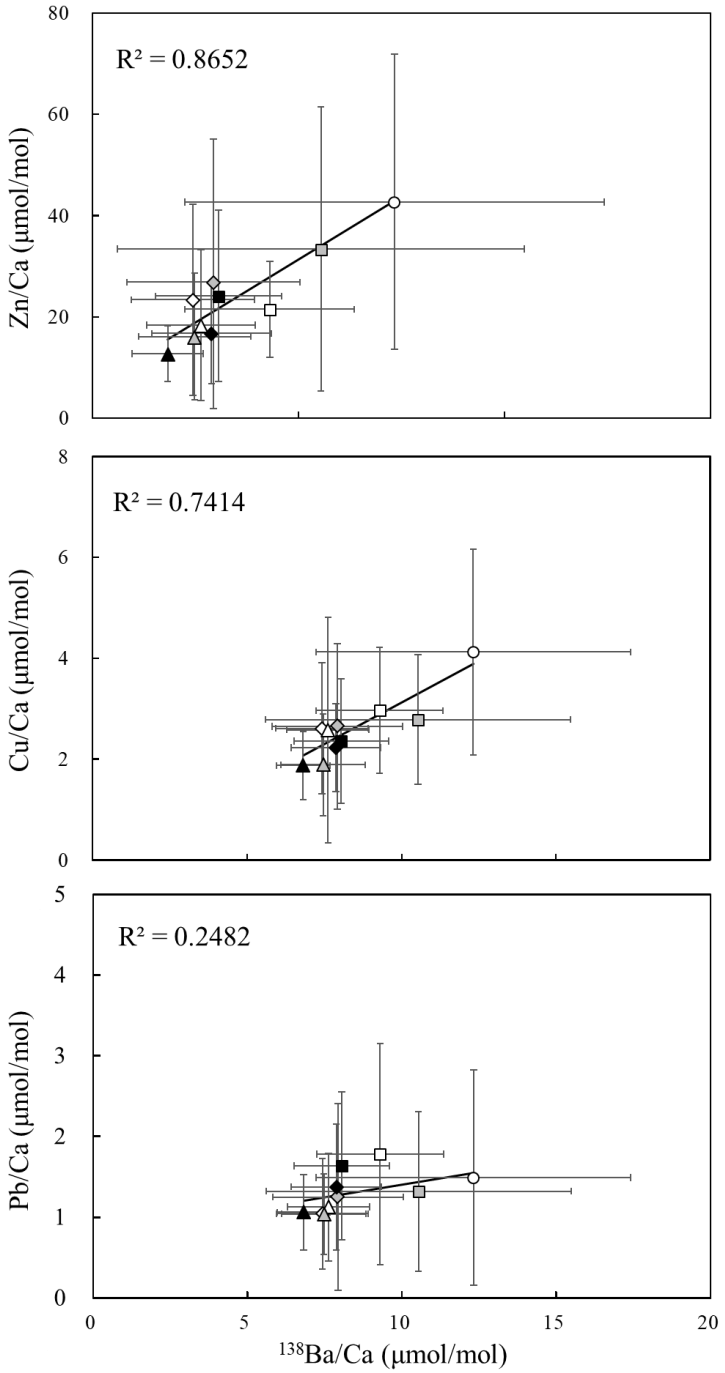

Figure 4 Linear regressions between mean element : Ca ratios and ^{138}Ba : Ca in the statoliths of hatchlings. Symbols indicate different treatment durations (circle, control; square, 1 day; diamond, 3 days; triangle, 7 days) and difference ^{137}Ba spike concentrations (white, 0.2 ppm; grey, 0.5 ppm; black, 1 ppm). Error bars indicate the s.d..

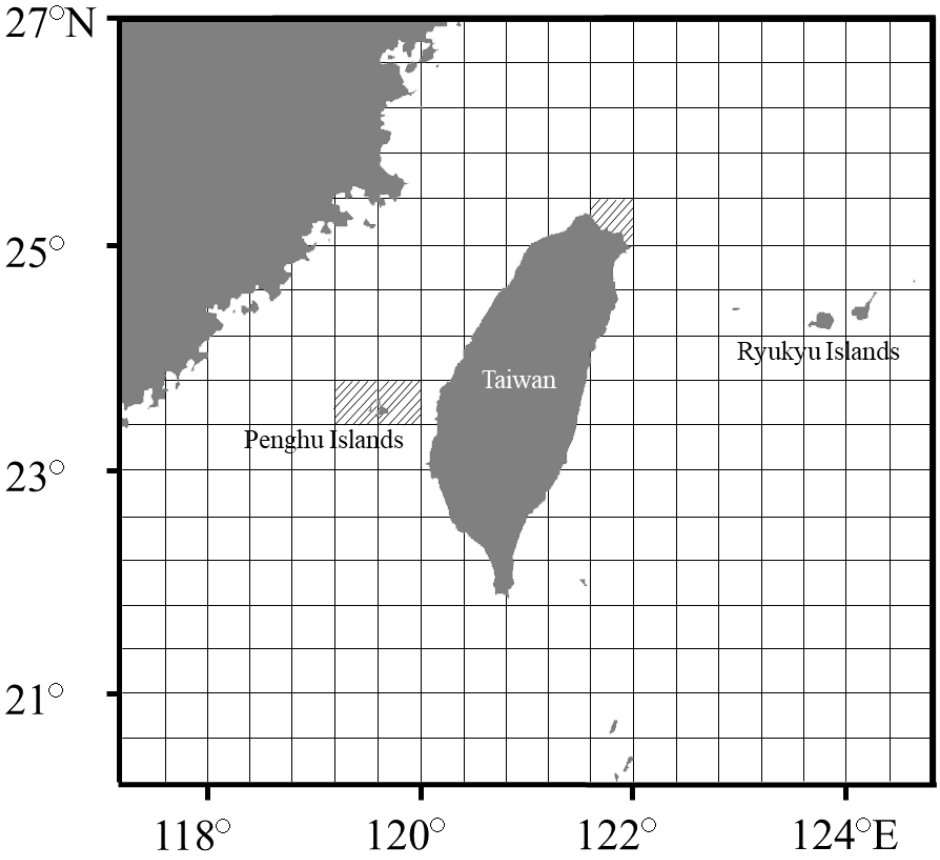

Figure 5 Map showing the collection locations (slanted lines). The unit of spatial grids was 0.4° × 0.4° for the establishment of occurrence probability.

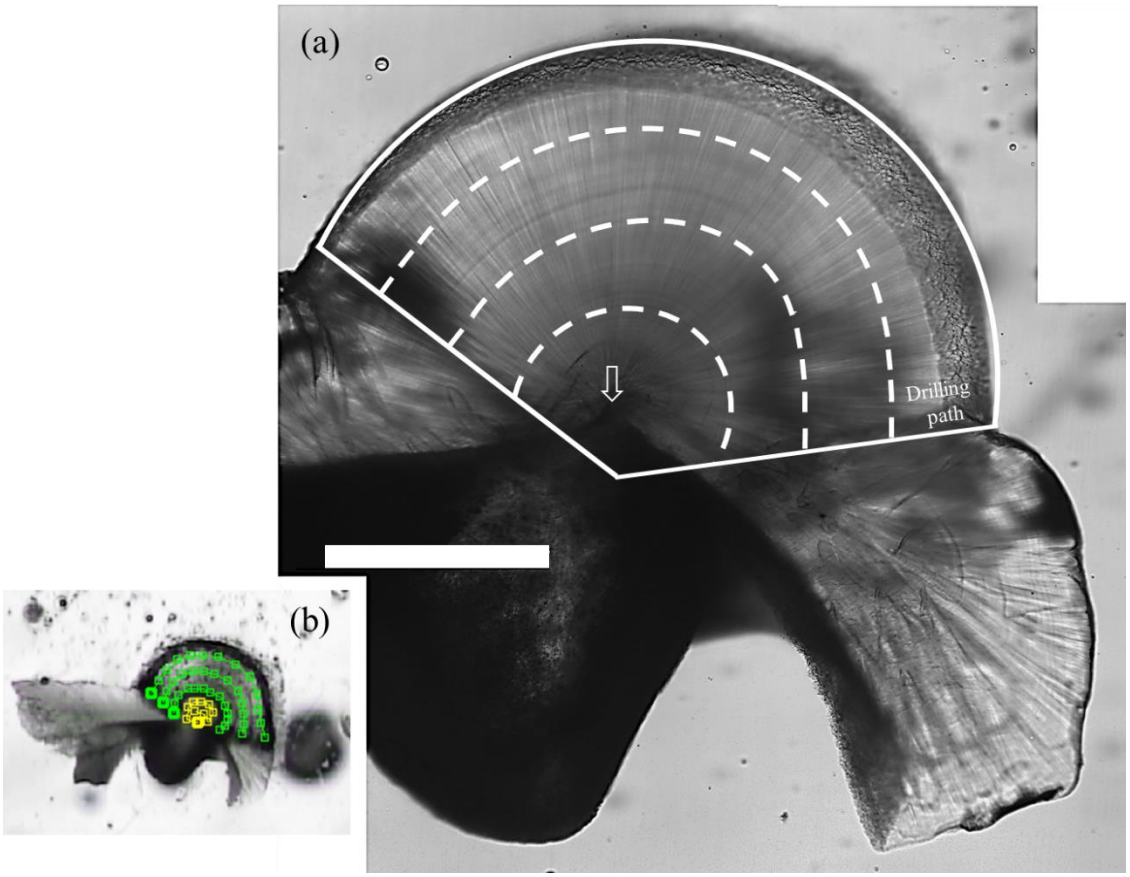

Figure 6 Polished *S. lessoniana* statolith (K180116012) with the drilling paths for powder collection. (a) White solid lines indicate the entire powder collection area at the lateral dome region and dashed lines indicate approximate boundaries of the drilling path. Arrow indicates the statolith core. Scale bar = 400 μm. (b) The setting of the drilling path. Yellow and green lines indicate the paths of drill tip at the core and the outers of the core, respectively, square as a turning point. The intervals between lines are 134–192 μm.

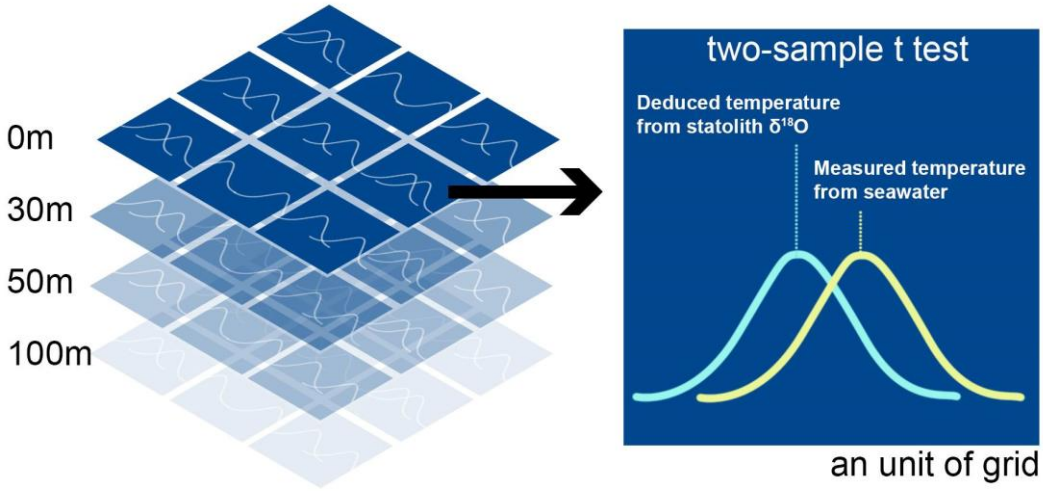

Figure 7 Determination of matching between deduced and measured temperature from the two-sample t test. The deduced temperature was based on the statolith $\delta^{18}O$ values and measured temperature was the data extracted from the HYbrid Coordinate Ocean Model website. The test was conducted in each spatial grip ($0.4^{o} \times 0.4^{o}$) at depths for each specific life stage of *S. lessoniana*. The criteria of matching was set as the *P*-value of 0.05.

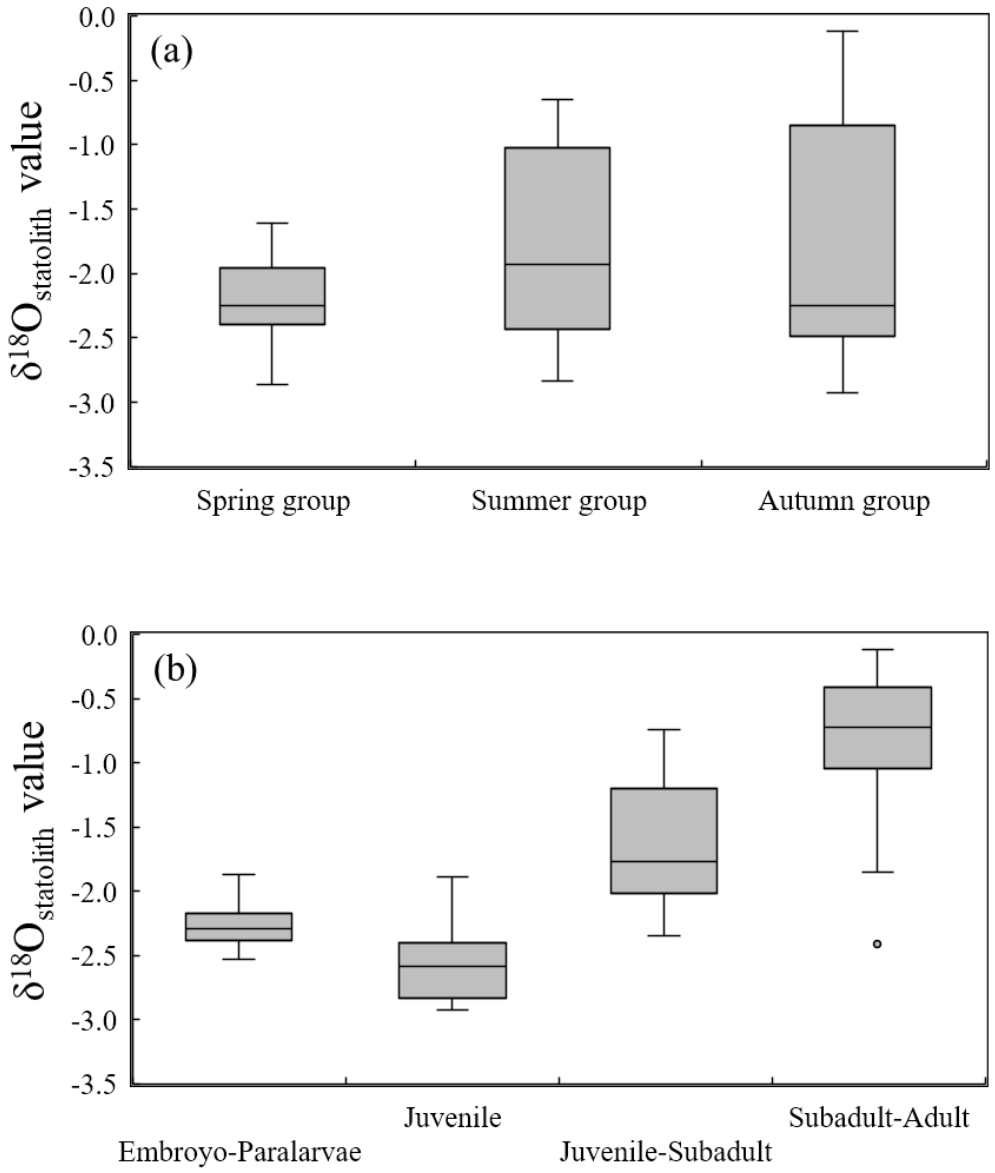

Figure 8 $\delta^{18}O_{statolith}$ values in *S. lessoniana* hatched in 2017 from northern Taiwan in three seasonal groups and at four ontogenetic stages. The box plots show the interquartile range, with the median value indicated by the horizontal line; whiskers show the range. Circles indicate outliers.

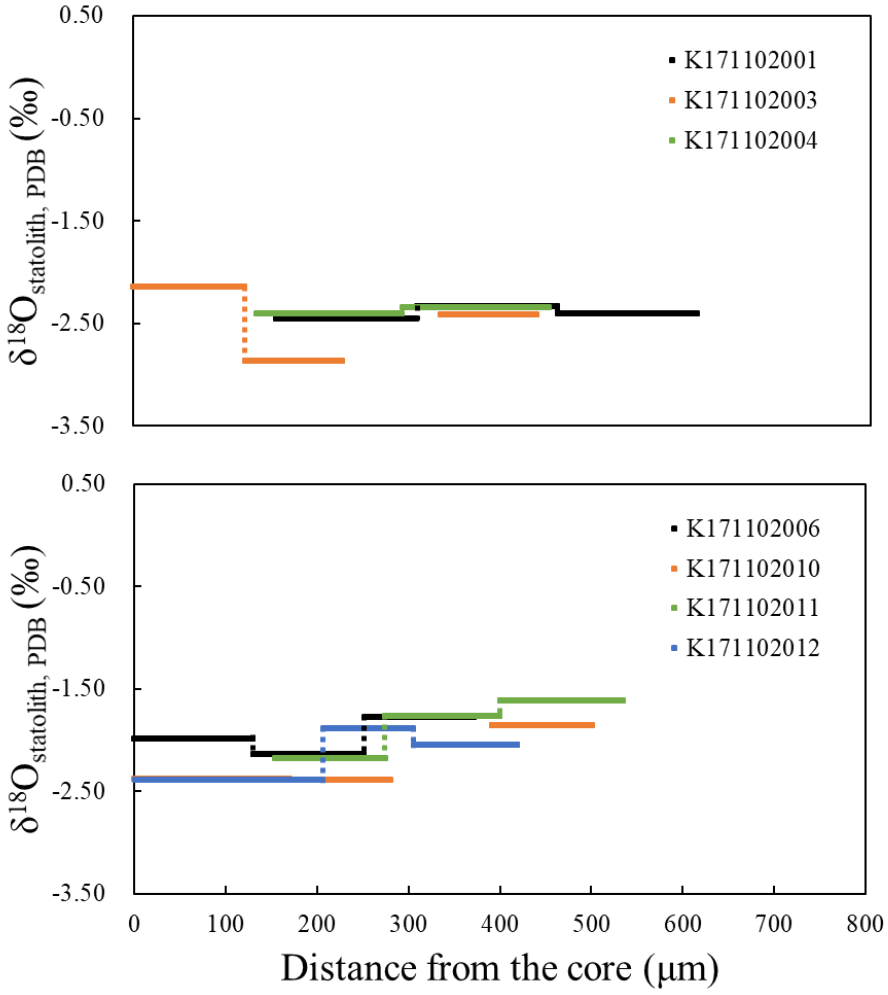

Figure 9 $\delta^{18}O_{statolith}$ profiles of *S. lessoniana* from the statolith core to the edge of each individual in the spring group of 2017-Northern Taiwan.

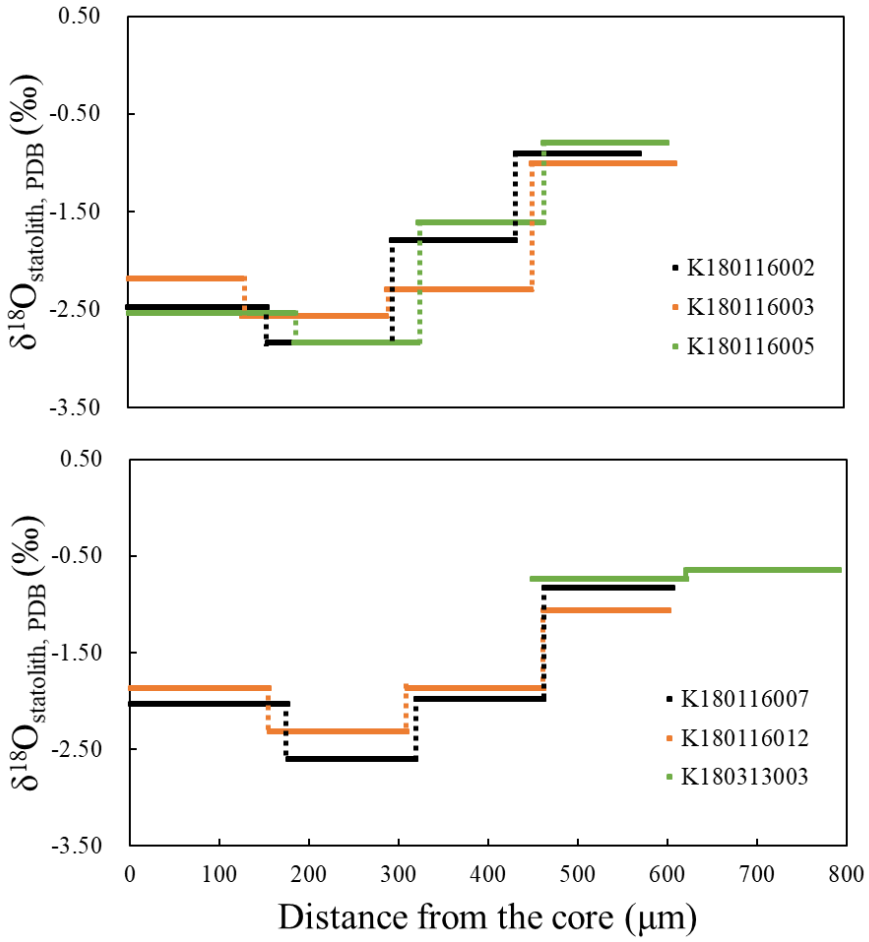

Figure 10 $\delta^{18}O_{statolith}$ profiles of *S. lessoniana* from the statolith core to the edge of each individual in the summer group of 2017-Northern Taiwan.

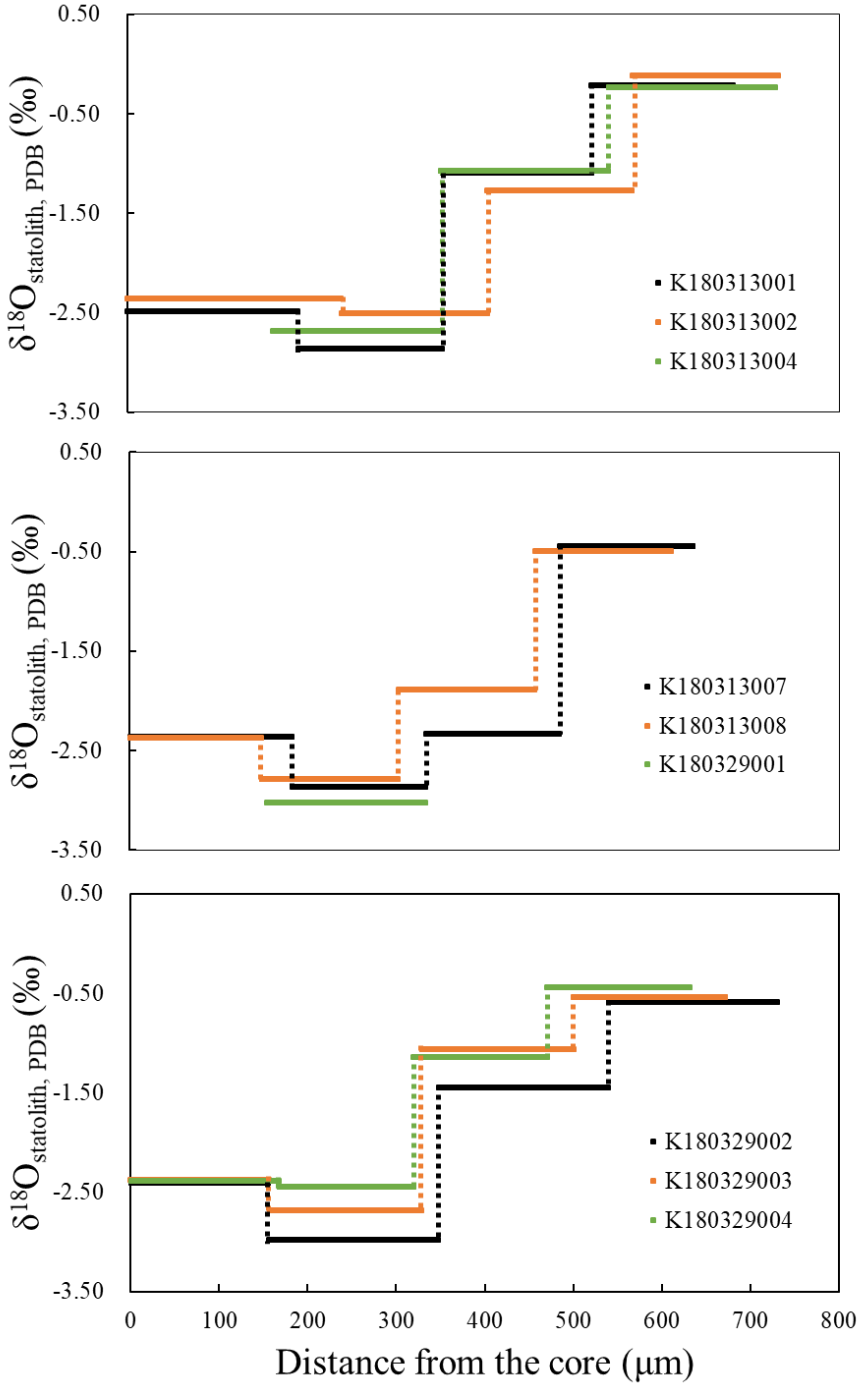

Figure 11 $\delta^{18}O_{statolith}$ profiles of *S. lessoniana* from the statolith core to the edge of each individual in the autumn group of 2017-Northern Taiwan.

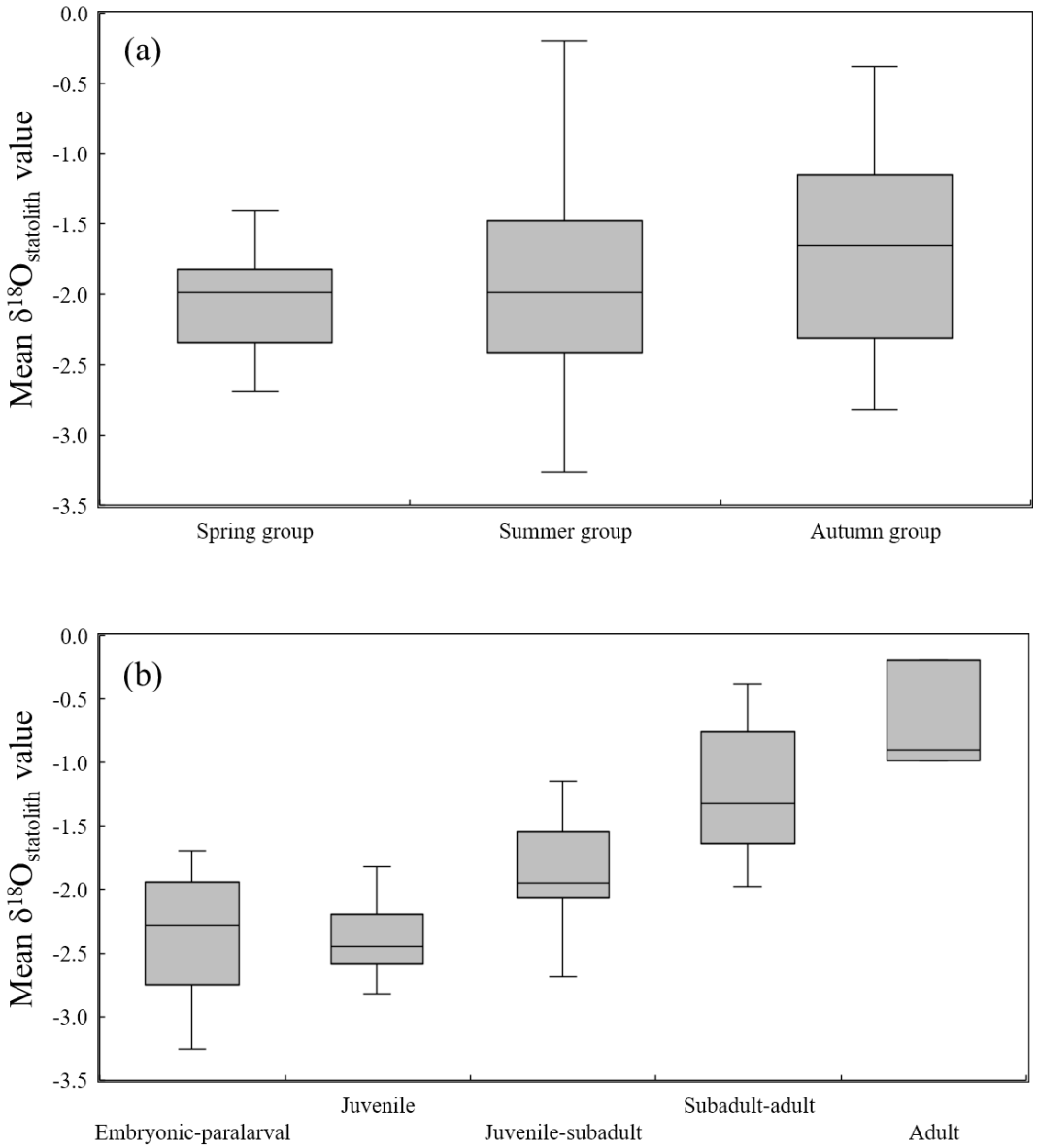

Figure 12 $\delta^{18}O_{statolith}$ values in *S. lessoniana* hatched in 2017 from Penghu Islands in three seasonal groups and at five ontogenetic stages. The box plots show the interquartile range, with the median value indicated by the horizontal line; whiskers show the range.

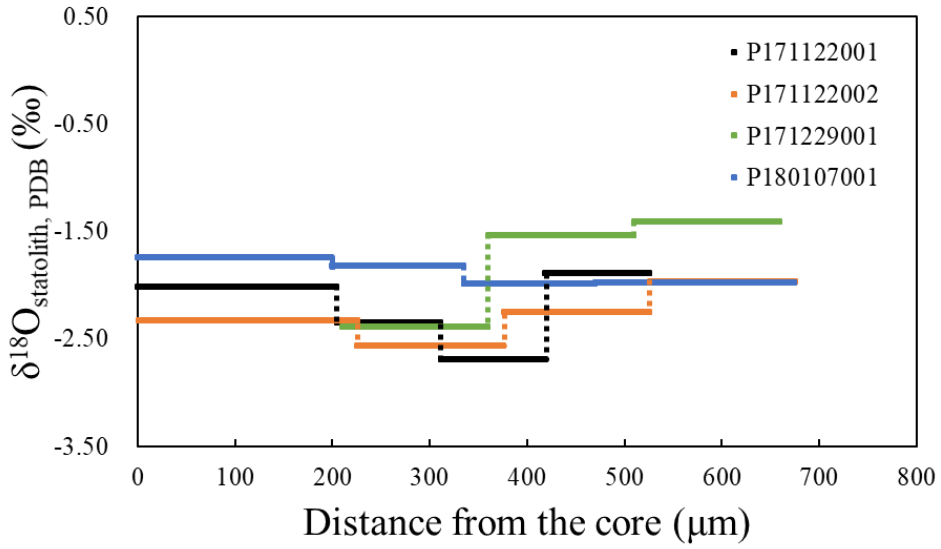

Figure 13 $\delta^{18}O_{statolith}$ profiles of *S. lessoniana* from the statolith core to the edge of each individual in the spring group of 2017-Penghu Islands.

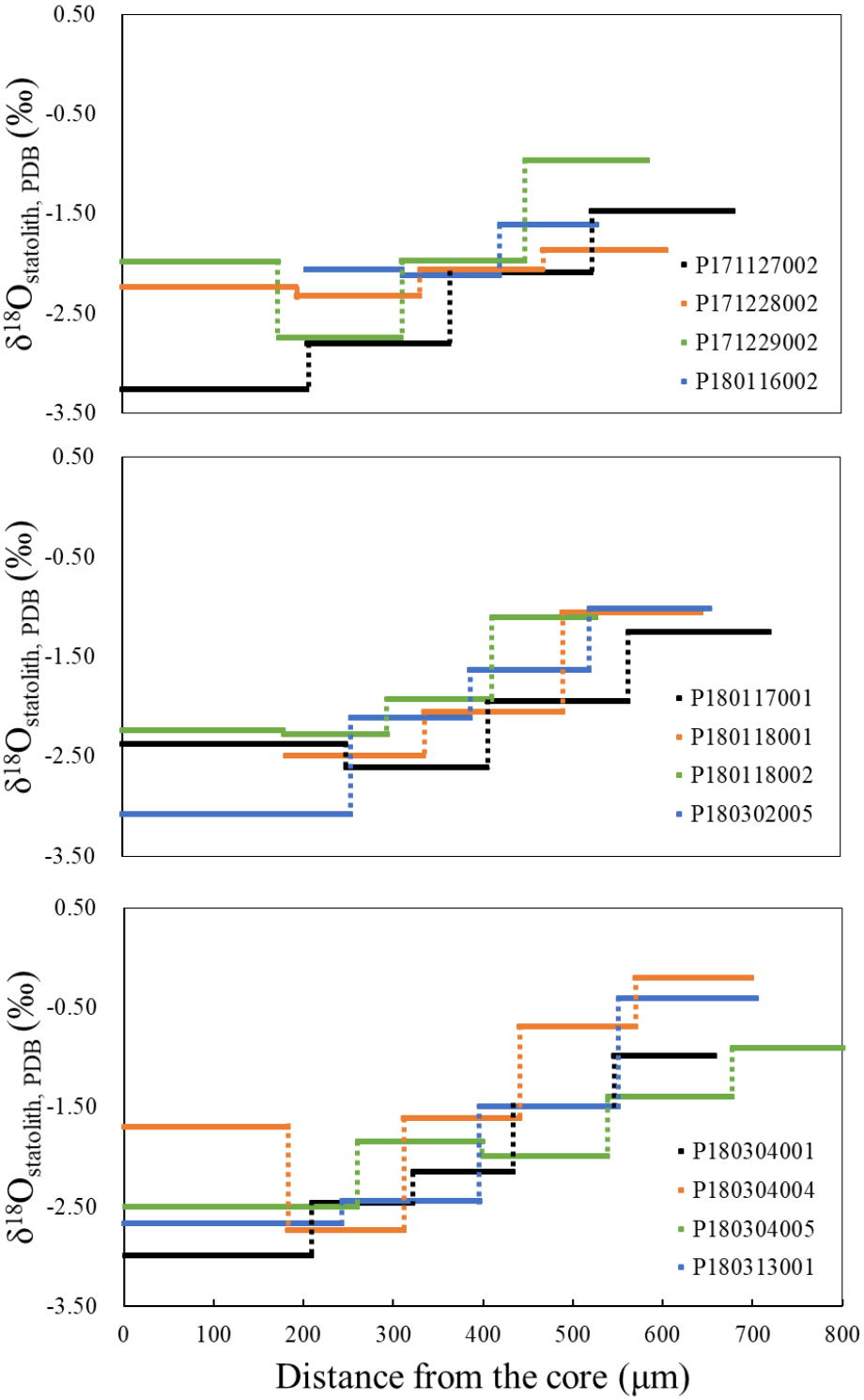

Figure 14 $\delta^{18}O_{statolith}$ profiles of *S. lessoniana* from the statolith core to the edge of each individual in the summer group of 2017-Penghu Islands.

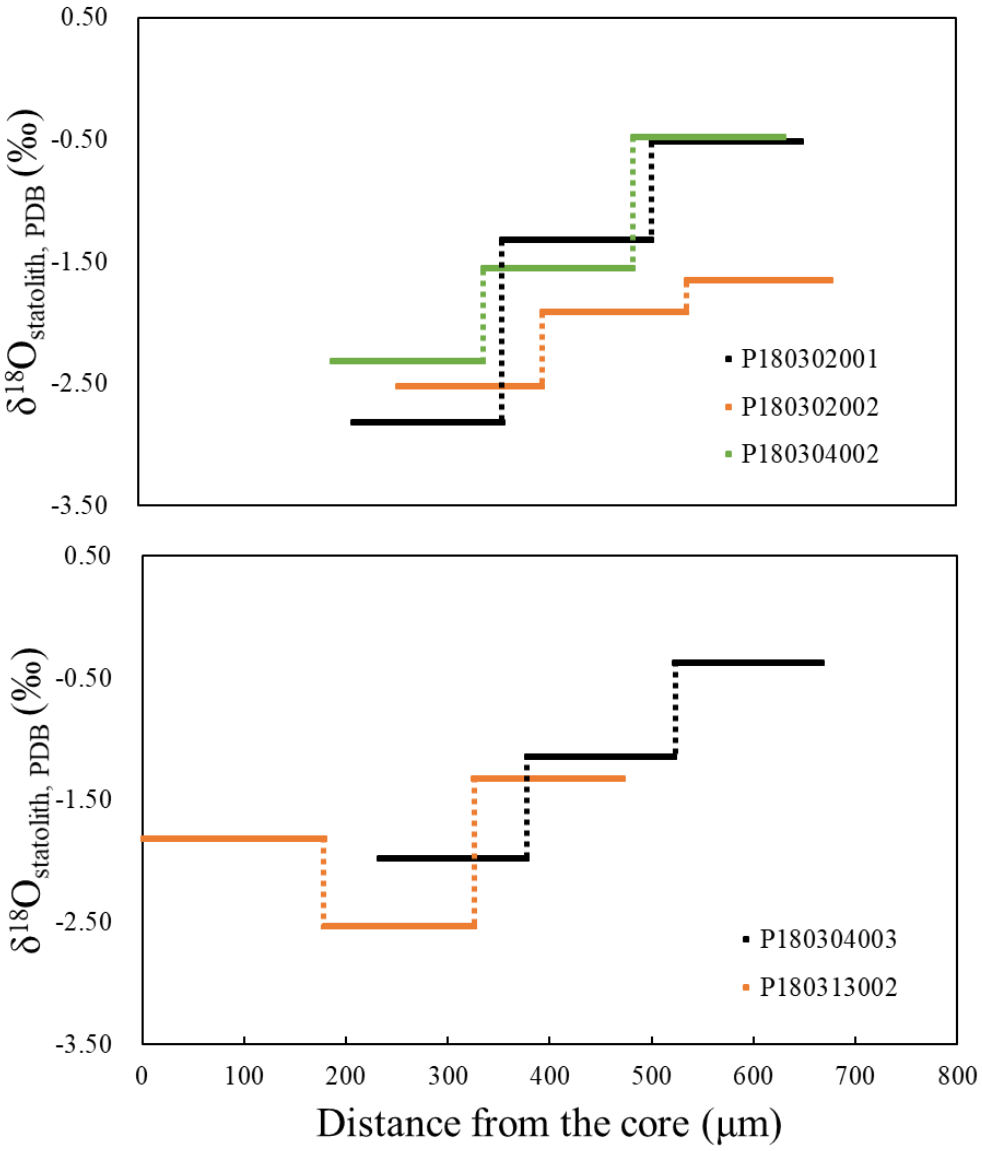

Figure 15 $\delta^{18}O_{statolith}$ profiles of *S. lessoniana* from the statolith core to the edge of each individual in the autumn group of 2017-Penghu Islands.

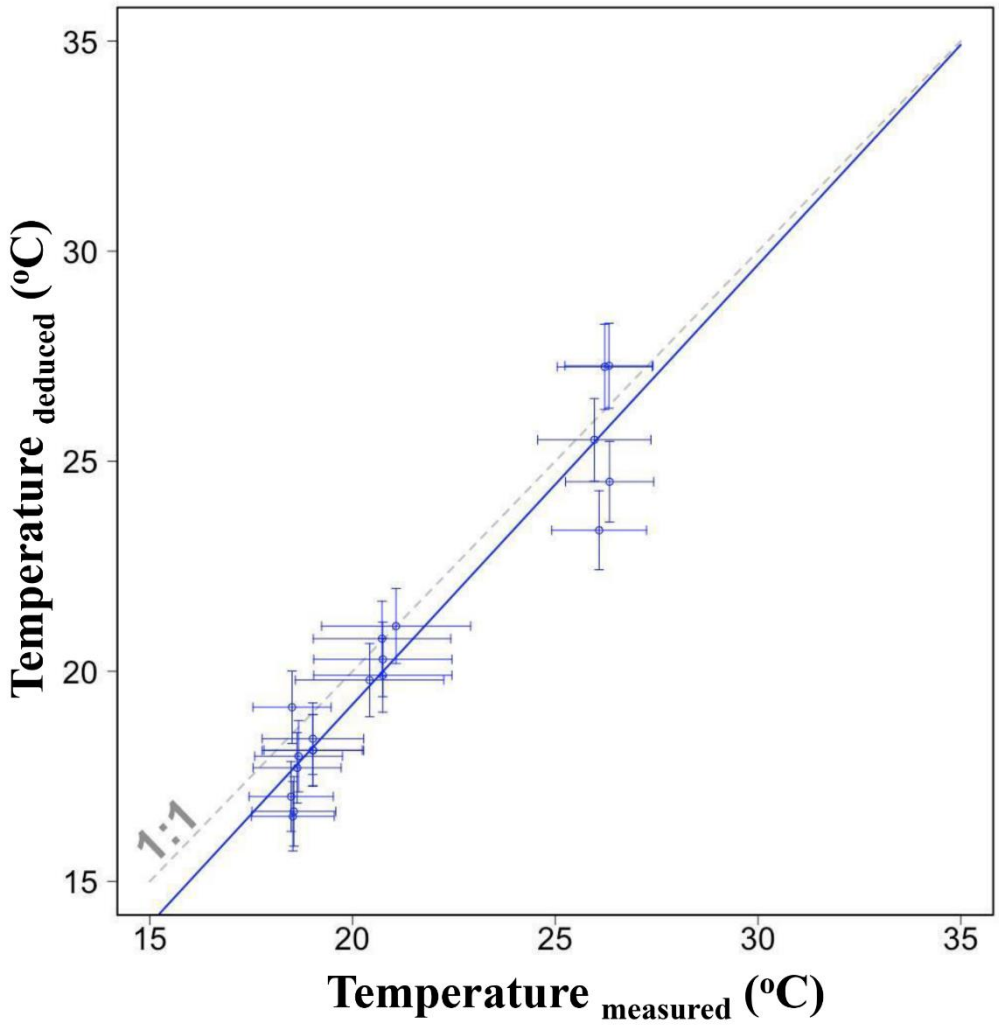

Figure 16 The linear relationship between deduced temperatures from $\delta^{18}O$ values of individual statolith edges and corresponding measured temperatures in the same period. Horizontal error bars indicate one standard deviation of measured temperature; vertical error bars indicate one standard deviation evaluated by using Monte Carlo Simulations and considering uncertainty caused from salinity and parameter variation in the equation. Dashed line indicates the 1:1 correspondence.

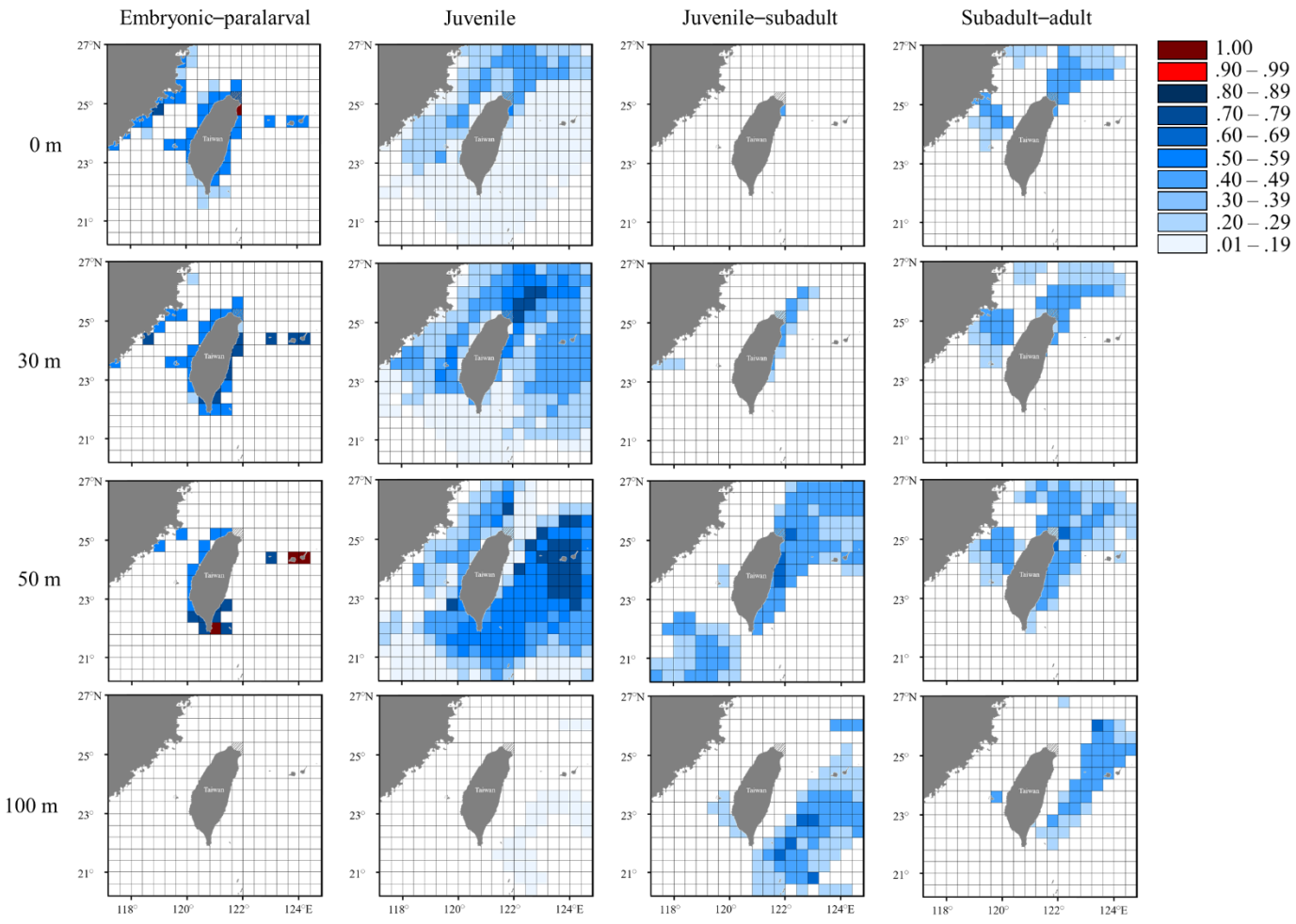

Figure 17 Probability distribution based on experienced temperatures in *S. lessoniana* individuals in the spring group at each life stages of 2017-Northern Taiwan. The legend indicates the probability value of occurrence.

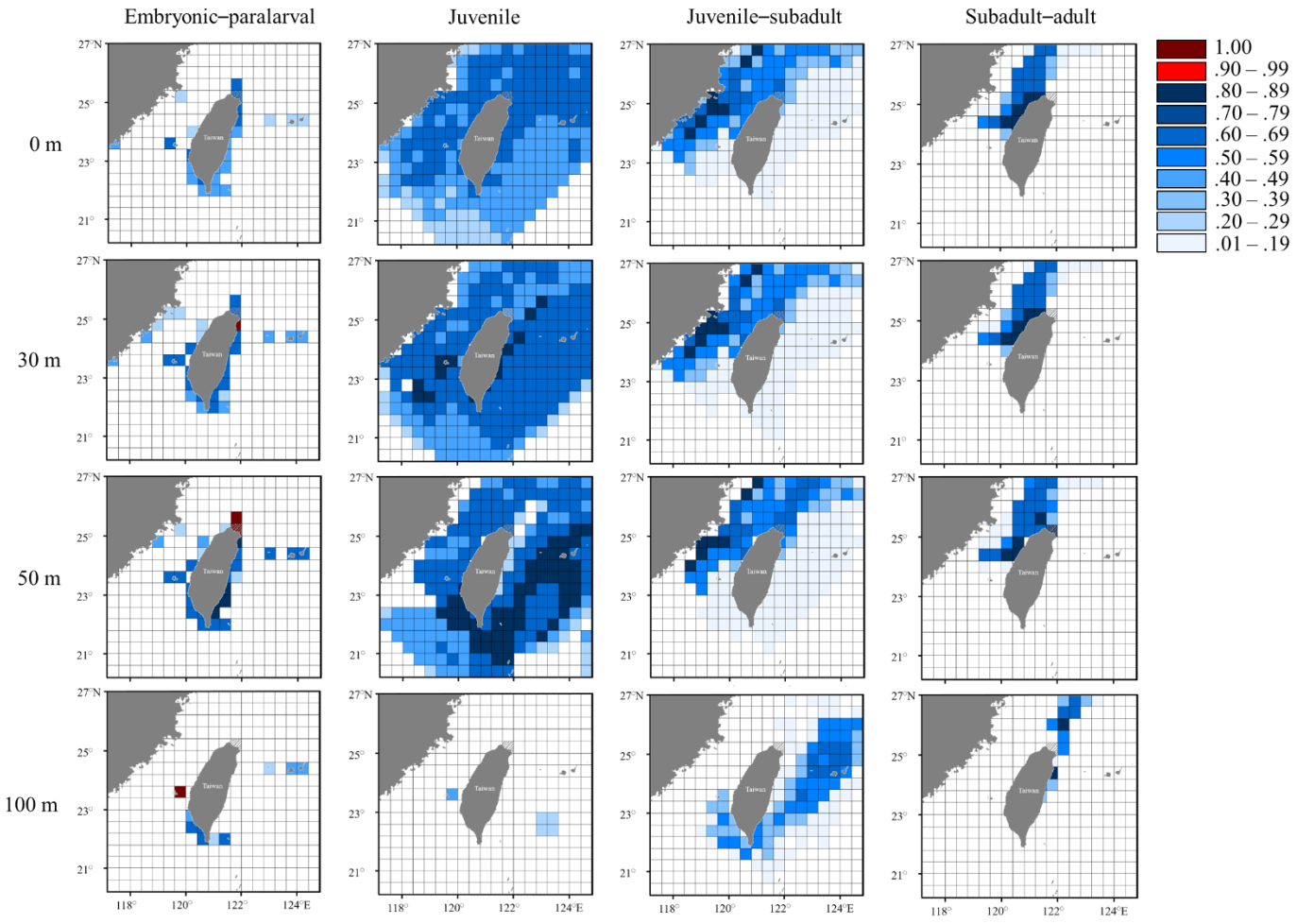

Figure 18 Probability distribution based on experienced temperatures in *S. lessoniana* individuals in the summer group at each life stage of 2017-Northern Taiwan. The legend indicates the probability value of occurrence.

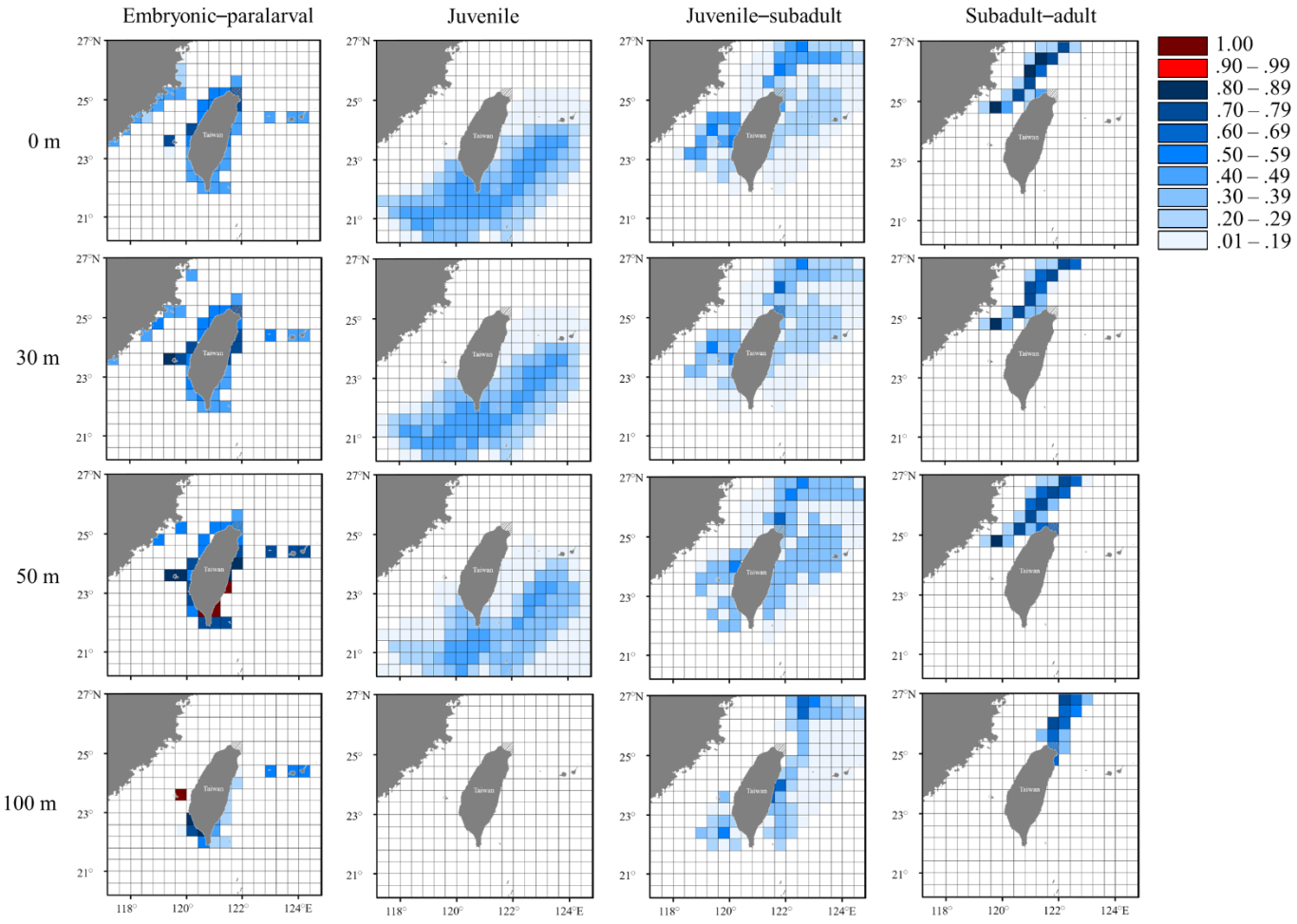

Figure 19 Probability distribution based on experienced temperatures in *S. lessoniana* individuals of the autumn group at each life stage of 2017-Northern Taiwan. The legend indicates the probability value of occurrence.

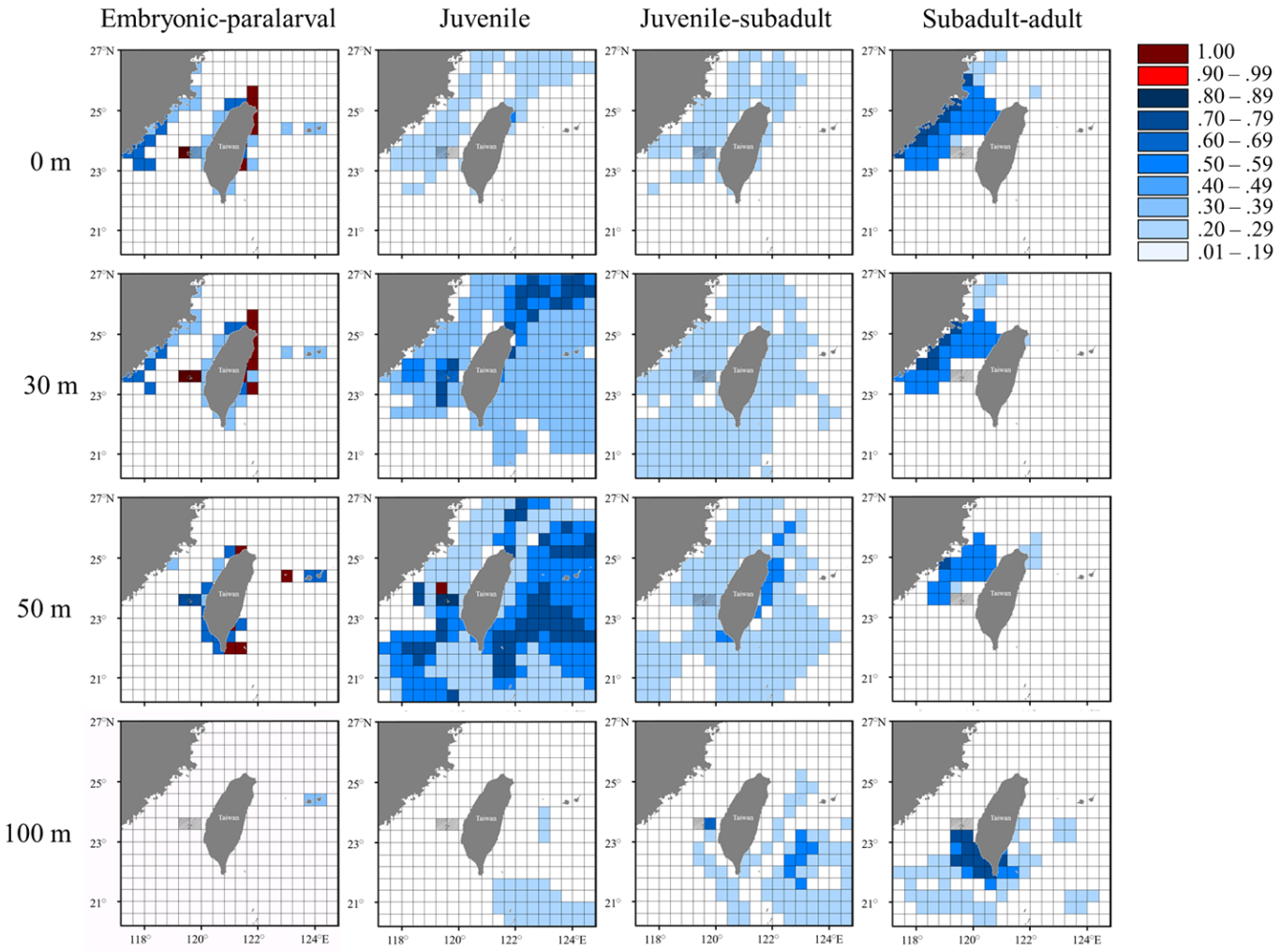

Figure 20 Probability distribution based on experienced temperatures in *S. lessoniana* individuals of the spring group at each life stage of 2017-Penghu Islands. The legend indicates the probability value of occurrence.

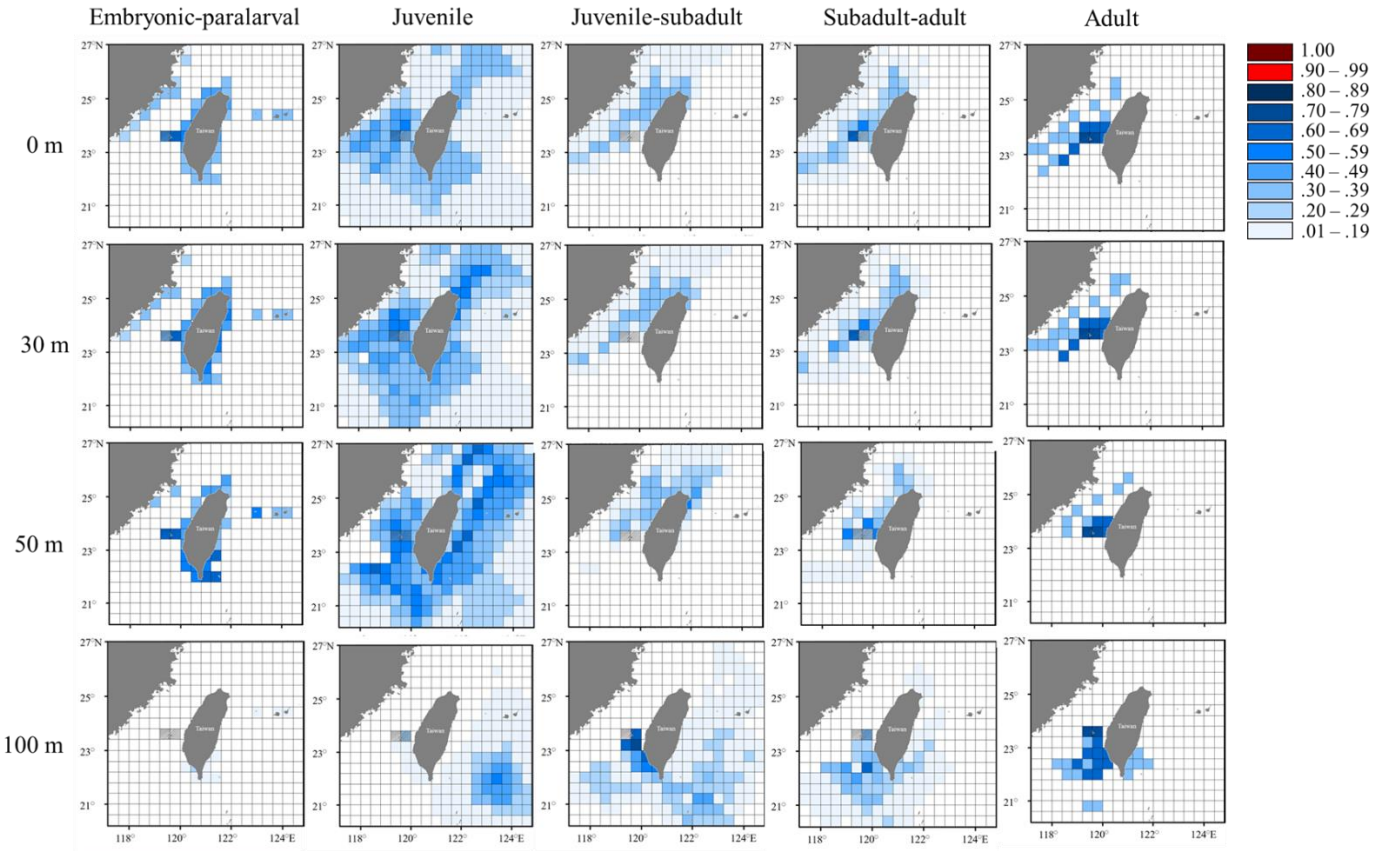

Figure 21 Probability distribution based on experienced temperatures in *S. lessoniana* individuals of the summer group at each life stage of 2017-Penghu Islands. The legend indicates the probability value of occurrence. Note that the adult stage was only shown in the summer group in 2017-Penghu Islands.

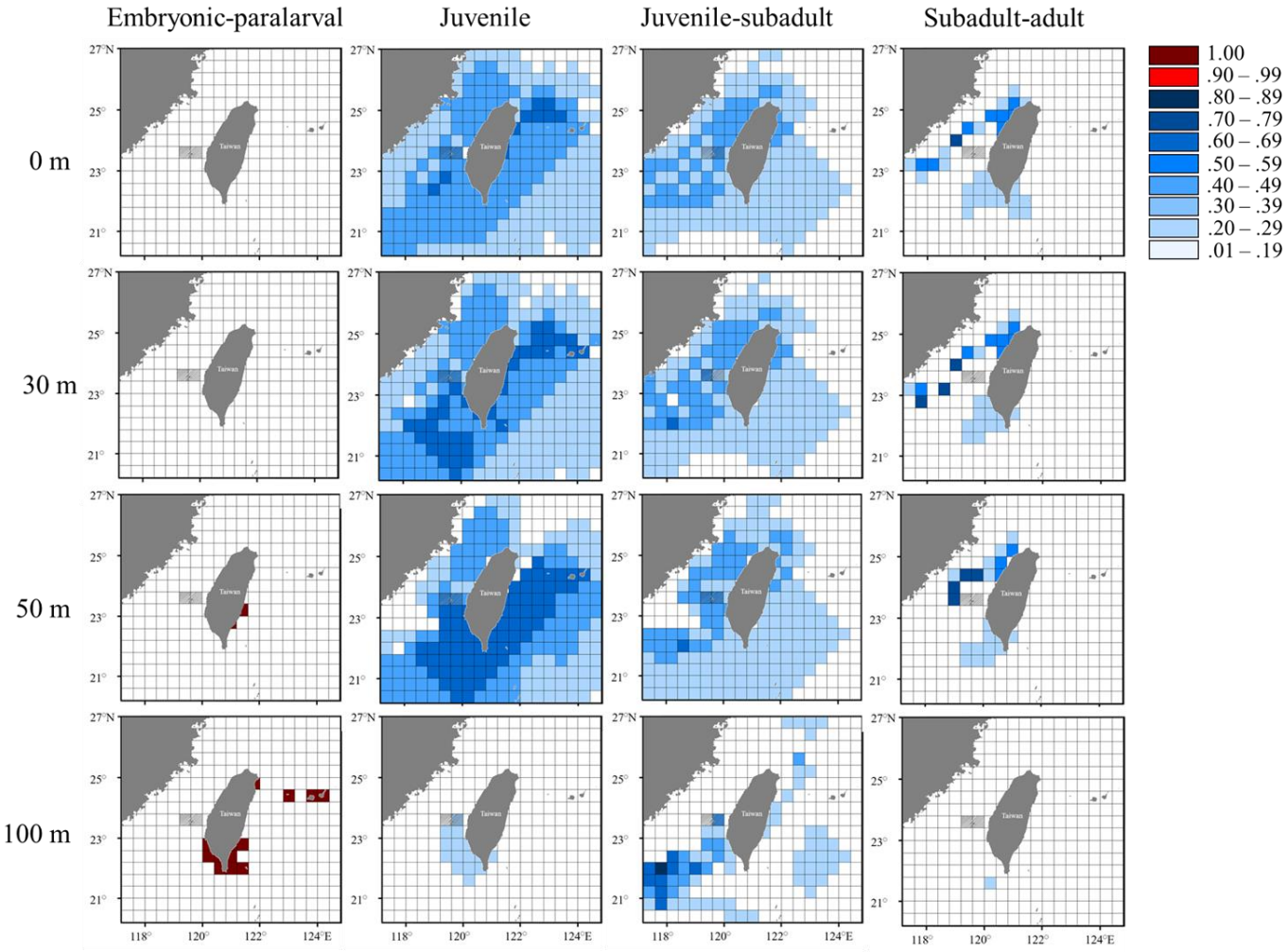

Figure 22 Probability distribution based on experienced temperatures in *S. lessoniana* individuals of the autumn group at each life stage of 2017-Penghu Islands. The legend indicates the probability value of occurrence.

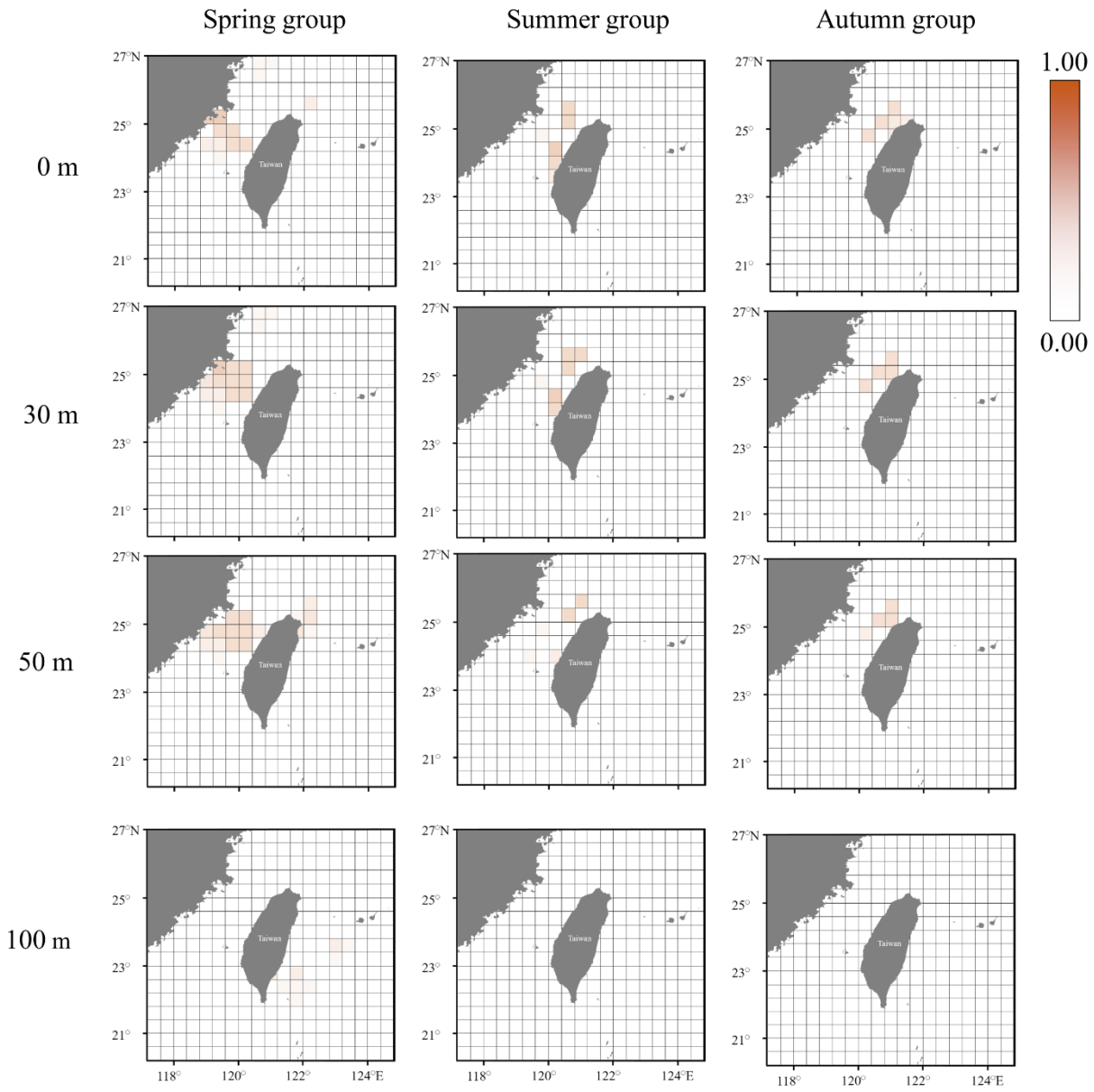

Figure 23 Overlapping rates at the subadult-adult stages of *S. lessoniana* individuals among three seasonal groups between northern Taiwan and the Penghu Islands. The legend indicates the probability value of geographical overlap.

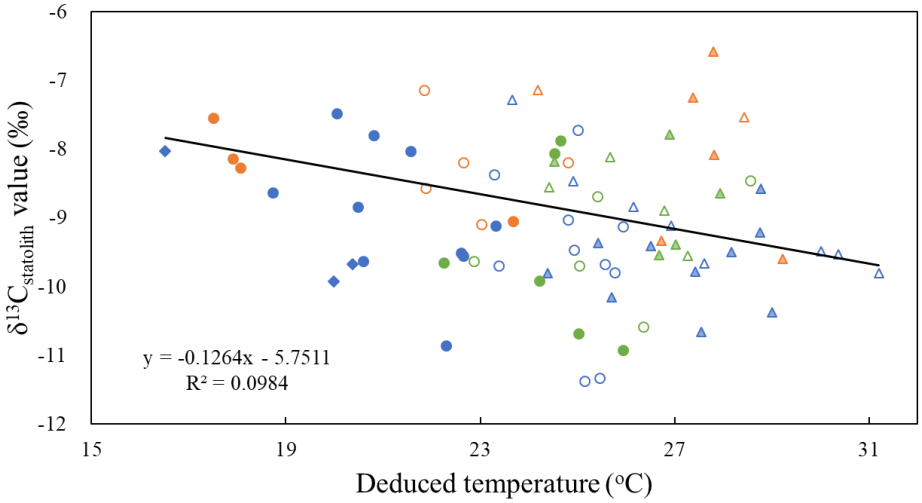

Figure 24 The relationship between deduced temperature and $\delta^{13}C_{statolith}$ value for all life history stages of Penghu Islands individuals. Symbols indicate different life history stages (open triangle: embryonic-paralarval; solid triangle: juvenile; open circle: juvenile-subadult; solid circle: subadult-adult; solid diamond: adult) and seasonal hatching groups (green: spring; blue: summer; orange: autumn).

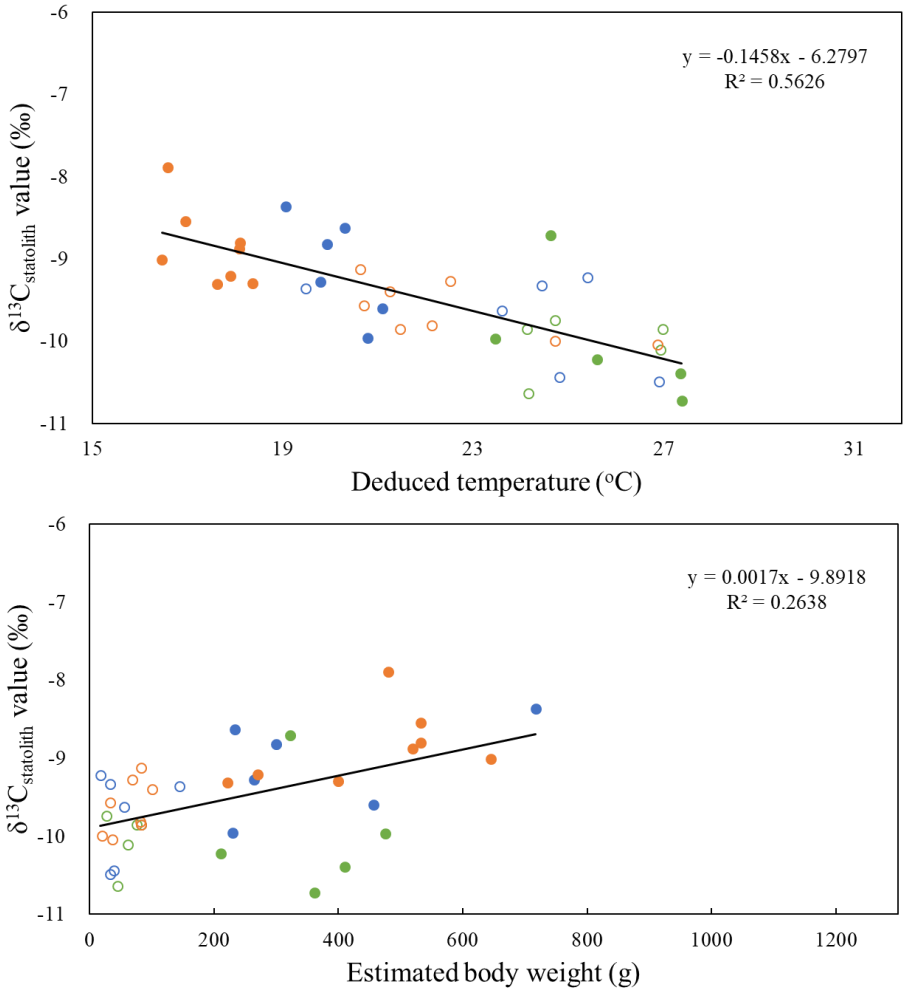

Figure 25 The relationship between alternative metabolic indexes (deduced temperature and estimated body weight) and $\delta^{13}C_{statolith}$ value for the later life history stage of northern Taiwan individuals. Symbols indicate different life history stages (open circle: juvenile-subadult; solid circle: subadult-adult) and seasonal hatching groups (green: spring; blue: summer; orange: autumn).

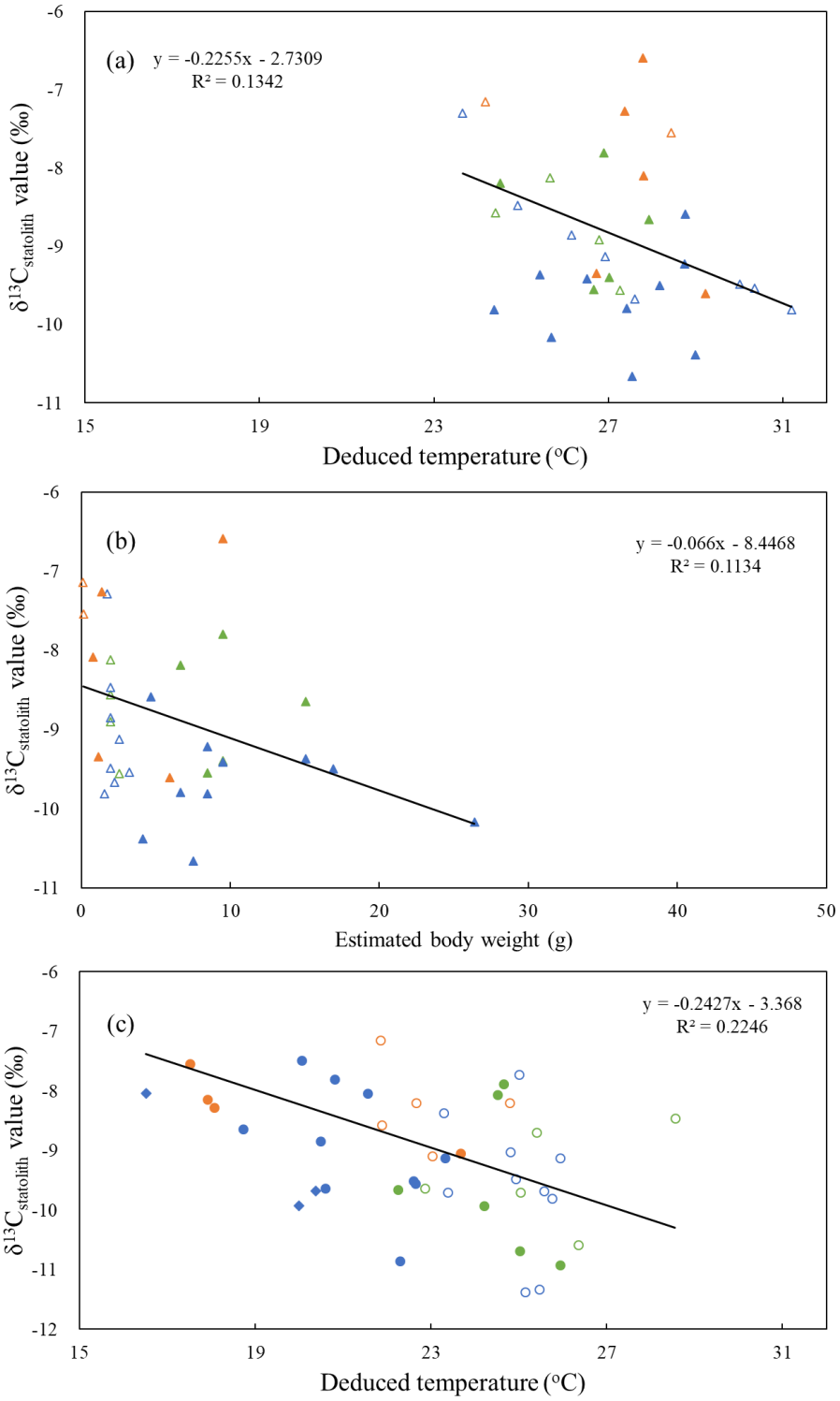

Figure 26 The relationship between alternative metabolic indexes (deduced temperature and estimated body weight) and $\delta^{13}C_{statolith}$ value for the (a, b) early and (c) later life history stage of Penghu Islands individuals. Symbols indicate different life history stages (open triangle: embryonic-paralarval; solid triangle: juvenile; open circle: juvenile-subadult; solid circle: subadult-adult; solid diamond: adult) and seasonal hatching groups (green: spring; blue: summer; orange: autumn).

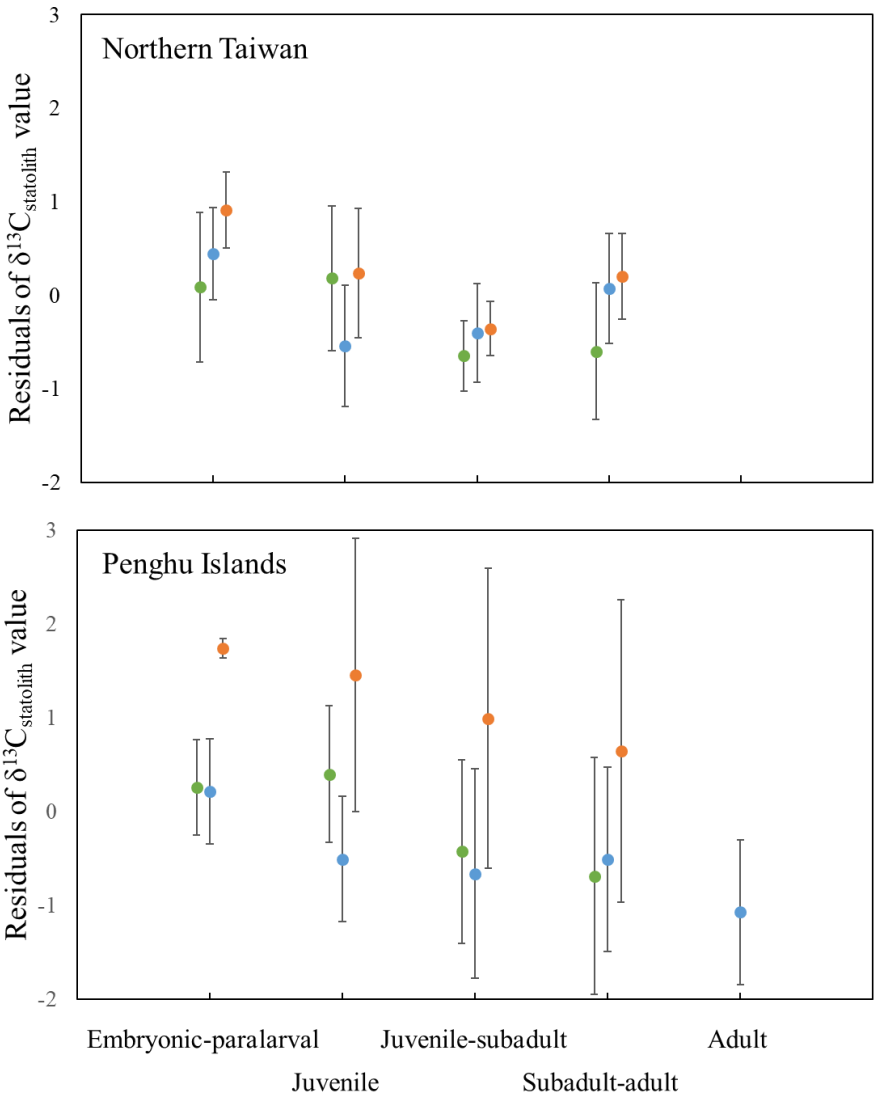

Figure 27 The variations of residual values of seasonal hatching groups (green: spring; blue: summer; orange: autumn) among different life history stages. These residual values were acquired from a linear regression of $\delta^{13}C_{statolith}$ values on the deduced temperatures. Error bars indicate the s.d..

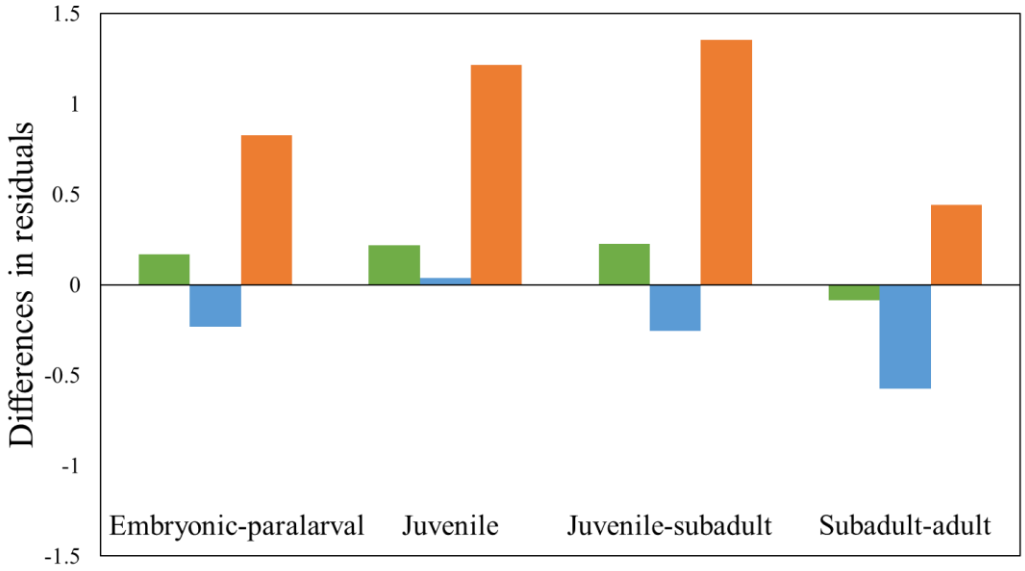

Figure 28 The residuals of the Penghu Islands minus these of northern Taiwan at each life history stage. The colors indicate seasonal hatching groups (green: spring; blue: summer; orange: autumn).

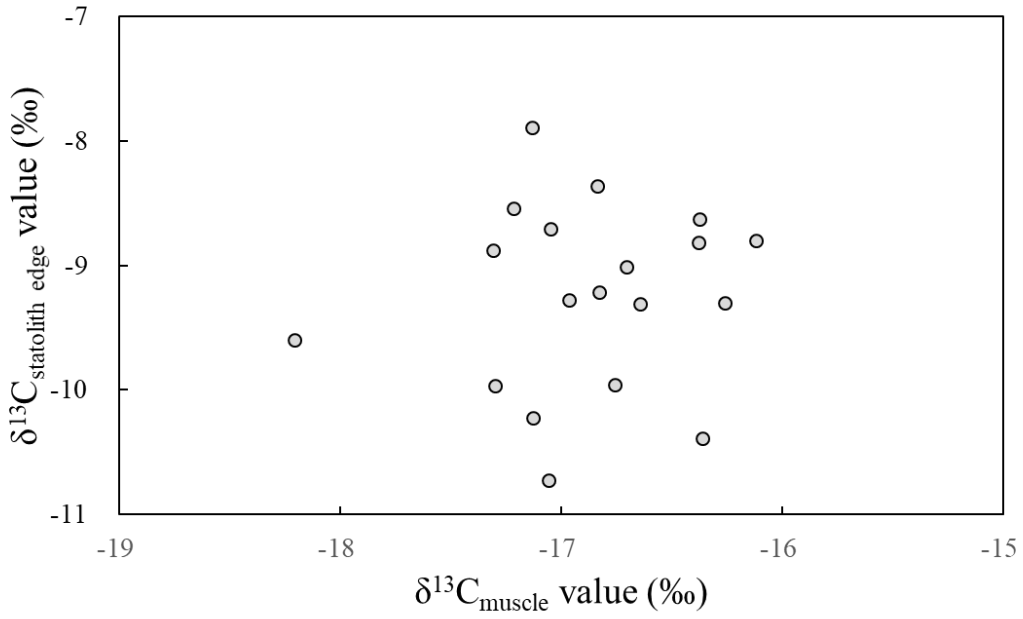

Figure 29 $\delta^{13}C$ values in muscles and statolith edge of northern Taiwan individuals (n = 19).

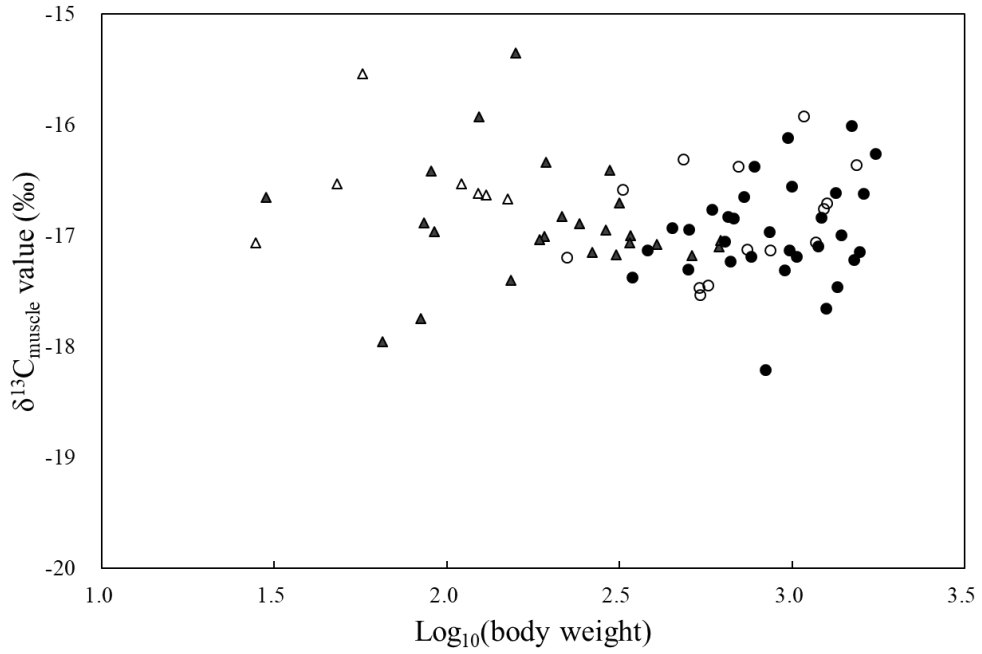

Figure 30 The relationship between $\log_{10}$(body weight) and $\delta^{13}C_{muscle}$ values of northern Taiwan individuals (n = 77). Note that symbols here indicate different sexual maturity stages (open triangle: I; solid triangle: II; open circle: III; solid circle: IV).

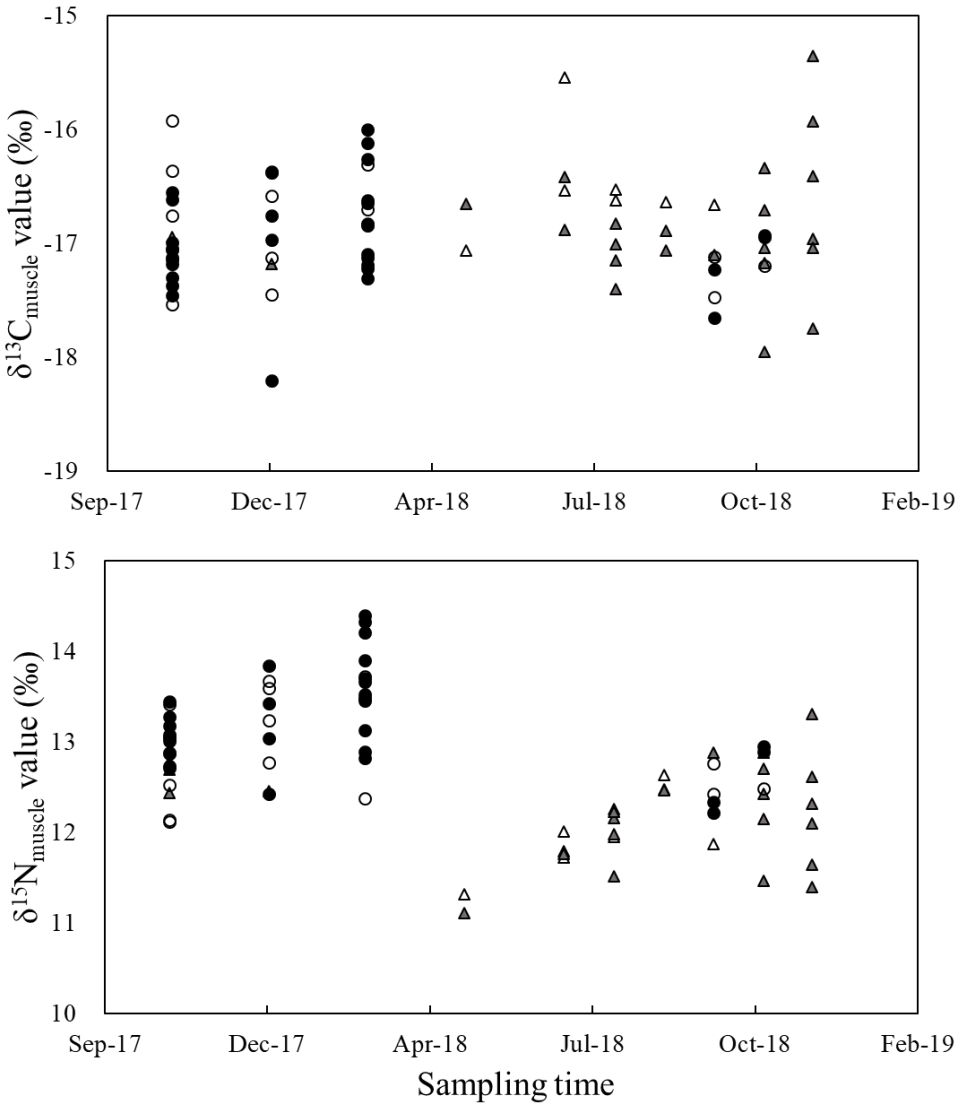

Figure 31 The variations of $\delta^{13}C_{muscle}$ and $\delta^{15}N_{muscle}$ values of northern Taiwan individuals (n = 77) over the sampling duration. Note that symbols here indicate different sexual maturity stages (open triangle: I; solid triangle: II; open circle: III; solid circle: IV).

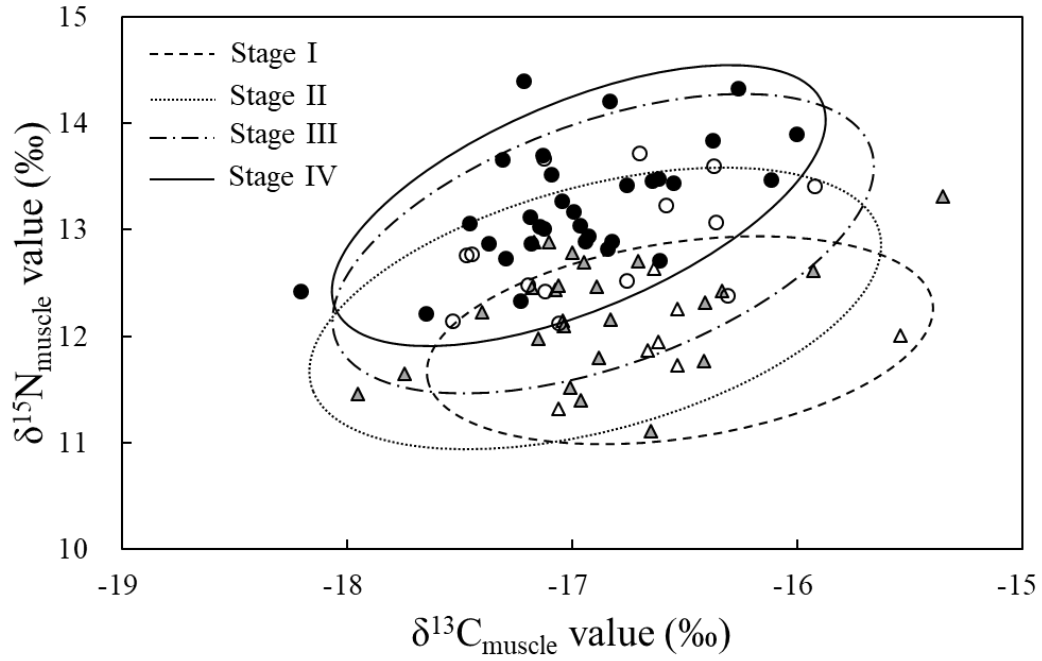

Figure 32 $\delta^{13}C$ and $\delta^{15}N$ values in muscles of northern Taiwan individuals. Ellipses represent the standard ellipse area (SEA) estimated for each sexual maturity stage. Note that symbols here indicate different maturity stages (open triangle: I; solid triangle: II; open circle: III; solid circle: IV).